Carter, R.M., McCave, I.N., Richter, C., Carter, L., et al., 1999
Proceedings of the Ocean Drilling Program, Initial Reports Volume 181

4. Site 1120: Central Campbell Plateau[1]

Shipboard Scientific Party[2]

BACKGROUND AND OBJECTIVES

General Description

Site 1120 is located ~650 km southeast of Stewart Island, near the middle of the Campbell Plateau. The site was drilled in a water depth of 543 m and was located at the crossing of National Institute of Water and Atmospheric Research (NIWA) multichannel seismic line 3034 (Fig. F1). A 3.5-kHz profile (NIWA, Tangaroa CR-3034, 23/2/97) reveals an acoustically reflective seafloor that is underlain by three shallow reflectors, perhaps unconformities, at depths of ~5, 13, and 18 m subseafloor. Multichannel profile NIWA 3034-20 penetrated the complete thickness of the Cretaceous–Holocene Campbell Plateau succession (e.g., Beggs, 1978), including probable Cretaceous nonmarine rift-fill sediments at the base.

The seismic succession is punctuated by seven conspicuous reflectors (R1–R7), which probably represent unconformities. Three of these reflectors (R2, R4, and R5) are used to divide the succession into four major parts, corresponding to subdivisions of the New Zealand Plateau–wide Cretaceous–Holocene, Kaikoura Synthem (Carter, 1988; Fig. F2). Between reflectors R6 (basement) and R5, a thin unit (0–0.18 two-way traveltime [TWT]) of probable upper Cretaceous–Eocene terrigenous sands and silts has its thickest occurrence within rift-axis depocenters (sediments up to 0.55 TWT thick) and thins to almost nothing where it onlaps block-faulted basement highs. Reflector R5, which caps the basal part of the succession, is the first flat-lying reflector that is traceable throughout the region, and it probably marks the inception of widespread biopelagic carbonate sedimentation. If this correlation is correct, then reflector R5 corresponds to the contact between the Garden Point

F1. Locality map of Site 1120, p. 25.

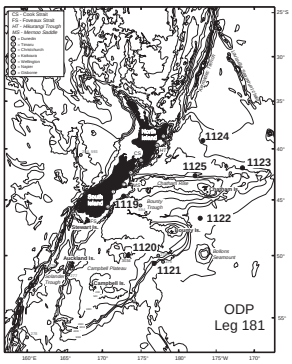

F2. Portion of seismic line, p. 26.

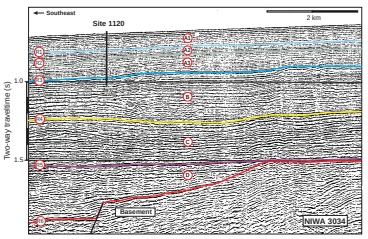

[1]Examples of how to reference the whole or part of this volume.
[2]Shipboard Scientific Party addresses.

and Amuri Limestones on nearby Campbell Island (Beggs, 1978). Few basement highs remained on the Campbell Plateau to shed terrigenous sediment after the late Cretaceous, and the entire succession above reflector R5 is therefore probably biopelagic carbonate (i.e., Amuri Limestone facies). Times of water-mass change, perhaps accompanied by current activity and sublevation, are indicated by the subtle but marked changes in seismic character that take place across reflectors R4 to R1. Two obvious episodes of current drift deposition occur above reflectors R5 and R4 respectively, starting at ~0.7 s and ~0.5 s TWT subseafloor, and minor channeling is apparent along reflector R2 at ~0.15 s TWT subseafloor. The railroad-track, flat-lying nature of the reflections of the biopelagic carbonates across profile NIWA 3034 is disturbed only by minor faulting, seemingly concentrated along reflector R3 but which sometimes extends to the seabed above and into older sediments below.

Site Objectives

Site 1120 was drilled to establish the age of the major unconformities in the Campbell Plateau sequence, and to determine the history of the shallow parts of the Antarctic Circumpolar Current (ACC) where it sweeps past and over the southeast corner of the Plateau. The analysis of seafloor magnetic anomalies indicates that the ACC had its inception in the Oligocene, at ~32 Ma, when Australia separated from Antarctica and allowed circumpolar flow to commence (Molnar et al., 1975; Lawver et al., 1992). At this time, the Campbell Plateau was situated immediately down-current from the opening Southern Ocean, and, like eastern South Island, New Zealand (Carter et al., 1996b), was therefore probably exposed to vigorous current activity. It was anticipated that reflector R3 would be of middle–late Miocene in age, thus correlating with the phase of known volcanism and minor faulting in eastern South Island between ~13–10 Ma (Benson, 1969; Field and Browne, 1989). The expanded section of Eocene and Oligocene carbonates below this unconformity is one of the thickest known in the entire New Zealand region and should yield an unparalleled record of the paleoceanographic events associated with the opening of the Tasmania-Antarctica gateway, and the early evolution of the ACC system.

OPERATIONS

Hole 1120A

The 319-nmi voyage to Site 1120 (proposed site SWPAC-6B) was accomplished through calm seas at an average speed of 11.0 kt. The vessel proceeded directly to the Global Positioning System coordinates of the location. The positioning beacon was dropped at 0045 hr on 28 August 1998. The advanced hydraulic piston core/extended core barrel (APC/XCB) bottom-hole assembly was assembled using a 9⅞-in PDC bit with a lockable float valve (LFV) and deployed. Hole 1120A was spudded with the APC at 0550 hr on 28 August. The recovery indicated that the water depth was 542.9 m below sea level (mbsl). The hole was scheduled for only a mudline sample and the single APC Core 1H was taken from 0 to 4.6 meters below seafloor (mbsf) (Table **T1,** also in **ASCII format**).

T1. Site 1120 coring summary, **p. 47.**

Hole 1120B

The second hole of the site was spudded with the APC at 0650 hr on 28 August. The seafloor depth inferred from recovery was 544.2 mbsl. APC coring advanced to 68.3 mbsf when Core 8H did not achieve a full stroke. Cores were oriented starting with Core 3H. Coring was continued with the XCB and deepened the hole to 188.0 mbsf (Table T1) when operations were put on standby because of excessive heave (2 m with an occasional 3-m event) generated by 2.0- to 2.5-m seas combined with a 4.0–5.5-m swell from the southwest. The hole was abandoned, the bit clearing the seafloor at 2020 hr on 28 August.

Hole 1120C

A force 9 gale, with sustained winds up to 45 kt and gusts to 60 kt (force 10), prevailed in the drilling area from the evening of 28 August until 0045 hr on 30 August, when it was decided to continue site operations even though environmental conditions were borderline for shallow-water operations. After positioning the bit at 543 mbsl, Hole 1120C was spudded with the APC at 0613 hr on 30 August. The seafloor depth based upon recovery was 545.9 mbsl. Piston coring advanced to 44.6 mbsf (Table T1) when an incomplete stroke was encountered at Core 5H. While recovering the core, the wireline broke. In an attempt to fish the parted wireline, monel sinker bars, and APC assembly, the drill pipe was pulled back. The bit cleared the seafloor at 0613 hr on 31 August.

A wireline spear was made up and run in the pipe. It tagged the broken wireline at 183 mbsl. Attempts to work the broken wireline back up the pipe were unsuccessful and the spear slipped off. The drill pipe was pulled back in stands until the broken end of the wireline was found. After the broken wireline was recovered, the APC core barrel containing Core 5H was retrieved at 1055 hr. Environmental conditions were too extreme to continue, and operations were placed in standby mode while awaiting improved weather.

Hole 1120D

At 1600 hr on 31 August, Hole 1120D was spudded and drilled ahead to 157.4 mbsf, where XCB coring was initiated. XCB coring advanced from 157.4 to 220.7 mbsf (Table T1) when operations again had to be terminated because of excessive heave. It was decided to discontinue coring at this location and move on to Site 1121. As the drill string was being retrieved, the beacon was recalled and recovered. At 0600 hr on 1 September, the vessel began the transit to Site 1121.

LITHOSTRATIGRAPHY

The sedimentary regime of the 500- to 1500-m-deep Campbell Plateau is not well known. Summerhayes (1969) ran a reconnaissance survey of surficial sediments, which were mainly foraminifer ooze. In the 1960s and early 1970s, the *Eltanin* surveyed the shallow structure and sediment thickness using a single-channel air gun system. Results from those surveys have been summarized by Davey (1977). *Eltanin* seismic profiles were used to select a series of holes for Deep Sea Drilling Project (DSDP) Leg 29 (Kennett, Houtz, et al., 1975). Two of the sites, 275 and 276, were located at the eastern and western margins of Campbell Pla-

teau and were characterized by a series of pronounced disconformities, which Kennett, Houtz, et al. (1975) related to erosion under an extremely active, shallow western boundary current (nominally the northern edge of the ACC). Site 275, in particular, had a disconformity encompassing the entire Cenozoic and part of the Upper Cretaceous. Accordingly, Site 1120 was located toward the central plateau within a Cenozoic sedimentary sequence anticipated to be 700 m thick.

Lithology

Cores from Site 1120 penetrated a succession of calcareous biogenic oozes. With the exception of one sample containing 85% calcium carbonate, all other ooze samples had more than 90% $CaCO_3$, with two-thirds in the range of 94% to 96%. Despite this high degree of lithologic homogeneity, four basic units are recognized on the basis of subtle changes in the calcareous biogenic and noncarbonate components, along with variations in bedding and color (Table T2). The resulting lithologic logs, together with physical properties and biostratigraphic control, are summarized in Figure F3. Of note is the improved correlation, compared with Site 1119, between light reflectance and calcium carbonate percentage (Fig. F4). At Site 1119, a much poorer correlation was realized because the spectrophotometer was too high above the core surface, thereby allowing reflectance scatter. By altering the sensor height to as close to the sediment surface as possible, better results were obtained. These results are too preliminary to act as a proxy for calcium carbonate. This is in part caused by the limited color range associated with the sediment's high concentration and restricted range (>90%) of $CaCO_3$.

Unit I

Interval: Sections 181-1120A-1H-1 through 1H-CC; Sections 181-1120B-1H-1 through 2H-CC; Sections 181-1120C-1H-1 to 1H-4
Depth: 0–4.6 mbsf (Hole 1120A); 0–4.3 mbsf (Hole 1120B); 0–4.6 mbsf (Hole 1120C)
Age: late Pleistocene

The youngest lithostratigraphic unit occupies the top 4.6 m of Hole 1120C, where it rests above more lithified sediment; the contact is interpreted as an unconformity (Fig. F5). The younger sediments are thinly bedded with layers typically <0.5 m thick. Contacts are generally bioturbated and are disrupted further by one layer injecting into another—a process of soft-sediment deformation that probably was caused by drilling. Beds are distinguished by color variations of white and light gray. Colors alternate between light gray (N7) and various hues of white (N8, 5Y8/1, 5Y8/2). However, some hues of white are not covered by the Munsell color chart. Of note are layers with a brilliant white resembling fluorescent toothpaste for which the term "bright white" has been coined for use on the visual core description sheets. The surface of the unconformity below this banded sequence is white with a yellow-red hue (10YR 8/2). Sediments are dominated by calcareous nannofossils and foraminifers in differing proportions so that the lithology varies between foraminifer nannofossil ooze and nannofossil foraminifer ooze. Lithologies containing mainly nannofossils tend to be "bright white." Accessory components include pyrite, found frequently lining or infilling the chambers of foraminifer tests, quartzofeldspathic silt, skeletal de-

T2. Main criteria used for distinguishing lithostratigraphic Units I–IV, p. 54.

F3. Summary logs for Site 1120, p. 27.

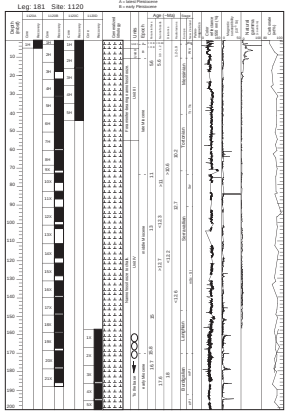

F4. Plot of light reflectance against $CaCO_3$, p. 29.

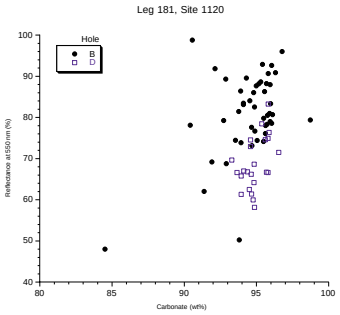

F5. Lithologic break at 4.6 mbsf, p. 30.

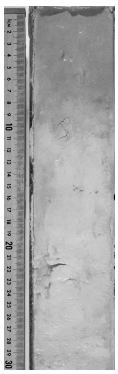

bris of uncertain genesis, and trace amounts of heavy minerals. Quartzofeldspathic grains were present in the upper 3 m of the core, below which they occur in only trace amounts.

Bioturbation is pervasive, but the lack of contrast in the various lithologies, together with soft sediment deformation, have precluded reliable identification of ichnofossils, although possible *Planolites* traces are present.

Unit II

Interval: Sections 181-1120B-2H-1 through 2H-5; Sections 181-1120C-1H-4 through 2H-4
Depth: 4.3–10.2 mbsf (Hole 1120B); 4.6–11.2 mbsf (Hole 1120C)
Age: early Pleistocene

The unit begins at the postulated unconformity at 4.6 mbsf (interval 1120C-1H-4, 10 cm). The sediment below is indurated, but not to the extent that it could be classified as chalk. However, further below the contact, the sediment again becomes softer, but individual beds are typically thicker than 1 m and are still discernible on the basis of color, although color differentiation is not as clear as in Unit I. There is a more substantial difference in composition. Unit II is mainly foraminifer nannofossil ooze, that is, the dominant biogenic component is nannofossils with foraminifers as a subordinate constituent, although still occasionally rivaling the nannofossils' abundance. Unit II also contains glauconite and rare pyritic concretions, both of which are absent in the overlying beds.

Bioturbation is again pervasive, but as the sediments are firmer than those of Unit I, burrows are better preserved and, in some instances, highlighted by pyrite stains (note that "pyrite" is used as a generic term for authigenic iron sulfides). Identified trace fossils include *Chondrites*.

Unit III

Interval: Sections 181-1120B-2H-5 through 7H-3; Sections 181-1120C-2H-4 through 5H-CC
Depth: 10.2–54.9 mbsf (Hole 1120B); 11.2–44.6 mbsf (Hole 1120C)
Age: late Miocene

A sequence of weakly bedded ooze extends from 10.2 to 54.9 mbsf. At this level, color differentiation is minimal and sediments range from white (N8) to white (5Y8/1). Bioturbation has ensured extensive but very subtle mottling of these differently hued whites. As in Unit II, foraminifer nannofossil ooze is the dominant lithology, but there the similarity ends. Glauconite disappears in Unit III, and its place is taken by siliceous sponge spicules. Pyrite continues to be a prominent accessory and, in two instances (Sections 181-1120C-4H-4 and 4H-5), it forms concretions with clusters of sponge spicules.

The color and lithologic similarity of the sediments in Unit III make identification of ichnofossils difficult, although some burrows are accentuated by dark gray pyrite staining. Identifiable forms are *Zoophycos* and *Planolites*.

Unit IV

Interval: Sections 181-1120B-7H-3 through 21X-CC; Core 181-1120D-1X through Section 181-1120D-9X-CC
Depth: 54.9–188.0 mbsf (Hole 1120B); 157.4–220.7 mbsf (Hole 1120D)
Age: early to late Miocene

Between 54.9 mbsf and the base of the core at 220.7 mbsf, the sediment exhibits a fairly uniform lithology. Sediment color varies mainly between two hues of white (N8 and 5Y8/1). Pervasive bioturbation results in a mottled white deposit, the monotony of which is interrupted by occasional ill-defined layers of light gray (N7) ooze, and dark gray stains associated with concentrations of pyrite. A rhythmic sequence of slightly dark bands (<1 cm wide) first appears in Section 181-1120B-18X-2 and is assumed to mark the onset of drilling biscuits. Biscuits have a rhythmic character and form across existing sedimentary features, such as primary bioturbation. Where unaffected by biscuiting and soft sediment deformation, the following trace fossils were identified: *Zoophycos, Terebellina, Planolites,* and *Palaeophycus*. A single echinoid spine was observed in Section 181-1120B-8H-5.

Compared to the younger units, Unit IV lithology is a nannofossil ooze with markedly reduced numbers of foraminifers (concentrations in the "Present" category), and a very reduced accessory assemblage. The noncarbonate mineralogy is dominated by pyrite, and quartzofeldspathic silt occurs only in trace amounts. Flakes of deformed mica, indicative of a probable metamorphic source, shards of colorless and brown glass, and diatoms all make sporadic appearances toward the base of the core below ~160 mbsf. Smear slides from the dominant lithology and a light gray layer (Section 181-1120D-6X-2) revealed the latter to have higher quantities of foraminifer tests (**"Site 1120 Smear Slides,"** p. 37). Of special note are small pebbles of gray, dense pumice in Section 181-1120B-16X-2 and of gray limestone in Section 181-1120D-8X-1.

Discussion

A feature of the pelagic drape sampled at Site 1120 is its high content of calcium carbonate which averages 93%. Such a high amount is consistent with the site's isolation from terrigenous sources. New Zealand is 500 km to the northwest of the site, and Campbell Plateau is topographically isolated from the main sediment conduits leading from New Zealand, namely Solander Channel, and Bounty Channel with its attendant canyon system draining the eastern margin of the South Island (e.g., Carter et al., 1996a). Flow across the plateau is mainly from south to north, coming from a region with negligible sources of terrigenous material. Furthermore, Site 1120 is over 300 km south of the main pathway of aeolian dust carried east of New Zealand under the vigorous westerly wind regime (e.g., Thiede, 1979). Nevertheless, during periods of northwesterly wind, some aeolian detritus is likely to reach Campbell Plateau both from local sources and Australia (Hesse, 1994).

The lowest carbonate concentrations are within the upper Pleistocene sequence of alternating light and dark nannofossil and foraminifer oozes represented by Unit I (Fig. **F3**). Kasten cores from elsewhere on Campbell Plateau suggest that these alternations are interglacial (light beds)/glacial (dark beds) cycles (e.g., Carter et al., unpubl. data).

The glacial periods were times of increased windiness, a response to enhanced thermal gradients associated with the equatorward migration of cold water (e.g., Stewart and Neall, 1984). Thus, the horizons of lower carbonate in Unit I may be caused by an increased aeolian input—a supposition that is supported by higher concentrations of angular quartzofeldspathic silt grains in this unit. Carbonate continues to increase downward through the upper core to reach a local peak at the base of Unit II. Below this it decreases to a minimum around the middle part of upper Miocene Unit III before climbing to high values (~92%–96%) that are more or less maintained to the base of the core. The cause of the reduced carbonate in upper Unit III is unknown. It may be related to the arrival of siliceous organisms, in particular sponges, which at times were also accompanied by diatoms. Such an incoming of siliceous species often heralds a change to cooler waters (e.g., Weaver et al., 1998), which in turn may influence carbonate production and preservation.

As discussed above, the alternations of light and dark colors in Unit I are likely to represent glacial/interglacial cyclicity as noted elsewhere off eastern New Zealand (e.g., Griggs et al., 1983; Nelson et al., 1986). However, the components responsible for the contrasts in plateau sediments differ slightly from other examples because the plateau is largely isolated from terrigenous sources. Light layers have a dominance of nannofossils that impart a "bright white" color to individual layers. By comparison, the darker glacial beds have a higher proportion of aeolian detritus and foraminifers, whose tests are rendered darker by the formation of pyrite within test chambers. Carbonate curves, magnetic susceptibility profiles, and stable isotope measurements made on kasten cores from the region (Neil, 1998; Carter et al., unpubl. data) demonstrate that the glacial/interglacial cyclicity commenced at isotope Stage 6 and continued through to the present Stage 1. If this cyclicity holds for Site 1120, and it is continuous through to the unconformity at 4.6 mbsf, then the oldest sediments in Unit I could be about Stage 21. However, the biostratigraphy indicates a break at ~3 mbsf. This level approximates isotope Stage 16 with a top age of 620 ka (again assuming there is no undetected break in cyclicity between 0–3 mbsf).

BIOSTRATIGRAPHY

Introduction and Summary

From Site 1120, drilled on the western part of the Campbell Plateau, sediments were recovered from ~550 m water depth. The sediments are foraminifer-bearing nannofossil oozes, and calcareous microfossils (including *Bolboforma*) are well preserved with diverse assemblages, which provide a wealth of information. Through the upper and middle Miocene part of the section, moreover, siliceous microfossils are present in sufficient numbers to provide paleoceanographic information, as well as first and last appearance datums for age control. Because of the paleolatitudinal position of the site, both subantarctic species and cosmopolitan species were used to date the sediments.

The Pleistocene–Pliocene stratigraphic sequence recovered is very thin. The Pliocene is probably missing completely because of hiatuses caused by intensified flow of water masses across the Campbell Plateau. The upper 2.5–3 meters composite depth (mcd) are late Pleistocene in age (mostly younger than 0.24 Ma). Down to ~10–12 mcd, a middle

Pleistocene age was determined (0.9–1.2 Ma). A large part of the upper and lower Pleistocene thus is missing.

A 219-m-long lower to upper Miocene section was recovered from interval 181-1120B-2H-CC to 181-1120D-9X. A detailed age control is provided through the Miocene at this site by numerous datum levels from calcareous and siliceous microfossils (Table T3). As the site is located near the northern occurrence of subantarctic species, their last and/or first occurrence datums may deviate from the ages published in the literature. Unfortunately, magnetostratigraphy, which would allow us to check whether any datum levels are time transgressive, is not available for this site (see "Paleomagnetism," p. 15). Using the published ages (compare Tables T2, p. 59, T3, p. 60, T4, p. 63, and T5, p. 64, all in the "Explanatory Notes" chapter), and depending on which species are selected for the age-depth plot, either a number of short hiatuses can be detected (Fig. F6; see also "Age Models and Sedimentation Rates," p. 17) or a more-or-less complete section from ~5.5–22 Ma results, with only one possible hiatus (detected by calcareous nannofossil analysis, but not by foraminifer biostratigraphy) between 168.7 and 171.2 mbsf, where sediment representing ~1.5–3.0 m.y. is missing. Sedimentation rates in the upper and middle Miocene are 10–20 m/m.y.

Benthic foraminifers indicate that this site's paleoenvironment has been middle to upper bathyal throughout the Neogene–Quaternary. Characteristics of all planktonic microfossil groups show that, during the Pleistocene, surface waters and intermediate water masses above the Campbell Plateau were cold. For the Miocene, the calcareous microfossils reflect alternations between warmer and colder conditions. The planktonic foraminifers and calcareous nannofossils show, in addition, a general trend toward colder planktonic faunas and floras from the early/middle Miocene to the late Miocene. For radiolarians, an opposite trend is observed: although subantarctic species are present in the lower and middle Miocene, they are lacking in the upper Miocene.

At this site, the abundance of diatoms cannot simply be related to paleoproductivity but is clearly also influenced by diagenetic processes. This is evident from the inverse correlation between diatom abundance and the abundance of the authigenically formed zeolite, clinoptilolite, in the acid-insoluble residue (Fig. F7). The sediments from the lower Miocene and uppermost Miocene are strongly affected by silica diagenesis, with the exception of sediments at ~184 mbsf core depth, which probably represent an altered tephra.

T3. Biostratigraphic events identified in Site 1120, p. 55.

F6. Age-depth curve, p. 31.

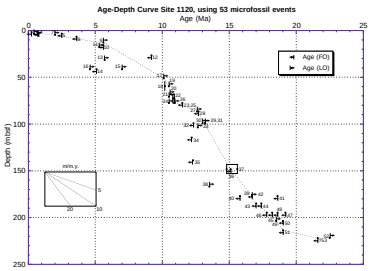

F7. Relative abundance of diatom valves, zeolite, clinoptilolite vs. core depth and age, p. 32.

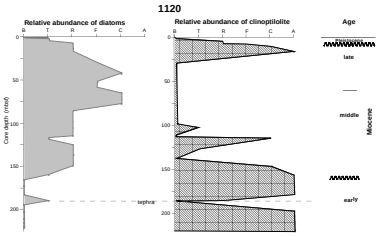

Age

The biostratigraphy of Site 1120 is largely based on the onboard study of core-catcher samples. Samples from Holes 1120A, 1120B, and 1120C were used for the uppermost part of the section, samples from Hole 1120B for the bulk of the sequence and of Hole 1120D for the lowest part. Additional samples were taken from within selected cores to address specific questions concerning age and paleoenvironment. The absolute ages assigned to biostratigraphic datums follow the references listed in the "Explanatory Notes" chapter (Tables T2, p. 59; T3, p. 60; T4, p. 63; T5, p. 64).

Calcareous Nannofossils

More than 45 nannofossil species were recognized and recorded at Site 1120 (Table T4). Nannofossils are generally well preserved, showing both cool subtropical/temperate and subantarctic assemblages.

Samples collected in the uppermost portion of the first core (from the mud-line to Sample 181-1120A-1H-2, 28–29 cm) yield very abundant and well-preserved nannofossil assemblages, characterized by abundant *Calcidiscus leptoporus, Gephyrocapsa* spp. (small), *Helicosphaera carteri, Emiliania huxleyi, Gephyrocapsa* spp. (medium), *Reticulofenestra* spp. (small), and a few *Coccolithus pelagicus,* indicating an age of latest Pleistocene (<0.24 Ma).

A drastic change in nannofossil assemblage occurs between Samples 181-1120A-1H-2, 86 cm, and 1H-3, 30–32 cm). The nannofossil assemblages from Samples 181-1120A-1H-3, 30–32 cm, to 1H-3, 130–132 cm, are characterized by the dominance of small-sized *Gephyrocapsa,* and disappearance of medium-sized *Gephyrocapsa*. In association with the presence of *Pseudoemiliania lacunosa,* this interval is correlatable to the middle Pleistocene "small *Gephyrocapsa* Zone," with an estimated age of 0.9–1.2 Ma. This drastic change in assemblage composition requires a hiatus between the depth of 2.35 and 3.3 mbsf occupying most of the upper Pleistocene (~0.25–0.9 Ma).

Late Miocene nannofossil assemblages occur from Sample 181-1120B-2H-CC downward. The assemblages are characterized by abundant *Dictyococcites antarcticus, Reticulofenestra pseudoumbilica/gelida,* medium-sized *Reticulofenestra* (~5 µm), and *Sphenolithus moriformis*. The absence of Pliocene assemblages indicates a major hiatus between 4.3 and 12.8 mbsf.

Below 12.8 mbsf to the bottom of this site (Core 181-1120D-9H, 221.86 mbsf), the nannofossil assemblages are well preserved and indicate a more or less continuous record of Miocene sediment deposition. As a result of the paucity of subtropical species (e.g., the genera *Amaurolithus* and *Discoaster*) in the upper part of this site (above Core 181-1120B-12X), the correlation to the standard nannofossil zonation is difficult. The only datum level we adopted for this upper part of the Miocene was the last occurrence of *Calcidiscus miopelagicus,* dated at 10.4 Ma (Raffi and Flores, 1995). For the intervals below 92 mbsf with more warm-water species present, 11 datum levels were recognized. The depths and ages of these datum levels are summarized in Table T5. An age-depth curve was constructed accordingly (see "Age Models and Sedimentation Rates," p. 17), which indicates that there is probably a continuous sedimentary sequence deposited between 23 and 11 Ma. However, the occurrence of the age-diagnostic species, *Sphenolithus heteromorphus* (with a range of 18.5–3.5 Ma, Raffi and Flores, 1995) in only a short interval (177–166.9 mbsf), suggests that the top of the lower Miocene and the lowest part of the middle Miocene might be missing. It is also possible that the short occurrence of this species results merely from the sporadic occurrence of this species in the subantarctic area, and we may have recorded only the acme. The hiatus, if it exists, would be short, no more than 3 m.y. duration. Assuming that there is no hiatus at ~170 mbsf (see "Age Models and Sedimentation Rates," p. 17), we calculated that the sedimentation rate of the upper and middle Miocene is ~15 m/m.y.

For the lower Miocene interval between 167 and 200 mbsf, we have recognized four bioevents, namely, the FO of *Calcidiscus premacintyrei,* the LO of *Sphenolithus dissimilis,* the FO of *Geminilithella rotula,* and the

T4. Identification and abundance of nannofossils, p. 57.

T5. Calcareous nannofossil datum levels and assigned age estimates, p. 58.

FO of *Calcidiscus leptoporus*. However, the estimated ages given by these four events are conflicting.

The age of the lowest part of the Hole 1120D is constrained by two age markers, *Ilselithina fusa* and *Discoaster druggi*. We found two specimens of *Ilselithina fusa* in Sample 181-1120D-8X-2, 138 cm, which has an estimated LO at 22.5 Ma (Gartner, 1992). On the other hand, the lowermost portion of the core, from 213.5 to 221.86 mbsf, contains *Discoaster druggi,* an early Miocene indicator with its FO at 23.2 Ma (Berggren et al., 1995). This means that the age of the lowermost part of the core (215 to 221.86 mbsf) is bracketed between 22.5 and 23.2 Ma. The sedimentation rate of the interval between 200–222 mbsf is estimated to be 5.5 m/m.y. Given the uncertain reliability of the datum levels adopted and the coarse resolution, we are not sure whether this interval is a condensed section or whether hiatuses exist.

Foraminifers

Foraminiferal assemblages are generally rich and well preserved, with planktonic forms composing ~95% of the total (Table T6). Throughout the section, the assemblages are dominated by *Globigerina* and *Globorotalia* taxa, with *Globigerinoides* and *Globoquadrina* being sporadically present in the lower half of the section.

T6. Identification and abundance of planktonic foraminifers, p. 59.

From the highest sample down to Sample 181-1120A-1H-2, 85–87 cm, *Globorotalia truncatulinoides* and abundant *Globorotalia inflata* are present. This top interval is assigned an age of no older than 0.7 Ma (late Pleistocene, Castlecliffian–Haweran Stages, Wc–Wq), based on the local age ranges of these two species in this cool region.

Samples 181-1120A-1H-3, 130–132 cm, 181-1120A-1H-CC, 181-1120B-1H-CC, 181-1120C-1H-CC, and 181-1120B-2H-4, 90–95 cm, are rich in left-coiling, encrusted *Neogloboquadrina pachyderma, Globigerina quinqueloba, G. bulloides, Globorotalia puncticuloides, G. crassaformis crassacarina,* and small 3- to 3.5-chambered *Globorotalia inflata; G. crassula* and *G. scitula* are rare. The assemblage is younger than 2.5 Ma, according to the biochronology shown in Table T3, p. 60, in the "Explanatory Notes" chapter, and is assumed to be stratigraphically below the local FO of *G. truncatulinoides,* discussed in "Foraminifers," p. 12, in the "Site 1119" chapter. The presence of *Plectofrondicularia advena, Orthomorphina jedlitschkai,* and *Haeuslerella pliocenica* (all of which became extinct during the *Stilostomella* Event) in Sample 181-1120B-2H-4, 90–95 cm, confirms that this interval is older than ~0.8 Ma. Tentatively, an age is assigned of latest Pliocene to early Pleistocene (0.8–2.5 Ma, Nukumaruan Stage, Wn).

Pliocene strata appear to be lacking, with Sample 181-1120B-2H-CC assigned a latest Miocene age (Kapitean Stage, Tk). The evidence stems from the finding of *Globorotalia margaritae evoluta,* a rather flat type, and *Neogloboquadrina dutertrei,* without *G. puncticulata* or *G. crassaformis*. Populations of the *Globorotalia miozea* lineage have forms spanning the range of *Globorotalia sphericomiozea* and *Globorotalia miotumida,* suggesting an age ~5.6 Ma (Table T2, p. 59, in the "Explanatory Notes" chapter). The benthic foraminifers include large *Haeuslerella pliocenica* (late Miocene to early Pleistocene).

Samples 181-1120C-2H-CC and 181-1120B-3H-CC have populations of *Globorotalia juanai,* which give a latest Miocene age of 5.2–6.6 Ma (Kapitean Stage, Tk). Samples 181-1120B-4H-CC to 8H-CC contain no short-ranged taxa that provide precise age estimates. The presence of common, random to left-coiling *Globorotalia miotumida* (~13.2–5.6 Ma)

is consistent with a late Miocene age inferred from foraminifer events above and below this interval. Common *Neogloboquadrina pachyderma* (common above 9.2 Ma) occur in Cores 181-1120B-3H and 4H. The last occurrence of *Rectuvigerina ongleyi* (~8 Ma), in Sample 181-1120B-3H-CC, is probably not a reliable datum as this benthic species is clearly facies controlled. Samples 181-1120B-4H-3, 35–37 cm, and 4H-3, 129–132 cm, are dominated by a high spiro-conical form of *Globorotalia* resembling *G. margaritae* (FO in New Zealand ~5.2 Ma), but having a fine pustular ornamentation on the tests (reminiscent of *G. hirsuta*) and weaker keels than typical forms. This acme is unusual in that it does not appear to have been recorded in the region previously. More study of the taxonomy of the populations in the samples is required before we can be confident of an age assignment.

Sample 181-1120B-9X-CC contains a right-coiling population of *Globorotalia miotumida* (Kaiti coiling event, 10.7–10.9 Ma), together with typical *Globorotalia panda* (LO 10.3 Ma), *Orbulina suturalis* (LO ~10.5 Ma), and rare *Globoquadrina dehiscens* (LO 9.9 Ma), indicating an early late Miocene age (10.7–10.9, early Tongaporutuan Stage). Sample 181-1120B-10X-3, 90–95 cm, again has the more usual left-coiling population of *Globorotalia miotumida.*

Samples from 181-1120B-12X-CC to 19X-CC are assigned a middle Miocene age on the basis of their planktonic foraminifers. Cores 181-1120B-12X to 17X contain *Orbulina suturalis* (FO 15.1 Ma), *Globorotalia conica, G. amuria* (LO for both 13 Ma), and common *Globorotalia praemenardii* (15.8–13.2 Ma), giving an age of 15.1–13.2 Ma (Lillburnian Stage). *Praeorbulina circularis* and *Praeorbulina glomerosa* (15.6–14.8 Ma) occur in Samples 181-1120B-17X-CC and 18X-4, 90–95 cm. No taxa of the *Orbulina* lineage occur below this level.

Samples from 181-1120B-18X, 181-1120B-19X and 181-1120D-2X-1, 50–55 cm (depth equivalent to 181-1120B-20X-1, 35 cm) are immediately below the lower/middle Miocene boundary. They contain common *Globorotalia miozea,* isolated *G. zealandica,* common *Sphaeroidinella disjuncta,* and rare *Globigerinoides trilobus;* an odd occurrence is *Dentoglobigerina altispira* s.s.; *Orbulina* lineage taxa were not observed. In New Zealand biostratigraphy, the assemblage is upper Altonian (16.7–16.3 Ma). In contrast, Sample 181-1120D-2X-6, 126–132 cm (depth approximately equivalent to 181-1120B-20X-CC) has no *G. miozea,* but contains abundant *G. praescitula* and *G. trilobus,* rare C*atapsydrax* sp., common "high-spired" "*Globoquadrina" venezuelana, Globigerina praebulloides, Globigerina woodi* s.s., but no *G. zealandica* nor *G. incognita.* This sample may be assigned to the early or middle Altonian Stage (early Miocene), presumably the latter, based on the presence of common *G. zealandica* in Sample 181-1120D-3X-CC. Thus, there is no foraminiferal evidence to support any hiatus as implied by nannofossils at this level.

The foraminiferal assemblage indicates an early Miocene age from Sample 181-1120B-20X-CC to the bottom of the section (Sample 181-1120D-9X-CC). The time ranges of the planktonic foraminifers allow us to subdivide this into three intervals. Samples 181-1120B-20X-CC to 181-1120D-4X-CC contain common *Globorotalia zealandica* (acme zone 18.5–16.7 Ma, middle Altonian Stage), *Globigerinoides trilobus* (FO ~19 Ma) and largely lack *Globoquadrina dehiscens*. The uppermost sample in this interval (181-1120B-20X-CC) contains a population with forms spanning the morphotype ranges of *Globorotalia praescitula* and *G. miozea,* indicating an age close to 16.7 Ma. Samples 181-1120D-3X-CC and 5X-CC contain small *Globorotalia praescitula* (FO 19 Ma) and

Globorotalia incognita (LO 18.5 Ma), giving an age of 19–18.5 Ma (early Altonian Stage). In all samples from 181-1120D-6X-CC and below, the planktonic assemblage is dominated by large globigerines and *Globoquadrina dehiscens*. The presence of rich populations of small *Globorotalia incognita* (FO 21.6 Ma) in Samples 181-1120D-6X-CC to 9X-CC indicates an age within the range of 21.6–19 Ma (Otaian Stage) for the bottom of the hole.

Bolboformids

Blooms of bolboformid taxa are present in lower upper Miocene samples (Cores 181-1120B-5H to 10X, Table T6). Specimen abundance is high and species diversity low. The spiny form *Bolboforma pentaspinosa* (regional time range ~7–11.5 Ma) occurs from Samples 181-1120B-5H-CC to 10X-CC. *Bolboforma subfragoris* (regional time range 10.5–11.5 Ma) occurs between Samples 181-1120B-7H-CC and 10X-CC. The ages are compatible with those from other microfossil groups.

Diatoms

Diatoms are present in the upper and middle Miocene (Table T7). Preservation is moderate to poor. As not all of the biostratigraphic marker species used for the Antarctic–subantarctic region are present, no zones were identified. But, where possible, the datums of biostratigraphically relevant species were determined. Five datums provided good age control and are in agreement with the datums from calcareous nannofossil analysis and planktonic foraminifers identified at this site. The species available for biostratigraphic age determinations were *Hemiaulus triangulus* (stratigraphic range 5.3–5.6 Ma), *Hemidiscus karstenii* f.1 (LO 5.7 Ma), and *Denticulopsis dimorpha* (10.6–12.2 Ma). Other datum levels such as the base of *H. karstenii* f. 1 could not be used, because of poor preservation of diatoms, which did not allow recognition of this species with certainty, and *Simonseniella barboi* was present but occurred too inconsistently to be useful stratigraphically.

Reworking of Paleogene diatoms was encountered in Samples 181-1120B-6H-CC, 12X-CC, 6X-CC, and 17X-CC. Some of the reworked species (e.g., *Cestodiscus reticulatus* and *Pyxilla prolongata),* have a relatively short stratigraphic range and appear to be reworked from lower Oligocene sediments.

T7. Identification and abundance of diatoms, p. 61.

Radiolarians

Radiolarian biostratigraphy at Site 1120 is based on the examination of 32 core-catcher samples and six core samples (Table T8). Radiolarian faunas are generally abundant from the top to the lower part of the section (Samples 181-1120A-1H-CC to 181-1120B-18X-CC, 0–158.5 mbsf). Although radiolarians are almost absent or very rare in the lowest section (181-1120B-19H-CC and below, 167 to 222 mbsf), two samples (181-1120B-21X-CC and 181-1120D-3X-CC) contain rare to common radiolarians that give age information.

Cyrtocapsella japonica is consistently present in varying numbers in the upper to lower part of the section (181-1120B-6H-CC to 16X-CC). *Cyrtocapsella tetrapera* occurs continuously throughout the lower half of the section from Sample 181-1120B-11X-CC to 181-1120D-3X-CC, and its occurrence represents an early to middle Miocene age.

T8. Identification and abundance of radiolarians, p. 62.

A single specimen of *Theocorythium vetulum* (LO 1.2–1.3 Ma; Alexandrovich, 1989) and abundant *Lithelius nautiloides* (FO 1.93 Ma) are present in Sample 181-1120A-1H-CC. Furthermore, the few to common occurrences of *Antarctissa denticulata, A. strelkovi, A. longa,* and of abundant *Lithelius nautiloides* in Sample 181-1120A-1H-CC give this sample an Antarctic–subantarctic character.

Samples 181-1120B-6H-CC to 8H-CC yield common to very abundant *Cyrtocapsella japonica* (LO 10.11 Ma, acme 10.2 Ma) and rare to few *Eucyrtidium calvertense,* which indicate an early late Miocene age.

Sample 181-1120B-10X-CC contains common *Cyrtocapsella japonica,* rare *Cycladophora bicornis amphora,* and few *Lithopera neotera,* together with rare *Cycladophora humerous* (LO 10.5 Ma). An evolutionary transition event from *Lithopera neotera* to *Lithopera bacca* is known to occur within the *Diartus petterssoni* Zone (RN6, 8.77–11.95 Ma, Sanfilippo and Nigrini, 1998). Although the stratigraphic marker species of the genera *Diartus* and *Didymocyrtis* are rare in this section, they indicate for Sample 181-1129B-10X-CC a late middle to early late Miocene age.

Sample 181-1120B-11X-CC yields a single specimen of *Dendrospyris megalocephalis* (FO 12.68 Ma) and abundant *Cyrtocapsella tetrapera*. Below, in Samples 181-1120B-12X-CC and 15X-CC *Cyrtocapsella tetrapera* is rare.

In Sample 181-1120B-16X-CC, very abundant *Cyrtocapsella tetrapera* (LCO 12.6 Ma) and rare *Eucyrtidium inflatum* (LO 12.3) are present, indicating a late middle Miocene age. Common to abundant *Eucyrtidium punctatum* (FO 17.02 Ma) are present in Samples 181-1120B-17X-CC, 18X-CC, and 181-1120D-3X-CC. This interval of the lower part of the section fits within the early to middle Miocene *Eucyrtidium punctatum* Zone of Lazarus (1992) and Abelmann (1992). The fauna, including *Eucyrtidium punctatum,* is characteristic of Antarctic–subantarctic waters.

Paleoenvironment

Calcareous Nannofossils

A major change in the flora occurs between Cores 181-1120B-11X and 12X (between 86.55 and 99.1 mbsf). Below this level, assemblages are more diverse, containing larger sized placoliths and helicoliths. The most conspicuous are those of *Calcidiscus premacintyrei, Cyclicargolithus floridanus,* and *Helicosphaera carteri*. Also present with more frequent occurrence is *Sphenolithus moriformis*. Above this middle Miocene (~12 Ma) change in nannofossil flora, there are virtually no discoasterids, whereas below this level discoasterids occur quite frequently. Based upon the more frequent occurrence of discoasterids and sphenoliths in the lower part of the sequence (Cores 181-1120B-15X to 181-1120D-9X, corresponding to 139–222 mbsf), we suggest that before 14 Ma, there were warmer water masses over this site than after that time. This climatic change, as indicated by the floral change, coincides well with major glaciation in Antarctica at ~14 Ma (Shackleton and Kennett, 1975; Margolis, 1975).

Foraminifers

There was insufficient time for detailed paleoenvironmental analysis of the benthic foraminiferal faunas during onboard studies. Throughout Site 1120, the samples contain rich benthic foraminiferal assemblages of rather similar overall composition, typical of middle to upper

bathyal depths, differing little from the Holocene fauna at this site. These include common *Sigmoilopsis schlumbergeri, Bolivina affiliata, Bulimina marginata, Cassidulina carinata, Ehrenbergina mestayeri, Globocassidulina subglobosa, Laevidentalina* spp., *Laticarinina altocamerata, L. pauperata, Lenticulina mammiligera, Melonis barleeanum, Oridorsalis umbonatus, Pullenia quinqueloba, P. bulloides, Planulina wuellerstorfi, Sphaeroidina bulloides, Trifarina bradyi, Uvigerina* spp., *Cibicidoides* spp., *Karreriella* spp., *Cassidulina* sp., and *Eggerella brady.*

The planktonic foraminiferal assemblages exhibit compositional differences related to near-surface paleo–water-mass temperatures. For example, the upper Miocene Sample 181-1120B-3H-CC contains a colder water mass assemblage, with dominant *Globigerina bulloides, G. umbilicata,* and *Neogloboquadrina pachyderma,* together with rare to common *Globigerina praebulloides, Globigerina woodi woodi, Orbulina universa, Globorotalia scitula, G. miotumida (*no preferential coiling), and *Paragloborotalia continuosa*. Samples 181-1120B-4H-3, 35–37 cm, and 4H-3, 129–132 cm, contain a comparable, but more temperate, water mass assemblage, with frequent *Globorotalia* cf. *margaritae* and rare *Paragloborotalia mayeri*.

Diatoms and Silica Diagenesis

Diatoms are present in Hole 1120B from 15 to ~150 mbsf core depth with varying abundance. The diatom assemblages at this site consist exclusively of planktonic diatoms with cosmopolitan species and species characteristic of the subantarctic belt. The diversity of the assemblages is low with species of the genera *Actinocyclus, Azpeitia, Coscinodiscus, Denticulopsis, Thalassionema* dominating the assemblages, and additional characteristic neritic species occurring (e.g., of the genera *Stephanopyxis, Paralia,* and *Pseudopodosira*).

At this site, the abundance of diatoms is not predominantly controlled by primary production but is strongly influenced by silica dissolution and diagenesis. This is shown by the inverse correlation between diatom abundance and the abundance of the authigenic zeolite clinoptilolite in the sediments (Fig. **F7**). This silicate is obviously formed here out of the high silica concentrations in the pore water after dissolution of siliceous microfossils. Only in one interval (Samples 181-1120B-21X-CC and 181-1120D-3X-CC) in the lower Miocene does silica diagenesis deviate in its character. This sample is practically free of zeolites, but has a few diatoms preserved in the acid-insoluble residue together with clay minerals. Because there is a well-known relation between the occurrence of tephra and siliceous microfossils, which mutually protect each other, this sediment is interpreted as an altered tephra.

Radiolarians

The early Pleistocene radiolarian fauna from the Sample 181-1120A-1H-CC, which is characterized by occurrences of southern high-latitude species (e.g., *Antarctissa strelkovi, Antarctissa denticulata, Antarctissa longa,* and *Lithelius nautiloides*), shows strong Antarctic/subantarctic affinity. Also the lower and middle Miocene faunas at Holes 1120B and 1120D from 148 to 185 mbsf (Samples 181-1120B-17X-CC to 21X-CC, and 181-1120D-3X-CC) are of Antarctic/subantarctic affinity. Whereas the radiolarians of middle and late Miocene at this site are quite unique in their species composition, they are not Antarctic/subantarctic assemblages. They rather show enhancement of cosmopolitan species,

including *Cyrtocapsella japonica,* which may allow these assemblages to be correlated with Northern Hemisphere mid-latitude faunas.

PALEOMAGNETISM

Core archive halves from Holes 1120B and 1120D were measured on the shipboard pass-through cryogenic magnetometer. Declination, inclination, and intensity of natural remanent magnetization (NRM) and 10-mT and 20-mT alternating field (AF) demagnetization steps were routinely measured at 10-cm intervals. When time permitted, some core sections were measured at 5-cm intervals. In situ Tensor tool data were collected at the APC core tops to determine azimuthal orientation of the core to 160 mbsf. The measurements, however, proved inconsistent. At least two oriented discrete samples were collected from the working half of each core interval for progressive AF and thermal demagnetization and for rock magnetic studies. Whole-core magnetic susceptibility was measured routinely on all cores using a Bartington susceptibility loop on the automated multisensor track (MST).

All cores from Site 1120 were very carbonate rich (92%–98%; see **"Lithostratigraphy,"** p. 3), susceptibility was mostly negative (diamagnetic), and NRM intensities were very weak (10^{-5} A/m on average). More than 50% of the remanence intensity was lost after demagnetization in an alternating field of 10 mT. At this level, intensities were at background levels of the pass-through cryogenic magnetometer, and the signal was too noisy and random to reliably ascertain polarity. Susceptibility and NRM intensity values were much higher in the upper 1–3 m of each core interval (NRM ranged as high as 10^{-1} A/m and susceptibility up to 10^{-3} SI; Fig. **F8**). Such a signal is clearly an artifact of drilling as paleomagnetic inclination and declination values do not show any less scatter within these intervals of increased intensity. Thermal demagnetization of selected discrete specimens demonstrates a small component of magnetization (<20%) that persists above 600°C, indicating hematite (Fig. **F9**). The most plausible explanation is that the signal is from rust contamination from the drill pipe. As each new core barrel is lowered (in the case of APC) or dropped (in the case of XCB) rust may be knocked from the drill pipe walls and accumulate at the sediment interface before each core is taken. It is also possible that the rust is suspended in the water column and injected into the sediment during coring and retained in any water between the core and coreliner. This would also explain increased intensities in intervals where the sediment was more fluid and included more drilling water (e.g., 212.0–213.5 mbsf; Fig. **F8**). This effect is more pronounced in XCB cores than in APC cores, as might be expected from dropping of the core barrel as opposed to lowering. Unfortunately, susceptibility values also show increases into positive values in the upper 1–3 m of each core interval, reflecting the increase in hematite. Smaller changes in susceptibility throughout the core may also reflect smaller amounts of disseminated hematite, and susceptibility values should be treated with caution when used for correlation. The reason that this effect was not seen at Site 1119 may be because of the very low intensity and susceptibility values, but also because the inside of the drill-stem was not cleaned before drilling at Site 1120, but it was at Site 1119.

Intensity of magnetization was too weak to investigate demagnetization behavior of discrete samples directly. Therefore, samples were first saturated with an isothermal remanent magnetization (IRM) and back-

F8. Whole-core magnetic susceptibility and NRM intensity, **p. 33.**

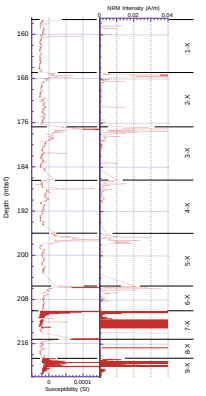

F9. Normalized intensity of magnetization, **p. 34.**

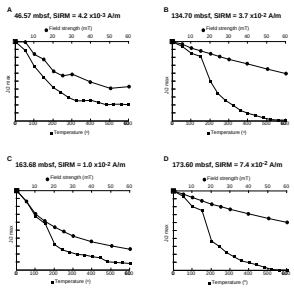

field IRM, and the IRM then demagnetized using first AF and then thermal methods. Typical IRM acquisition curves are shown in Figure F10. When saturation and backfield saturation values are compared, saturation was not reached by 600 mT for any sample measured, and mostly saturation was not reached by 1000 mT for many of the samples. Coercivity of remanence (B_{cr}) values were between 25 and 125 mT. Saturation values are low (10^{-3} 10^{-4} A/m), probably because of very low concentrations of magnetic minerals. AF demagnetization was not very effective in removing the saturation IRM (SIRM) and, in most cases, >50% of the remanence remained above 60 mT. Thermal demagnetization was more effective in removing the applied SIRM: in most cases 80% of remanence was lost by 300°C of heating, 90% by 400°C of heating, and all remanence was lost by 500°C (e.g., Figs. F9B, F9D). In many cases 20%–30% of remanence was lost in a single step between 150°C and 200°C (Fig. F9). The majority of the behavior described above suggests that the main carrier of remanence is a ferrimagnetic iron sulfide mineral present in very low concentrations, although characteristically different than at Site 1119. Site 1120 contained large pyrite nodules, and greigite was identified infilling foraminifer tests in smear slides ("Site 1120 Smear Slides," p.37) (distinguished from other sulfides by its gray nonmetallic luster in reflected light). Roberts and Turner (1993) also reported high SIRM values (900–1000 mT) for greigite samples from Upton Brook in New Zealand.

F10. IRM and backfield acquisition curves, p. 35.

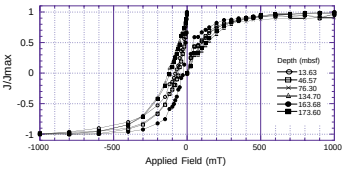

COMPOSITE DEPTHS

A composite section for Site 1120 was constructed using data from Holes 1120B, 1120C, and 1120D. Holes 1120B and 1120C yielded overlapping records for the upper ~52 mcd, although at least one gap in continuity exists in the composite record for this interval. Sediment composition at this site limited APC recovery to the upper ~50 m, thus the double-cored upper interval is relatively short. Holes 1120B and 1120D displayed some overlap between ~158 and 185 mcd, as planned by the drilling strategy at Hole 1120D. Four high-resolution data sets proved useful for correlation at this site: magnetic susceptibility (MS), natural gamma-ray intensity (NGR), and gamma-ray attenuation porosity evaluator (GRAPE), all measured on whole cores on the MST, and spectral reflectance at 550 nm (the center wavelength of the range measured), measured on split cores. Variations in all of these parameters decreased in amplitude downhole, yielding the best correlations in the upper section.

All four data sets defined the composite section from 0–52 mcd (Fig. F11). Low recovery in Core 181-1120B-3H (4.9 m) produced a break in continuity of the recovered section between Cores 181-1120B-3H and 181-1120C-3H (Fig. F11). Another gap may exist between Cores 181-1120B-4H and 181-1120C-4H, although we show an overlap between these two cores. This correlation, based on magnetic susceptibility records, includes only a small number of points, and may be suspect. The small section of overlap between Holes 1120B and 1120D from ~158 to 185 mcd also includes gaps between Cores 181-1120B-19X and 181-1120D-2X and between Cores 181-1120D-2X and 181-1120B-21X.

Downhole core offsets relative to mbsf depths roughly follow a model of 10% stretch between the mbsf and mcd depth scales in the upper section. Where gaps exist in the record, we assigned the top of the deeper core in one hole an mcd value equal to that at the base of

F11. Composite sections, p. 36.

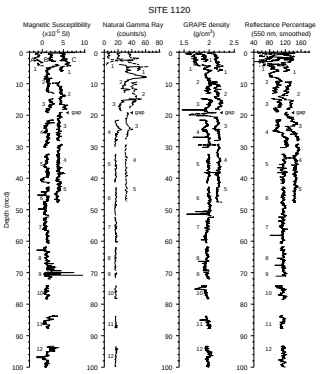

the overlying core in the other hole. Such an artificial closure of the gap between Cores 181-1120B-3H and 181-1120C-3H produced a shift in offsets for Cores 181-1120B-4H through 6H, although these cores follow a trend parallel to the ten-percent-stretch model (Fig. F12). Offsets for sections deeper than 50 mbsf are merely cumulative from cores above, producing a vertical trend in Fig. F12. Table T9 (also in ASCII format) contains the offsets between the mbsf and mcd scales resulting from composite section construction.

The spliced record, based primarily on GRAPE and reflectance data (Fig. F13), extends to 52 mcd. Wherever possible, splice tie points (Table T10, also in ASCII format) were picked at well-defined maxima or minima where the overlap in data from Holes 1120B and 1120C are correlated. Typically, parameter values differed by less than 10% at tie levels. In all cases, ties were selected so that the spliced record was as free from noise (high-frequency variability) as possible.

AGE MODELS AND SEDIMENTATION RATES

The combined nannofossil, foraminifer, diatom, and radiolarian biostratigraphy at Site 1120 yielded 53 event levels with age significance, using the shipboard stratigraphic framework (see "Time Scale," p. 11, in the "Explanatory Notes" chapter). The levels are shown in Table T11 and consist of 24 first occurrence (FO) events; eight acme, first common occurrence (FCO), or last common occurrence (LCO) events, and 21 last occurrence (LO) events. FO events may have been estimated to be too shallow, based on limited sampling. The position of arrows in Figure F6 reflects the possibility that further work may extend these datums downhole. Last occurrence events may have been estimated to be too deep, again as a result of the limited sampling interval. The position of arrows in Figure F6 reflects the possibility that further work may extend these datums uphole. The more reliable events, from the point of view of stratigraphic range established at the site and for the age depth plot (Figure F6) are listed in Table T11. The dashed line in Figure F6 shows the preferred age depth model using subjective weighting for areas where different events appear inconsistent.

Biostratigraphic control varies downcore. Three intervals (0–13, 51–100, and 175–215 mbsf) have particularly abundant occurrence datums in good agreement and these form the major control for the age depth correlation shown in Figure F6. The interval between 13 and 51 mbsf is poorly constrained. The two radiolarian datums FO *Prunopyle titan* (14) and LO *Helotholus praevema* (16) and the LO of the diatom *Hemidiscus karstenii* (13) appear to be older than expected (see "Time Scale," p. 11, in the "Explanatory Notes" chapter). The interval between 100 and 175 mbsf also has only a few apparently conflicting occurrence datums. The preferred line of correlation is constrained by the range of *Praeorbulina circularis (37)* and the FO of *Orbulina saturalis* (36). The FO of the diatom *Denticulopsis dimorpha* (34) and the radiolarian *Eucyrtidium inflatum* (35) are not considered reliable and may well be older than expected (see "Time Scale," p. 11, in the "Explanatory Notes" chapter). The LO of the nannofossil *Sphenolithus heteromorphus* (38) and the FO of the foraminifer *Globorotalia praemenardii* requires further scrutiny. Other bioevents that deviate from the best-fit line in Figure F6 may be a result of incomplete local range at Site 1120. These also require more scrutiny.

Summarizing the data and taking into account the above uncertainties, we conclude that average sedimentation took place in two major

F12. Downhole depth offsets, p. 38.

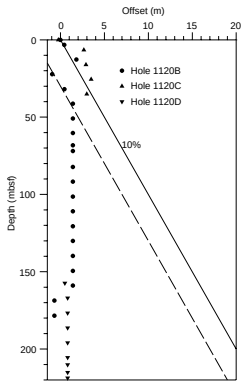

T9. Composite depth section, Site 1120, p. 66.

F13. Spliced record for Site 1120, p. 39.

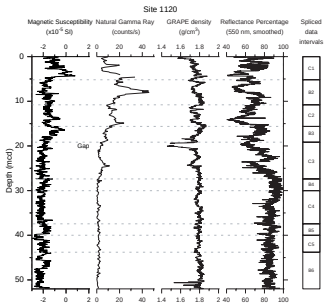

T10. Splice tie points, Site 1120, p. 70.

T11. Reliable biostratigraphic events, p. 71.

steps with a relatively rapid rate of ~20 m/m.y. from early to late Miocene and a slower sedimentation rate (~5 m/m.y.) from the late Miocene to present. Sedimentation rate values are simplified in Table T12. Bearing in mind that this sequence averages 94% $CaCO_3$, fluctuations in sedimentation rate are not attributable to tectonics and terrigenous sediment dilution or starvation. The variation is most likely a result of variation in productivity and the current strengths of AAIW. The relatively shallow depth of the site also means that dissolution is unlikely to have played a role in the fluctuations. The major change is the decline in sedimentation rate at ~10 Ma for which further work must find an explanation. It may well be related to growth of the Antarctic ice sheet and possible development of a vigorous AAIW circulation across the plateau.

T12. Age/sedimentation rate data, p. 72.

INORGANIC GEOCHEMISTRY

Interstitial Waters

Three interstitial-water samples were collected from each core from the upper 50 mbsf at Site 1120. Below this depth one sample per core was taken down to 100 mbsf and one from every third core between 100 mbsf and the total depth. In total, 27 interstitial-water samples were obtained at this site, 24 from Hole 1120B at depths ranging from 1.45 to 164.90 mbsf, and three from Hole 1120D between 163.30 and 211.50 mbsf. Analytical results are summarized in Table T13 (also in ASCII format) and the depth profiles of geochemical constituents are plotted in Figure F14.

T13. Interstitial-water geochemistry results, p. 73.

Salinity, Chloride, pH, and Sodium

Salinities of the interstitial-water samples vary slightly between 34.0 and 35.0 (Fig. F14). The topmost sample has the lowest value (34.0). The salinity remains constant throughout the hole, except for the uppermost samples and elevated values between 69.70 and 97.70 mbsf.

Chloride (Cl^-) concentrations increase gradually with depth (Fig. F14), except for the uppermost 26.65 m, where concentrations are almost constant. Below 26.65 m, there is a rapid increase in concentration from 550 to 555 mM, and then the concentration shows a steadily increasing trend with depth, reaching a maximum of 564 mM at 163.3 mbsf.

interstitial-water pH values vary from 7.17 to 7.83. Two extremely low values, of 7.02 at 45.70 mbsf and 6.90 at 102.80 mbsf, may be analytical errors considering that no significant lithologic change occurs (see "Lithostratigraphy," p. 3). The highest pH lies between 40 and 50 mbsf, below which it decreases with depth to 7.3 at the bottom of the hole.

Concentrations of sodium (Na^+) vary within a small range from 463 to 475 mM, generally following the salinity trend.

F14. Depth profiles of interstitial-water constituents, p. 40.

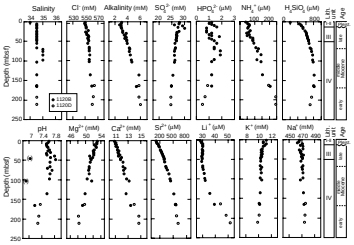

Alkalinity, Sulfate, Phosphate, Ammonium, and Dissolved Silica

The alkalinity increase from 2.99 mM at 1.45 mbsf to 5.96 mM at 211.5 mbsf is sharply different than Site 1119 (see "Inorganic Geochemistry," p. 18). The principal reasons for this trend are the lack

of active sulfate reduction throughout the profile and the influence of the diagenetic dissolution of carbonate sediments.

The profile of sulfate (SO_4^{2-}) concentration is inversely correlated with the alkalinity profile (Fig. F14). Below 23 mbsf, the sulfate concentration decreases slightly from 27.0 mM to 24.7 mM, which may be, together with the increase in alkalinity and ammonium, indicative of sulfate reduction. However, because of the low organic carbon content, there may be another contribution to the alkalinity increase, such as bicarbonate ion (HCO_3^-) from the dissolution of carbonate-rich sediments (see "Organic Geochemistry," p. 20).

The phosphate (HPO_4^{2-}) concentrations scatter considerably. Concentrations are below 2.0 µM in the upper part of the core, down to 69.70 mbsf (Fig. F14). The concentrations decrease slightly down to the bottom, below a maximum of 1.9 µM at 75–85 mbsf. The concentration of HPO_4^{2-} is possibly controlled by the oxidation of organic matter, the formation or dissolution of carbonate fluorapitite (CFA), and absorption reactions of $CaCO_3$. The decreasing trend in the lower part of the hole may be caused by the incorporation of phosphate into the reprecipitated carbonate.

Ammonium (NH_{4+}) concentrations are low in the upper 40 m of the hole and increase steadily with depth from 68 µM at 39.20 mbsf to 242 µM at 211.50 mbsf (Fig. F14). In general, ammonium, a by-product of organic matter degradation, increases systematically with decreasing sulfate (Gieskes, 1981).

Dissolved silica (H_4SiO_4) concentrations increase continuously from a value of 203 µM at 1.45 mbsf to 819 µM at 164.90 mbsf. The decrease in H_4SiO_4 in the bottom of Hole 1120D (Fig. F14) may be caused by a compositional change in the sediments. The silica concentration is controlled by the diffusion process of diagenetic dissolution of biogenic silica in the sediments.

Calcium, Magnesium, and Strontium

Calcium (Ca^{2+}) concentrations increase steadily from 10.8 mM at 1.45 mbsf to 14.7 mM at the bottom of the hole (Fig. F14). This increase is attributed to the dissolution of carbonate-rich sediments in the interstitial waters throughout the hole (see "Lithostratigraphy," p. 3). This dissolution effect is opposite to the magnesium profile and similar to the strontium concentration.

The profiles of magnesium (Mg^{2+}) concentrations are the mirror image of the calcium concentration profiles (Fig. F14). There is a gradual decrease of the Mg^{2+} concentration downhole, which can be explained by reactions that remove Mg^{2+} diagenetically from solution.

Dissolved strontium (Sr^{2+}) concentrations exhibit a similar pattern to calcium (Fig. F14). Strontium concentrations increase from 106 µM at 1.45 mbsf to 607 µM at 211.50 mbsf. The Sr^{2+} is supplied to pore fluids by the dissolution and recrystallization of carbonate to diagenetic low-Mg calcite. The variations of Sr^{2+} and Ca^{2+} concentrations at this site depend mainly on the lithologic characteristics (see "Lithostratigraphy," p. 3).

Potassium and Lithium

Potassium (K^+) concentrations are low (<11.2 mM), and show a slight decrease from the top to the bottom of the hole (Fig. F14). The low K^+

concentration is caused by the sediment properties (carbonate rich and organic-matter poor) because the K^+ concentration is partly controlled by the oxidation of organic matter (see "Organic Geochemistry," p. 20). Overall, changes in the Na^+ and K^+ gradients are similar and appear to be influenced primarily by depth.

The dissolved lithium (Li^+) remains almost constant above 75.50 mbsf, below which the concentration starts to increase, reaching 52 µM by 211.50 mbsf (Fig. F14). The Li^+ concentration depends on release of the element into the pore water from the sediments during recrystallization of biogenic carbonate. In addition, another source of Li^+ may be the occurrence of early diagenesis of opal-A (Gieskes, 1983).

Summary of Interstitial-Water Results

The biogenic sediments are the primary influence on many of the chemical gradients in the interstitial waters at Site 1120. The profiles of interstitial-water constituents at this site, controlled by simple diffusion diagenetic processes, show gradually increasing (alkalinity, H_4SiO_4, Cl^-, Ca^{2+}, Sr^{2+}, Li^+) and decreasing (K^+, Mg^{2+}) trends with depth and no signature of sulfate reduction. Such characteristics result from the uniform lithologic (calcareous dominated) features throughout the hole. The dominant chemical reactions are probably dissolution of carbonate, silica diagenesis, precipitation of low-Mg calcite, and possibly ion-exchange reactions in clay minerals.

ORGANIC GEOCHEMISTRY

Volatile Hydrocarbons

As part of the shipboard safety and pollution-prevention monitoring program, hydrocarbon gases were analyzed in each core of Holes 1120B and 1120D by the headspace technique. Methane and higher hydrocarbons could only be recognized in trace concentrations (<100 ppm). These low methane concentrations indicate only small bacterial postdepositional activity because of the lack of organic matter in the sediment. This result is corroborated by almost constant sulfate concentrations in the pore water throughout the hole (see "Inorganic Geochemistry," p. 18).

Carbonate and Organic Carbon

The abundance of total, inorganic, and organic carbon and of calcium carbonate in sediments from Holes 1120B and 1120D is summarized in Table T14 (also in ASCII format). Random sampling of all lithologies was performed for carbonate analysis. Organic-carbon measurements were conducted on only five samples because of the obviously low organic-carbon contents indicated by the light sediment color.

Carbonate contents are high throughout the section and range from 84.5 to 98.7 wt% (Fig. F15). These values strongly indicate carbonate-dominated sedimentation with a low supply of terrigenous clastic material. The lowest carbonate values were measured in the three uppermost samples (181-1120B-1H-1, 28–29 cm, 1H-1, 54–55 cm, and 1H-2, 84–85 cm).

T14. Organic chemistry data, p. 74.

F15. Carbonate contents in sediments, p. 41.

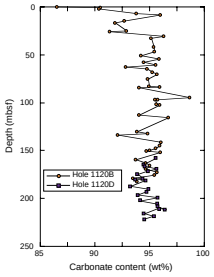

Organic-carbon contents in the five samples analyzed are low (<0.41%), suggesting the respiration of most of the organic matter occurred during settling through the water column and during early diagenesis caused by an oxic water column and low sedimentation rates.

PHYSICAL PROPERTIES

Index Properties

Index properties measurements were made at a resolution of one sample for every two sections in the cores from Holes 1120B and 1120D. Index properties were determined by a gravimetric method (see "Physical Properties," p. 24, in the "Explanatory Notes" chapter). Values of measured index properties (void ratio, porosity, water content, bulk density, and grain density) are presented in Table T15 (also in ASCII format). The properties show little variation downcore, indicating a relatively homogeneous section (Fig. F16). There was good correlation in an overlapping section between the deeper part of the core in Hole 1120B and the upper part of the core in Hole 1120D.

T15. List of index properties measurements, p. 76.

F16. Index properties measurements, p. 42.

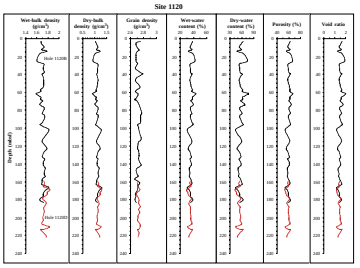

Multisensor Track Measurements

The shipboard physical properties program at Site 1120 included nondestructive measurements of bulk density, magnetic susceptibility, natural gamma-ray activity, and *P*-wave velocity on whole sections of all cores using the multisensor track (MST) (Fig. F17). Magnetic susceptibility was measured at 4-cm intervals and at high sensitivity (4-s measurement time) in all Site 1120 holes. Magnetic susceptibility is generally low but has occasional anomalously high values, especially in the deeper sections of the core. Natural gamma-ray activity was measured with a 15-s count every 14 cm in Holes 1120A, 1120B, 1120C, and 1120D. There is little variation downcore except in the upper part of the core (<15 mbsf), where high-amplitude fluctuations occurred. Gamma-ray attenuation porosity evaluator bulk density measurements were made at 4-cm intervals at all Site 1120 holes. The GRAPE bulk density measurements in Hole 1120D show a zone ~2 m thick that has significantly lower density values. Data from Hole 1120D correlate well with data from Hole 1120B and give indications of the nature of the unrecovered core (~17 to 22 mbsf) in Hole 1120B (Fig. F18) (see also "Composite Depths," p. 16). The zone of low-density sediment suggests that the lack of recovery in Hole 1120B may have been a result of unconsolidated sediment that was not retained by the core catcher.

The *P*-wave velocity measurements (PWL) were made at 4-cm intervals for Holes 1120A, 1120B (Cores 1H–7H), and 1120C but gave poor results.

F17. MST measurements, p. 43.

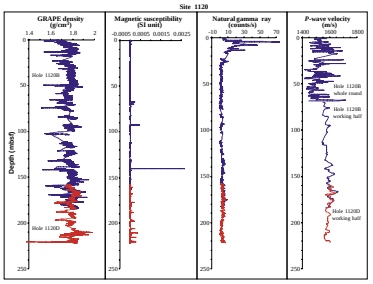

F18. GRAPE density measurements, p. 44.

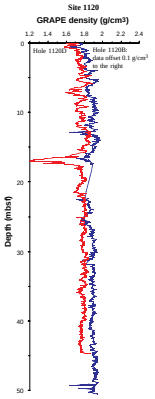

Shear Strength

Measurements of shear strength, using a mechanical vane, were made on split cores from Hole 1120B (Fig. F19). Samples were generally taken in fine-grained sediments at a resolution of one per section from Hole 1120B. Shear-strength measurements were taken using the Torvane method on cores from Hole 1120C at a resolution of one for every other section. No samples were taken from the XCB cores. Values are generally low with a range of near 0 to 25 kPa, indicating predomi-

nantly unconsolidated sediments. Shear-strength values obtained from the Torvane method correlate well with those from the vane shear test.

Compressional-Wave Velocity

Compressional-wave velocity was measured parallel to the core axis on split cores from Holes 1120B and 1120D using the digital sound velocimeter system. These measurements gave better results than the MST. There was good correlation of the values between the lower portion of Hole 1120B and the upper portion of Hole 1120D, indicating ~30 m of overlapping section. *P*-wave velocities range from 1540 to 1640 m/s.

Thermal Conductivity

Only one downhole temperature measurement was taken with the Adara temperature tool at the position of Core 181-1120B-6H, and temperature values were measured at two points in the coring process: the mudline and 45.9 mbsf (Fig. **F20**). At 45.9 mbsf, the Adara temperature tool measured a value that reached 17.5°C just after penetration because of the effect of frictional heat production; in the same location, and at near equilibrium with the in-situ sediments, it recorded 6.6°C just before pulling out. Thermal conductivity was measured in the shipboard laboratory on the same core where the Adara temperature tool was used; four measurements were made per core. The Adara temperature tool yielded good quality data; the results for Core 181-1120B-6H indicated a temperature of 8.877°C ± 0.18°C at 45.9 mbsf, and 6.244°C ± 0.02°C at the mudline, based on temperature equilibration curves. A thermal gradient of 5.74°C/100 m was then calculated from the two measurements. Using an average thermal conductivity of 1.29 W/(m·K) in Core 181-1120B-6H, heat flow was estimated to be 0.074 W/m^2. The thermal gradient and the estimated heat-flow value are similar to those determined from sediments recovered from the Weddell Sea (Barker, Kennett, et al., 1988), consistent with a similar age for the crust underneath both locations. However, the values were only determined from one Adara temperature profile and should be used with caution.

F19. Shear strength measurements, p. 45.

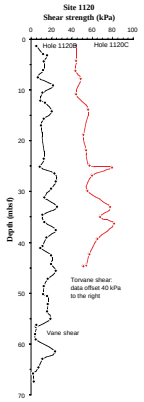

F20. Temperature measurements, p. 46.

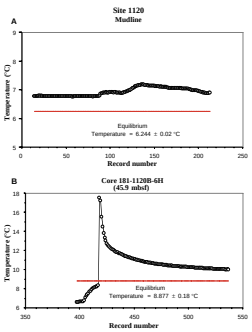

REFERENCES

Abelmann, A., 1992. Early to middle Miocene radiolarian stratigraphy of the Kerguelen Plateau, Leg 120. *In* Wise, S.W., Jr., Schlich, R., et al., *Proc. ODP, Sci. Results,* 120: College Station, TX (Ocean Drilling Program), 757–783.

Alexandrovich, J.M., 1989. Radiolarian biostratigraphy of ODP Leg 111, Site 677, eastern equatorial Pacific, late Miocene through Pleistocene. *In* Becker, K., Sakai, H., et al., *Proc. ODP, Sci. Results,* 111: College Station, TX (Ocean Drilling Program), 245–262.

Backman, J., and Raffi, I., 1997. Calibration of Miocene nannofossil events to orbitally tuned cyclostratigraphies from Ceara Rise. *In* Shackleton, N.J., Curry, W.B., Richter, C., and Bralower, T.J. (Eds.), *Proc. ODP, Sci. Results,* 154: College Station, TX (Ocean Drilling Program), 83–99.

Backman, J., Schneider, D.A., Rio, D., and Okada, H., 1990. Neogene low-latitude magnetostratigraphy from Site 710 and revised age estimates of Miocene nannofossil datum events. *In* Duncan, R.A., Backman, J., Peterson, L.C., et al., *Proc. ODP, Sci. Results,* 115: College Station, TX (Ocean Drilling Program), 271–276.

Beggs, J.M., 1978. Geology of the metamorphic basement and late Cretaceous to Oligocene sedimentary sequence of Campbell Island, Southwest Pacific Ocean. *R. Soc. N. Z. J.,* 8:161–177.

Benson, W.N., 1969. Geological map of Dunedin district, explanatory notes [1:50,000]. *N. Z. DSIR, Wellington.*

Berggren, W.A., Kent, D.V., Swisher, C.C., III, and Aubry, M.-P., 1995. A revised Cenozoic geochronology and chronostratigraphy. *In* Berggren, W.A., Kent, D.V., Aubry, M.-P., and Hardenbol, J. (Eds.), *Geochronology, Time Scales and Global Stratigraphic Correlation*. Spec. Publ.—Soc. Econ. Paleontol. Mineral. (Soc. Sediment. Geol.), 54:129–212.

Carter, L., Carter, R.M., McCave, I.N., and Gamble, J., 1996a. Regional sediment recycling in the abyssal Southwest Pacific Ocean. *Geology,* 24:735–738.

Carter, R.M., 1988. Post-breakup stratigraphy of the Kaikoura Synthem (Cretaceous–Cenozoic), continental margin, southeastern New Zealand. *N. Z. J. Geol. Geophys.,* 31:405–429.

Carter, R.M., Carter, L., and McCave, I.N., 1996b. Current controlled sediment deposition from the shelf to the deep ocean: the Cenozoic evolution of circulation through the SW Pacific gateway. *Geol. Rundsch.,* 85:438–451.

Davey, F.J., 1977. Marine seismic measurements in the New Zealand region. *N. Z. J. Geol. Geophys.,* 20:719–777.

Field, B.D., and Browne, G.H., 1989. *Cretaceous and Cenozoic Sedimentary Basins and Geological Evolution of Canterbury Region, South Island, New Zealand*. N. Z. Geol. Surv., Basin Stud., 2.

Gartner, S., 1992. Miocene nannofossil chronology in the North Atlantic, DSDP Site 608. *Mar. Micropaleontol.,* 18:307–331.

Gieskes, J.M., 1981. Deep-sea drilling interstitial water studies: implications for chemical alteration of the oceanic crust, layers I and II. *In* Warme, J.E., Douglas, R.G., and Winterer, E.L. (Eds.), *The Deep Sea Drilling Project: A Decade of Progress*. Spec. Publ.—Soc. Econ. Paleontol. Mineral., 32:149–167.

————, 1983. The chemistry of interstitial waters of deep-sea sediments: interpretation of deep-sea drilling data. *In* Riley, J.P., and Chester, R. (Eds.), *Chemical Oceanography* (Vol. 8): London (Academic), 221–269.

Griggs, G.B., Carter, L., Kennett, J.P., and Carter, R.M., 1983. Late Quaternary marine stratigraphy southeast of New Zealand. *Bull. Geol. Soc. Am.,* 94:791–797.

Hesse, P.P., 1994. The record of continental dust from Australia in Tasman Sea sediments. *Quat. Sci. Rev.,* 13:257–272.

Kennett, J.P., Houtz, R.E., et al., 1975. *Init. Repts. DSDP,* 29: Washington (U.S. Govt. Printing Office).

Lawver, L.A., Gahagan, L.M., and Coffin, M.F., 1992. The development of paleoseaways around Antarctica. *In* Kennett, J.P., and Warnke, D.A. (Eds.), *The Antarctic Paleoenvironment: a Perspective on Global Change (Pt. 1).* Am. Geophys. Union, Antarct. Res. Ser., 56:7–30.

Lazarus, D., 1992. Antarctic Neogene radiolarians from the Kerguelen Plateau, Legs 119 and 120. *In* Wise, S.W., Jr., Schlich, R., et al., *Proc. ODP, Sci. Results,* 120: College Station, TX (Ocean Drilling Program), 785–809.

Margolis, S.V., 1975. Paleoglacial history of Antarctica inferred from analysis of Leg 29 sediments by scanning-electron microscopy. *In* Kennett, J.P., Houtz, R.E., et al., *Init. Repts. DSDP,* 29: Washington (U.S. Govt. Printing Office), 1039–1043.

Molnar, P., Atwater, T., Mammerickx, J., and Smith, S., 1975. Magnetic anomalies, bathymetry and the tectonic evolution of the South Pacific since the Late Cretaceous. *Geophys. J. R. Astron. Soc.,* 40:383–420.

Naish, T., Abbott, S., Alloway, B., Beu, A., Carter, R., Edwards, A., Journeaux, T., Kamp, P., Pillans, B., Saul, G., and Woolfe, K., 1998. Astronomical calibration of a southern hemisphere Plio-Pleistocene reference section, Wanganui Basin. *N. Z. Quat. Sci. Rev.,* 17:695–710.

Neil, H.L., 1998. Late Quaternary variability of surface and deep water masses, Chatham Rise, SW Pacific [Ph.D. thesis]. Univ. of Waikato, Hamilton, New Zealand.

Nelson, C.S., Hendy, C.H., Cuthbertson, A.M., and Jarrett, G.R., 1986. Late Quaternary carbonate and isotope stratigraphy, subantarctic Site 594, Southwest Pacific. *In* Kennett, J.P., von der Borch, C.C., et al., *Init. Repts. DSDP,* 90: Washington (U.S. Govt. Printing Office), 1425–1436.

Raffi, I., and Flores, J.-A., 1995. Pleistocene through Miocene calcareous nannofossils from eastern equatorial Pacific Ocean. *In* Pisias, N.G., Mayer, L.A., Janecek, T.R., Palmer-Julson, A., and van Andel, T.H. (Eds.), *Proc. ODP, Sci. Results,* 138: College Station, TX (Ocean Drilling Program), 233–286.

Roberts, A.P., and Turner, G.M., 1993. Diagenetic formation of ferrimagnetic iron sulphide minerals in rapidly deposited marine sediments, South Island, New Zealand. *Earth Planet. Sci. Lett.,* 115:257–273.

Sanfilippo, A., and Nigrini, C., 1998. Code numbers for Cenozoic low latitude radiolarian biostratigraphic zones and GPTS conversion tables. *Mar. Micropaleontol.,* 33:109–156.

Sato, T., and Kameo, K., 1996. Pliocene to Quaternary calcareous nannofossil biostratigraphy of the Arctic Ocean, with reference to late Pliocene glaciation. *In* Thiede, J., Myhre, A.M., Firth, J.V., Johnson, G.L., and Ruddiman, W.F. (Eds.), *Proc. ODP, Sci. Results,* 151: College Station, TX (Ocean Drilling Program), 39–59.

Scott, G.H., 1995. Coiling excursions in *Globorotalia miotumida*: high resolution bioevents at the middle-upper Miocene boundary in southern temperate water masses? *Inst. Geol. Nucl. Sci.,* 443:299–308.

Shackleton, N.J., and Kennett, J.P., 1975. Paleotemperature history of the Cenozoic and the initiation of Antarctic glaciation: oxygen and carbon isotope analyses in DSDP Sites 277, 279, and 281. *In* Kennett, J.P., Houtz, R.E., et al., *Init. Repts. DSDP,* 29: Washington (U.S. Govt. Printing Office), 743–755.

Stewart, R.B., and Neall, V.E., 1984. Chronology of palaeoclimatic change at the end of the last glaciation. *Nature,* 311:47–48.

Summerhayes, C.P., 1969. Marine geology of the New Zealand subantarctic sea floor. *Mem.—N. Z. Oceanogr. Inst.,* 50:1–92.

Thiede, J., 1979. Wind regimes over the late Quaternary Southwest Pacific Ocean. *Geology,* 7:259–262.

Weaver, P.P.E., Carter, L., and Neil, H., 1998. Response of surface watermasses and circulation to late Quaternary climate change, east of New Zealand. *Paleoceanography,* 13:70–83.

Young, J.R., Flores, J.-A., and Wei, W., 1994. A summary chart of Neogene nannofossil magnetobiostratigraphy. *J. Nannoplankton Res.,* 16:21–27.

Figure F1. Locality map of Site 1120, showing location of seismic line NIWA 3034 of Figure F2, p. 26.

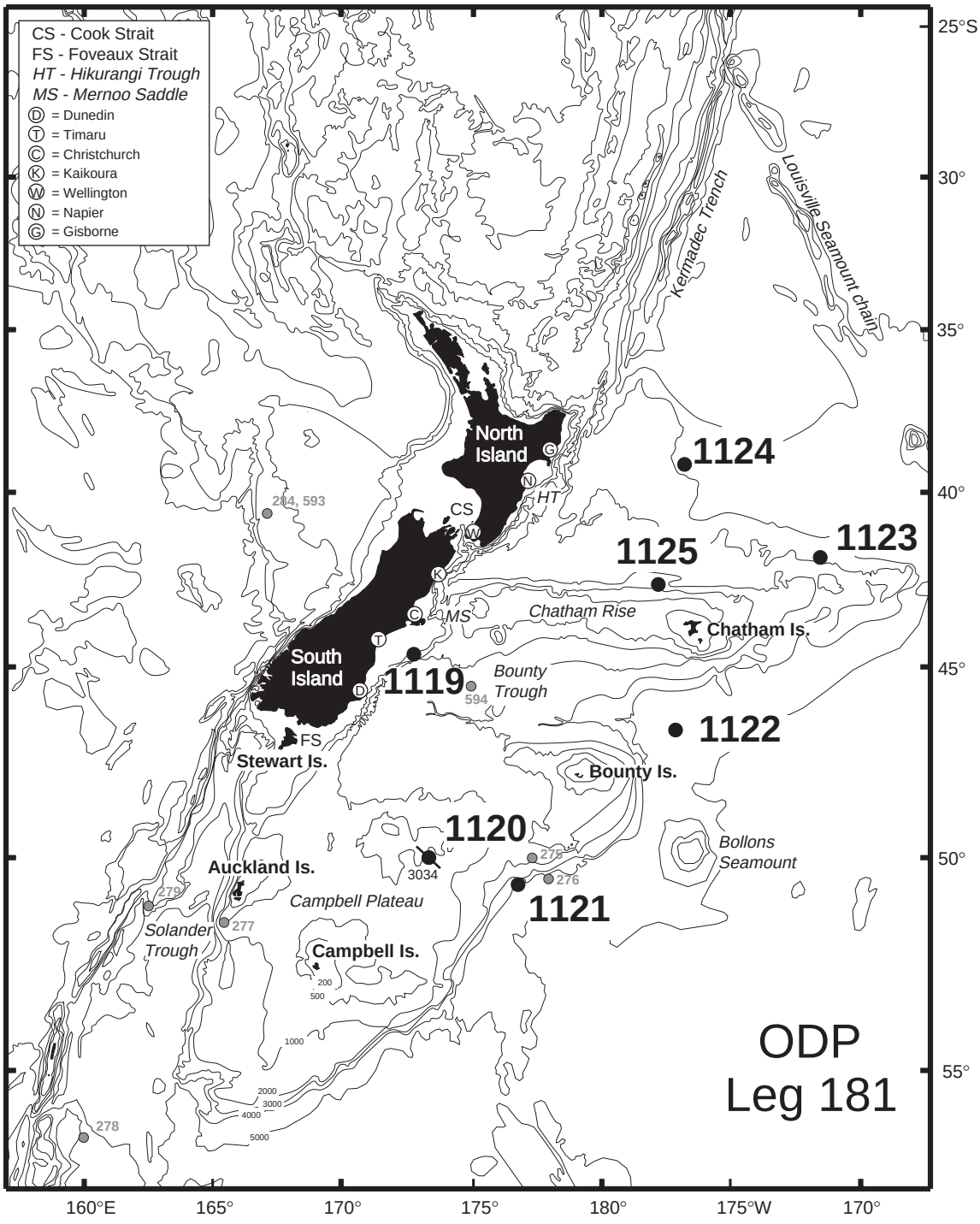

Figure F2. Portion of seismic line NIWA 3034 through Site 1120 (0130–0300 hr, 13 February 1997).

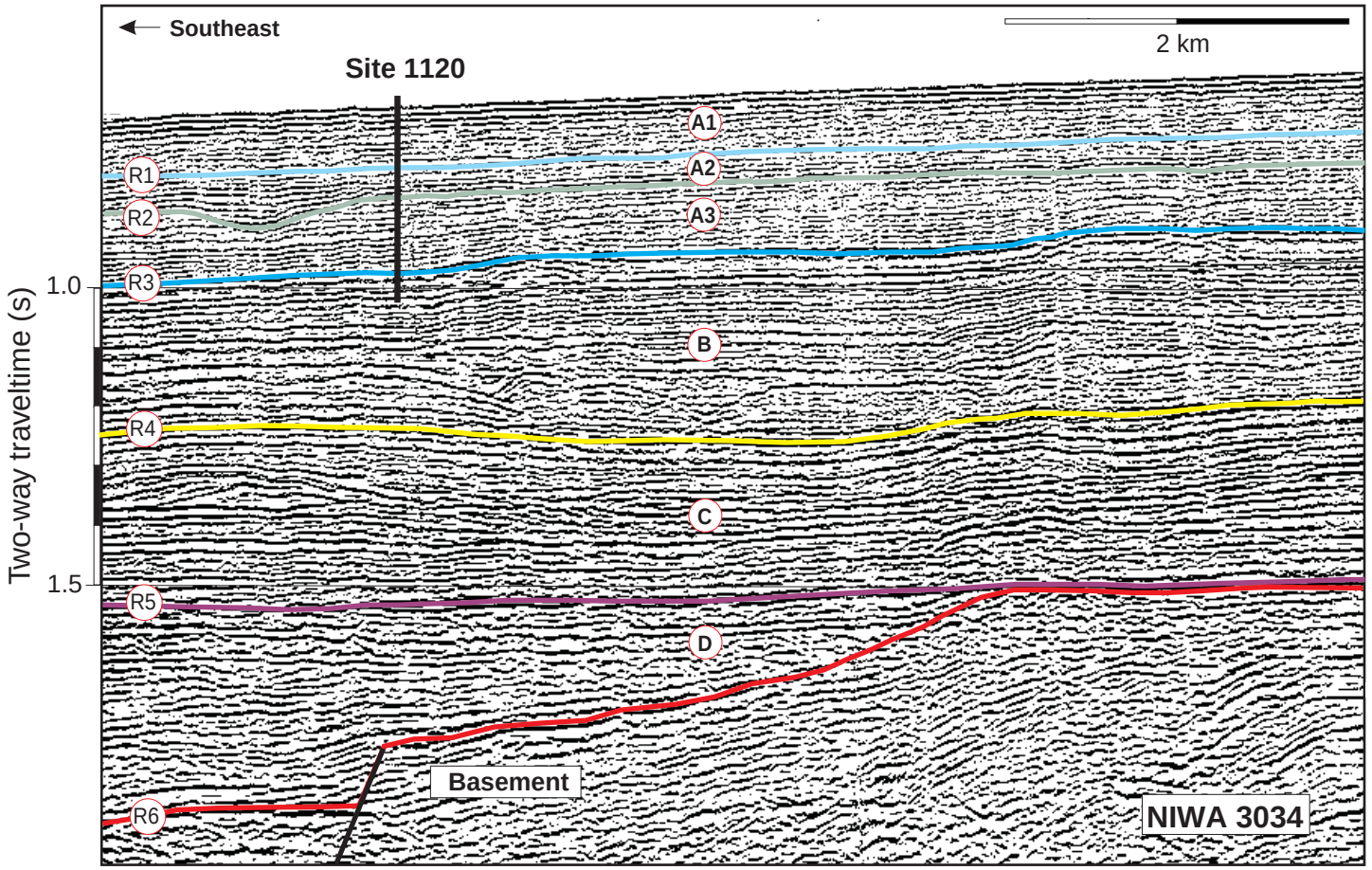

Figure F3. Summary logs for Site 1120. (Continued on next page.)

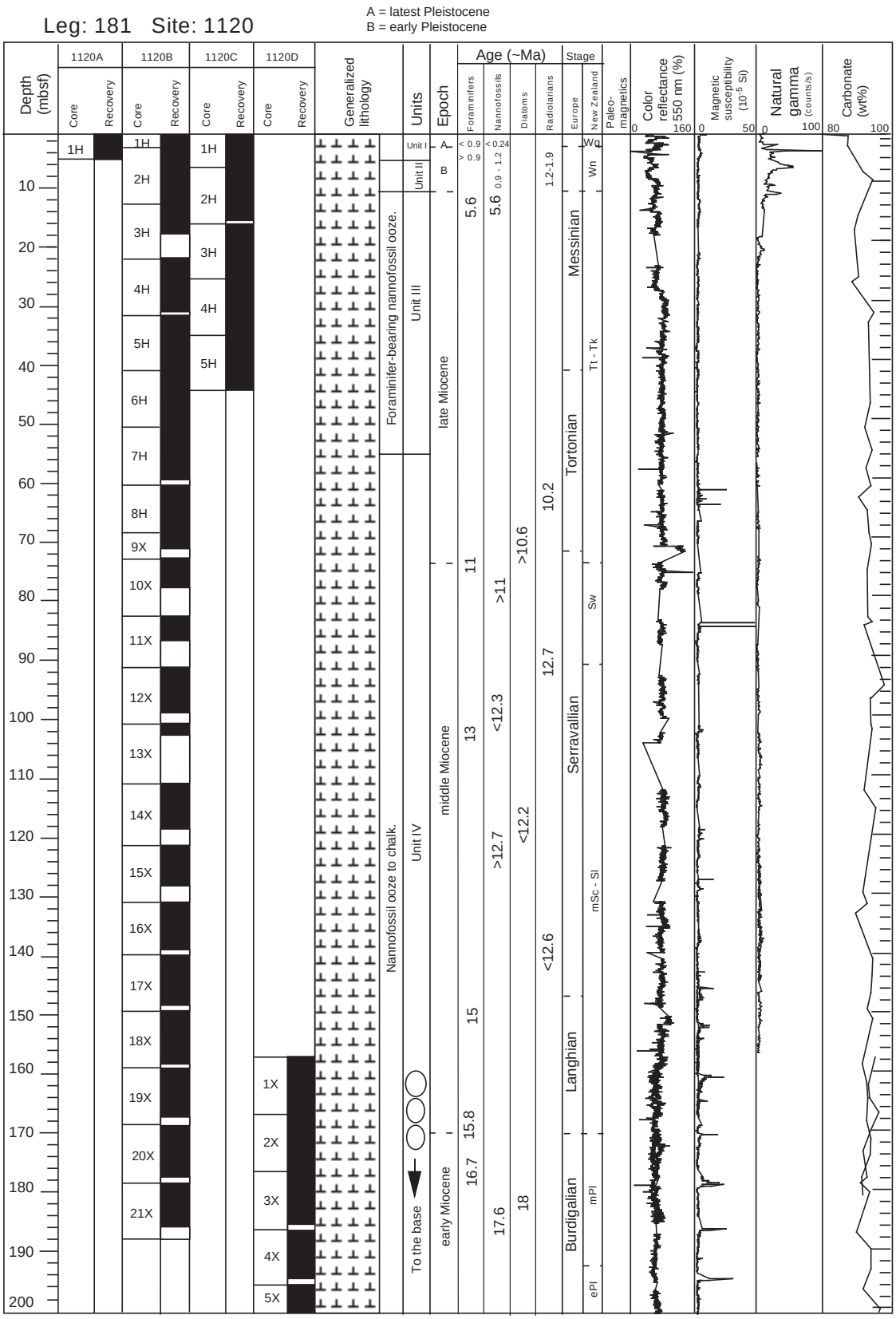

Figure F3 (continued).

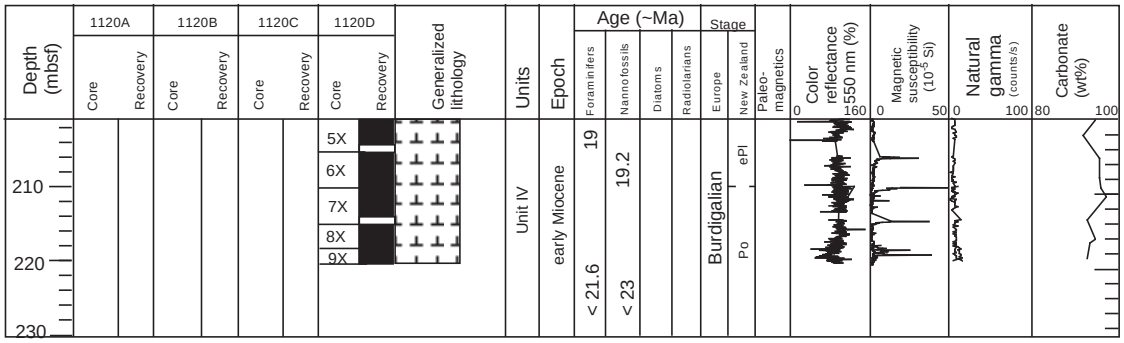

Figure F4. Plot of light reflectance against $CaCO_3$.

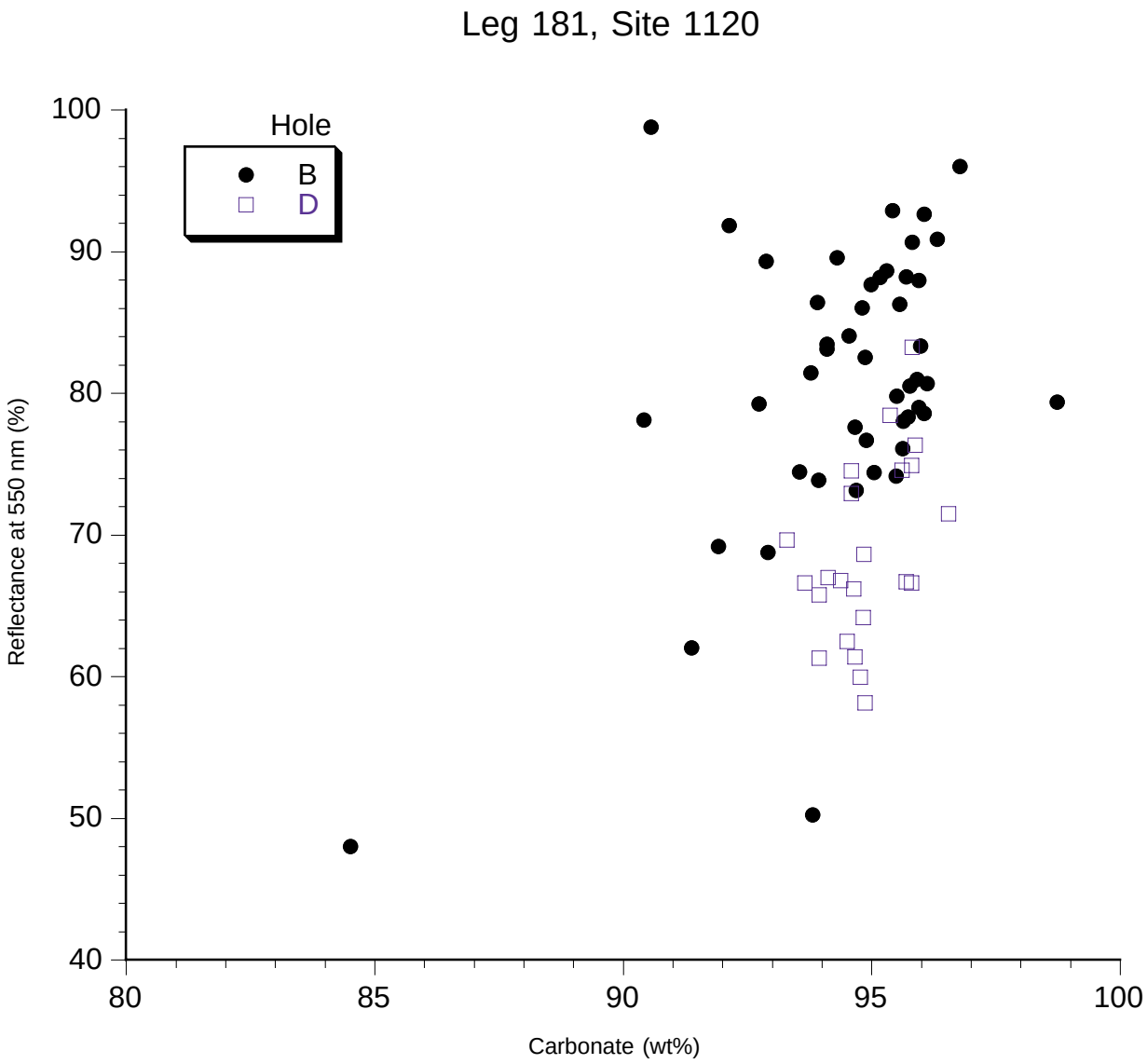

Figure F5. Lithologic break at 4.6 mbsf with minor hard ground that separates Units I (dark) and II (light) (interval 181-1120C-1H-4, 1–30 cm).

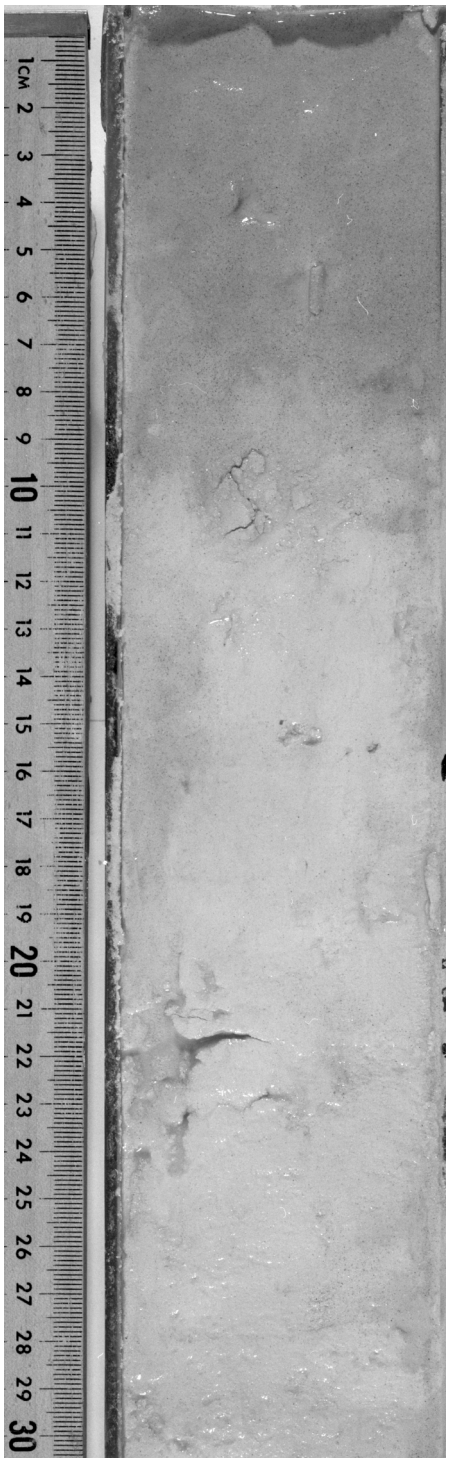

Figure F6. Age-depth curve using multiple microfossil datums for Site 1120. The best-fit line is drawn according to subjective weighting of the chronostratigraphic precision of the events listed in Table **T11,** p. 71, and it shows the preferred average sedimentation rate. Vertical lines on arrows indicate possible errors resulting from large sampling intervals (FO errors extend downcore, LO errors extend upcore). Vertical lines with no arrows represent acme events or total range boxes. The change in average sedimentation rate at 50 mbsf is consistent with an abrupt change in lithofacies at this level.

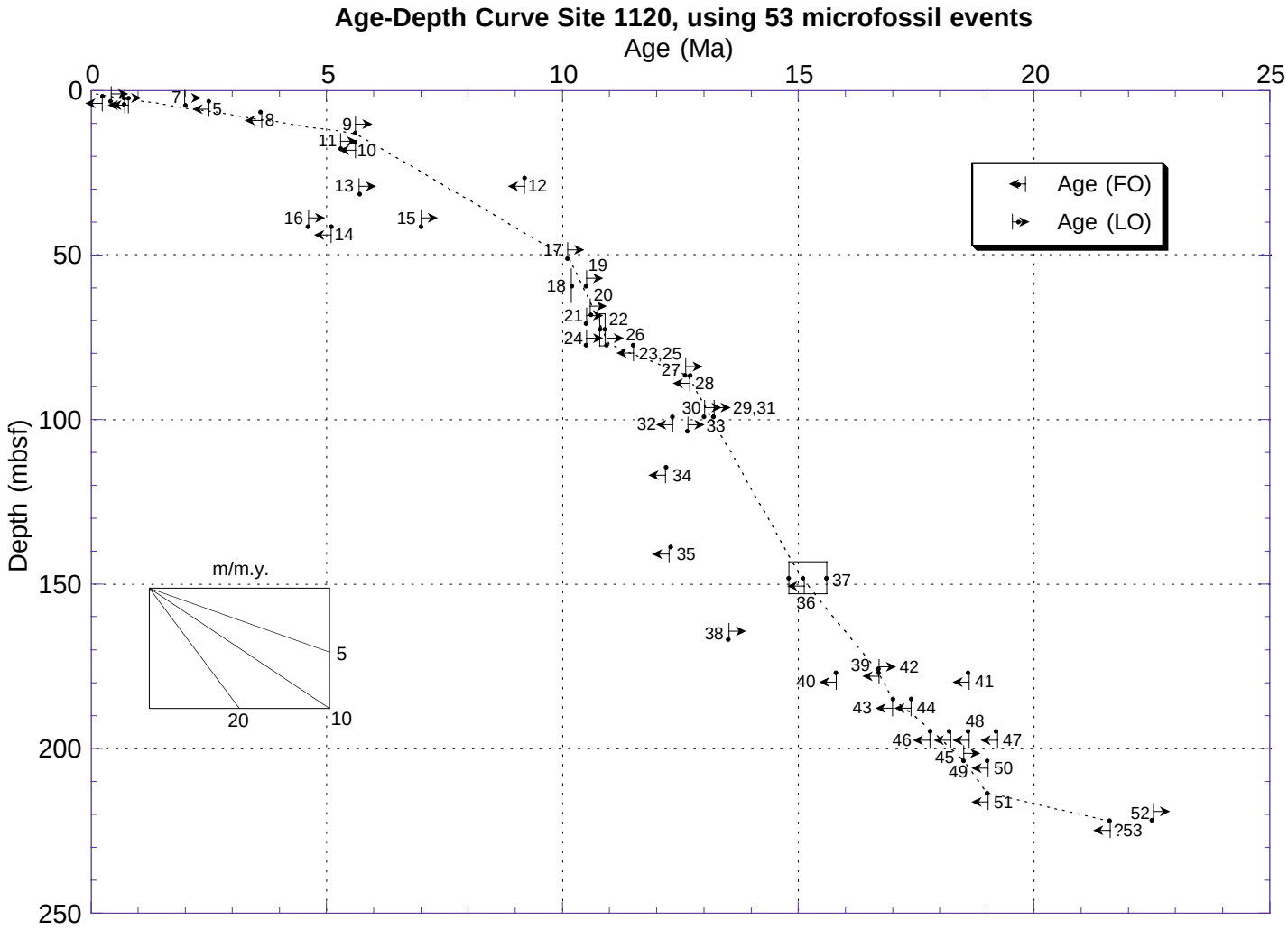

Figure F7. Relative abundance of diatom valves and of the authigenically formed zeolite and clinoptilolite vs. core depth at Site 1120. B = barren, T = trace, R = rare, F = few, C = common, A = abundant.

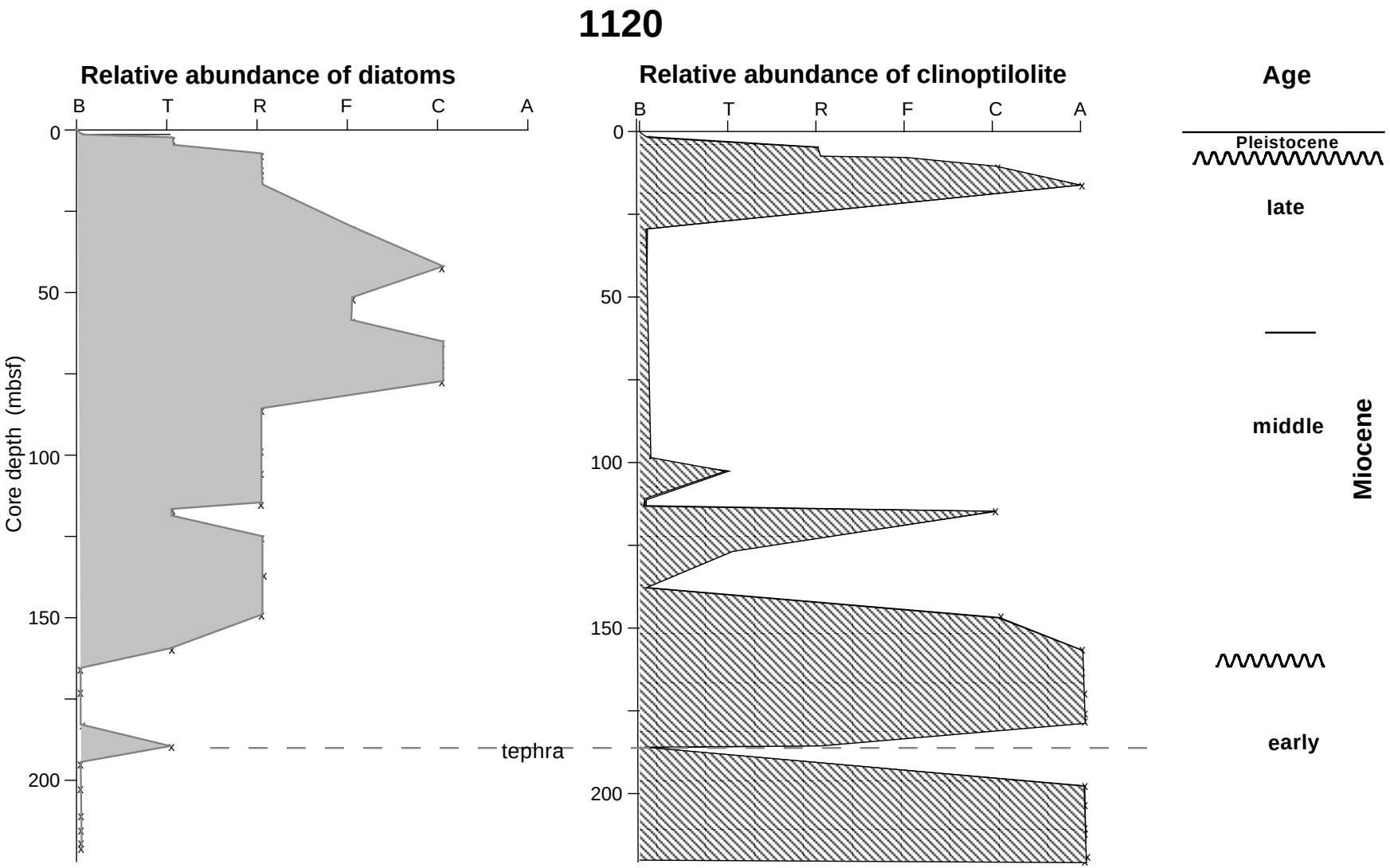

Figure F8. Whole-core magnetic susceptibility from Hole 1120D from the Bartington loop of the shipboard automated multisensor track and archive-half continuous measurements of NRM intensity from the pass-though cryogenic magnetometer. Bold horizontal lines mark core tops as labeled. Vertical and subvertical straight lines in the lower part of each core indicate intervals where measurement was not possible because of coring gaps. Note contamination signal in the tops of cores.

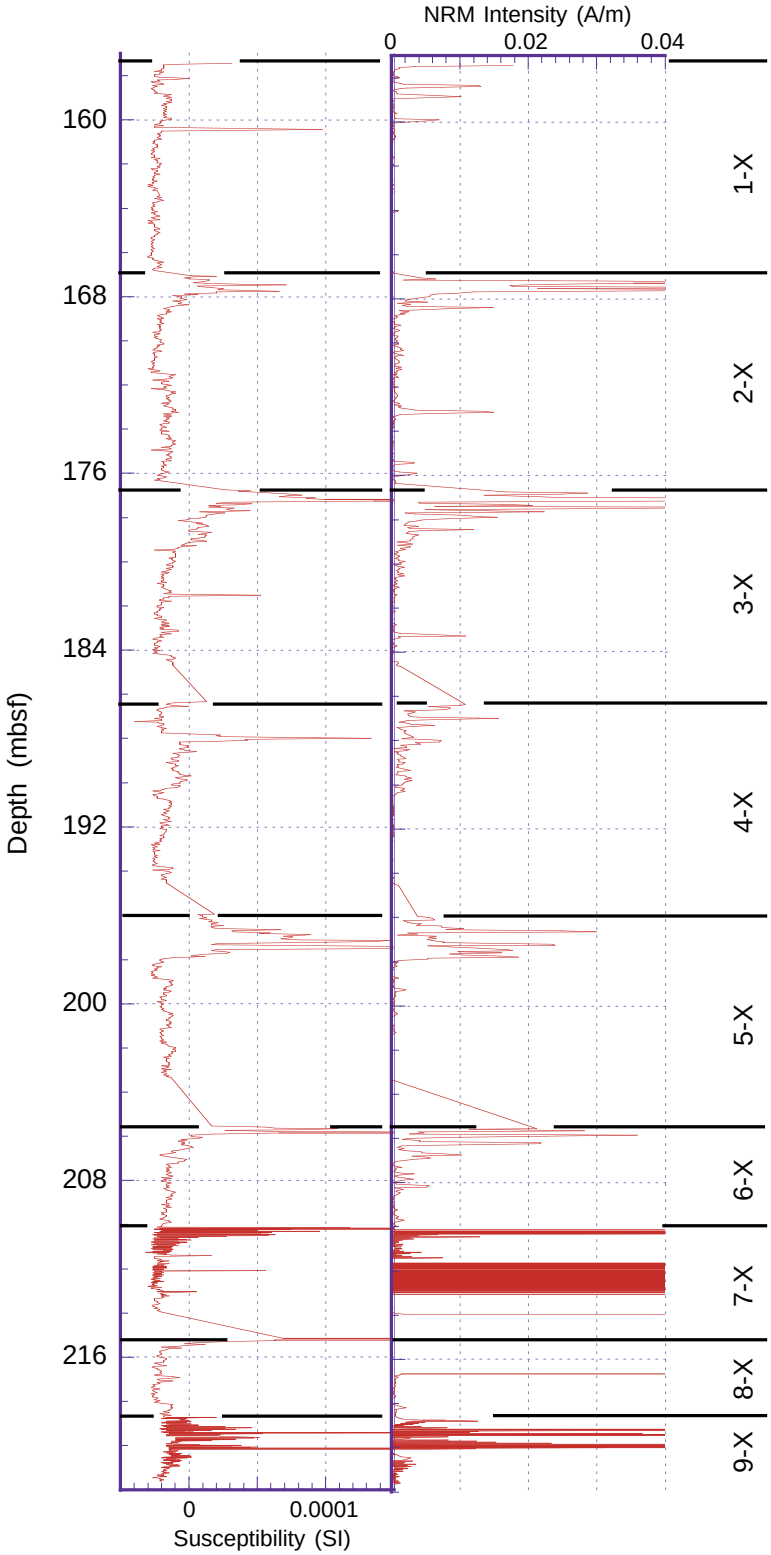

Figure F9. A–D. Plots of normalized intensity of magnetization with progressive AF and thermal demagnetization of saturation isothermal remanent magnetization (SIRM) for selected samples from Hole 1120B.

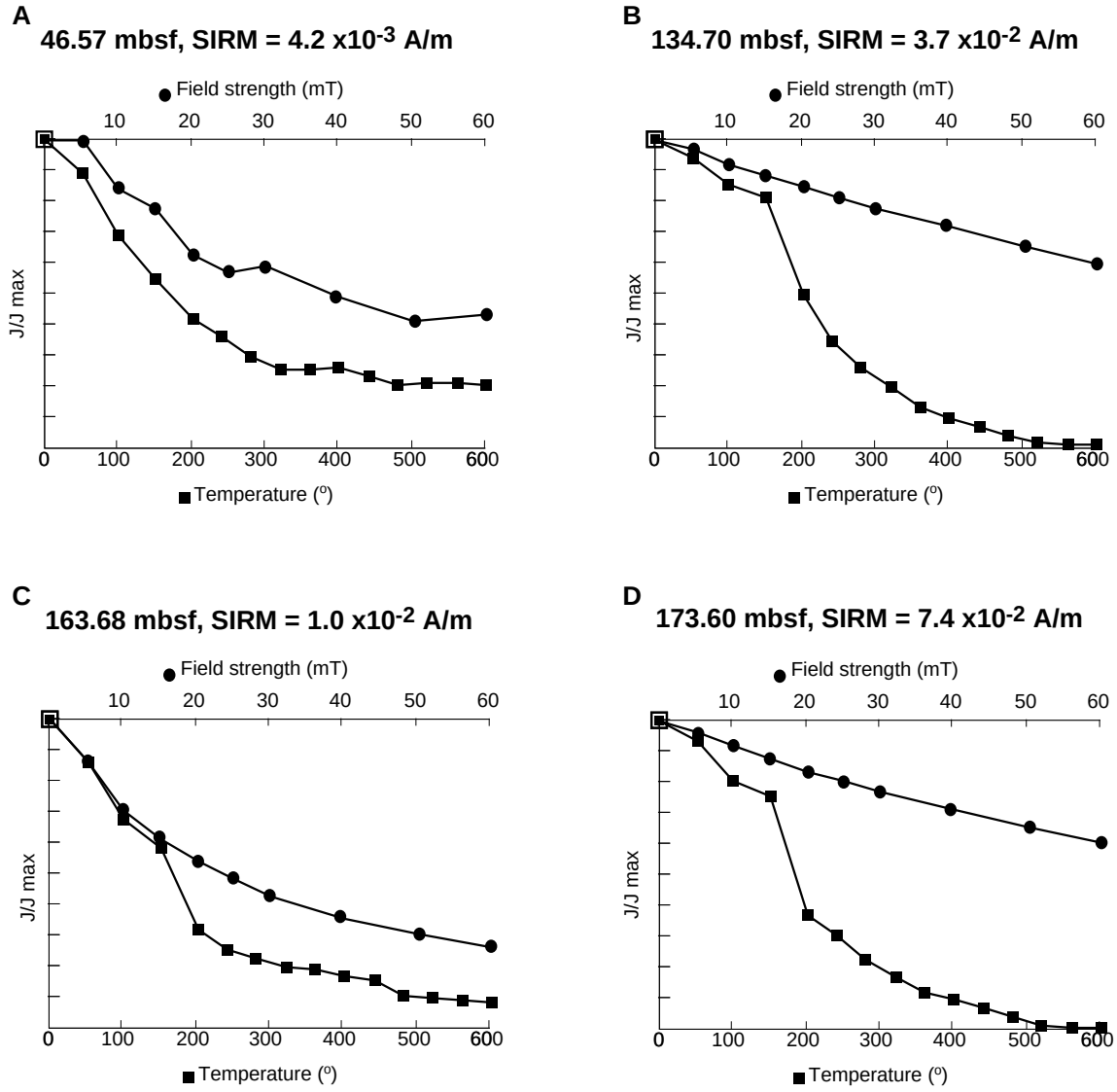

Figure F10. Isothermal remanent magnetization (IRM) and backfield acquisition curves for representative discrete samples from different depths in Hole 1120B. Remanence does not become saturated until 600–1000 mT, and B_{cr} is between 25 and 125 mT for all samples.

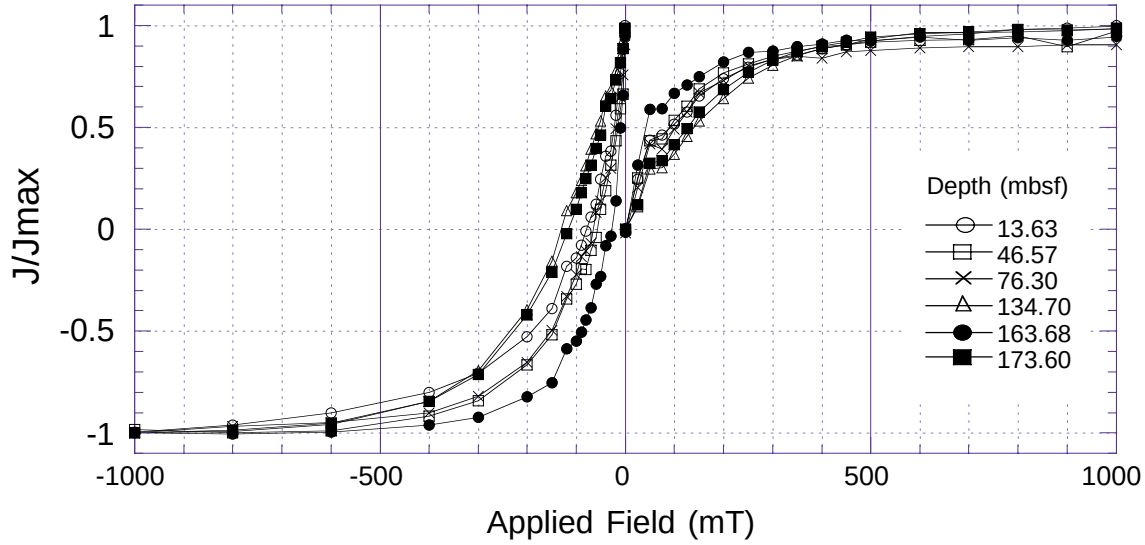

Figure F11. Composite sections for magnetic susceptibility, natural gamma ray, GRAPE, and reflectance percentage at 550 nm. For convenience, MS values from Holes 1120B, 1120C, and 1120D are offset by 3, 6, and 9×10^{-5}, respectively; NGR values are offset by 15, 30, and 45 counts/s, respectively; GRAPE values are offset by 0.2, 0.4, and 0.6 g/cm³, respectively; and reflectance values are offset by 40%, 60%, and 80%, respectively. Gaps in the composite section are indicated with triangles. Cores are indicated by small numbers. (Continued on next page.)

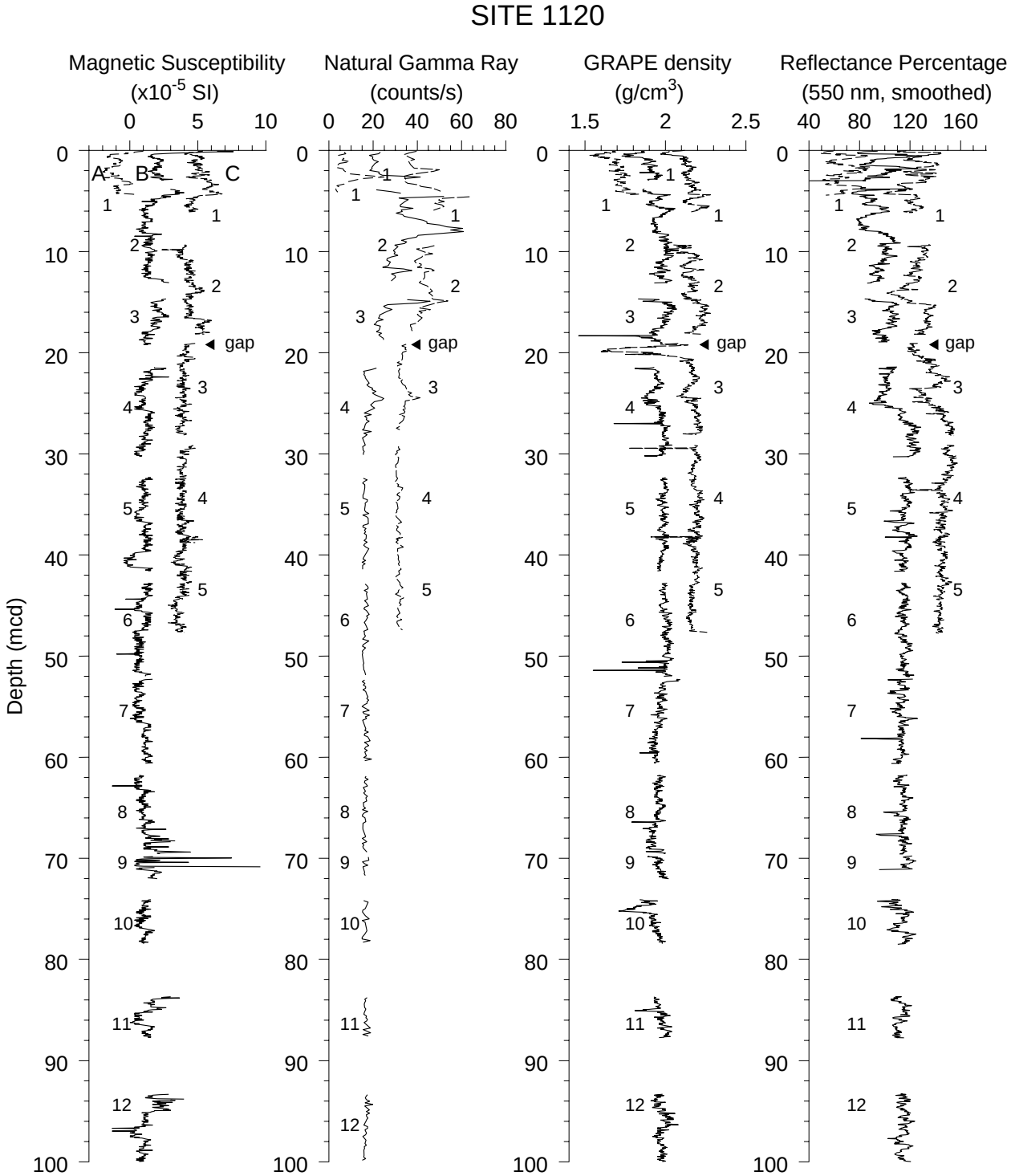

Figure F11 (continued).

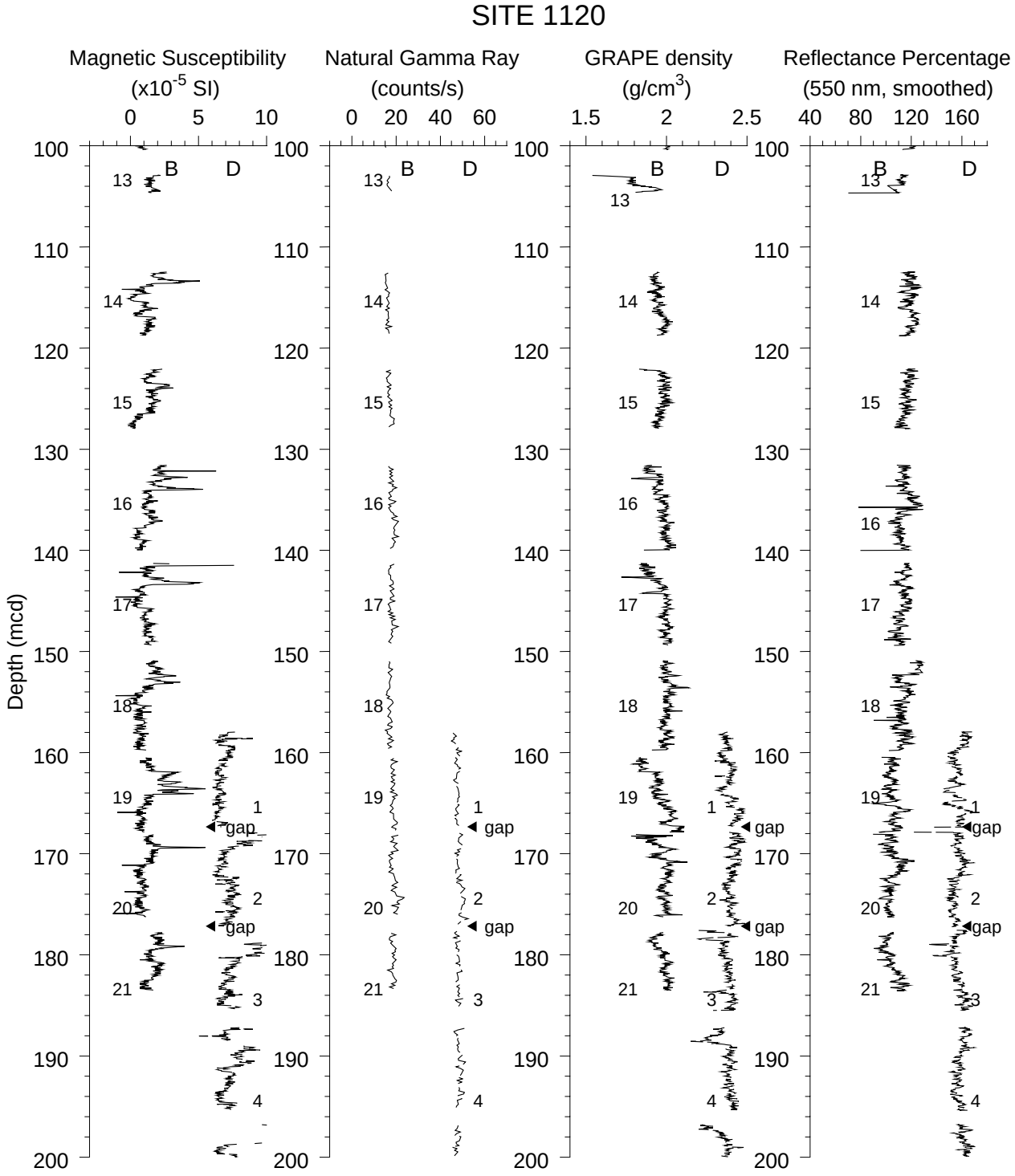

Figure F12. Downhole depth offsets between the mbsf and mcd scales for Site 1120. Solid line indicates the trend for a typical 10% stretch model between mbsf and mcd depths. The dashed line followed by Cores 181-1120B-4H to 6H parallels this trend.

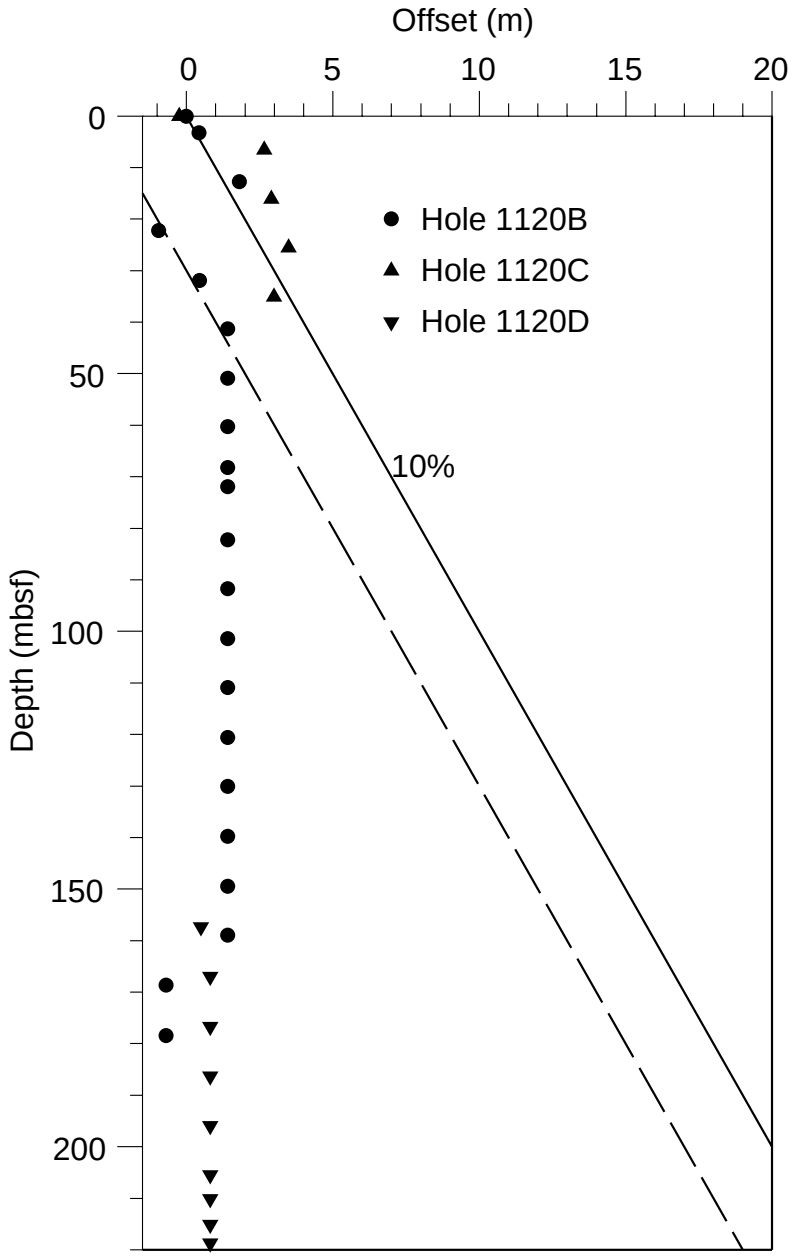

Figure F13. Spliced record for Site 1120. To reduce noise levels, the reflectance data illustrated were smoothed with a 10-cm Gaussian window.

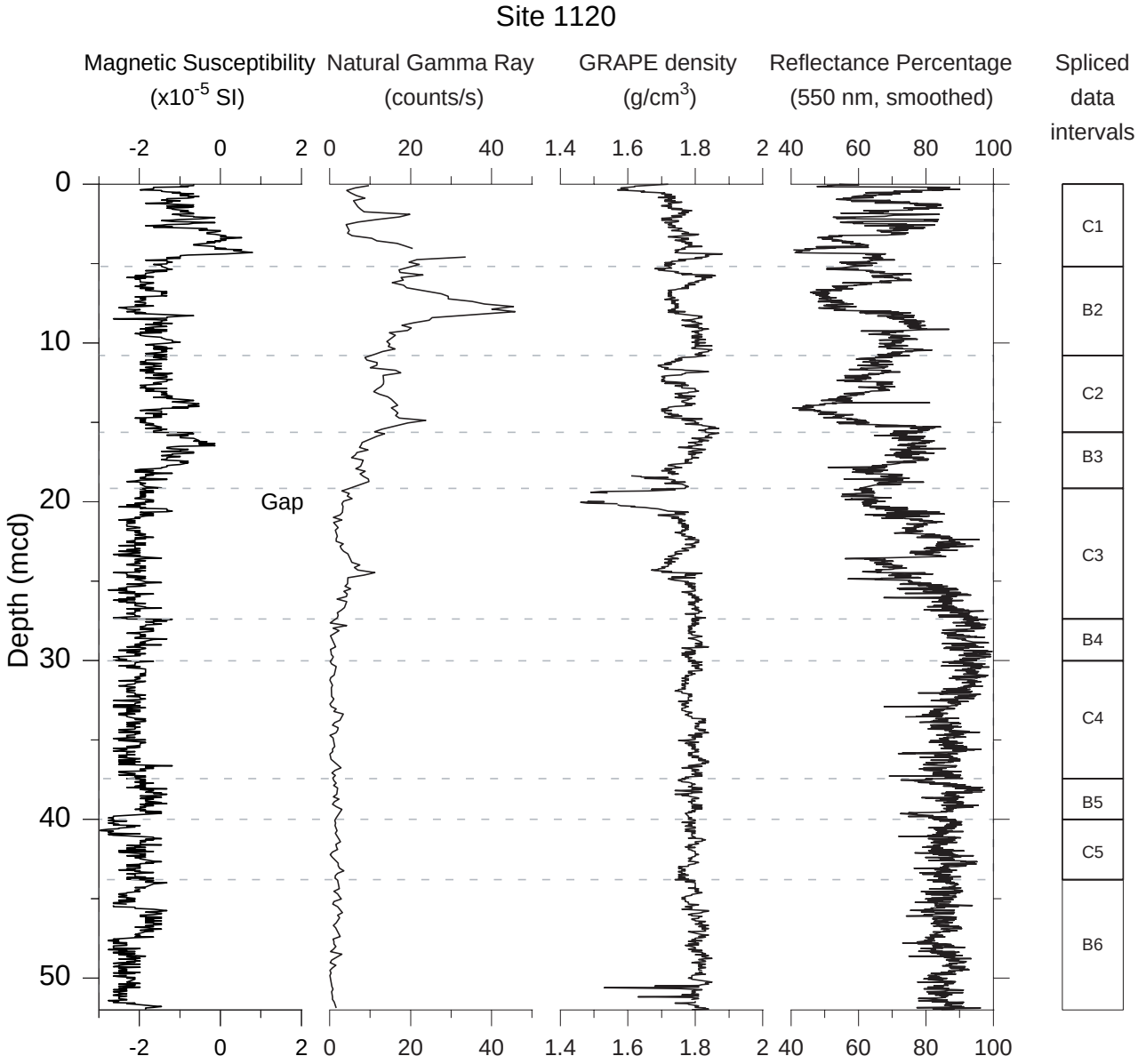

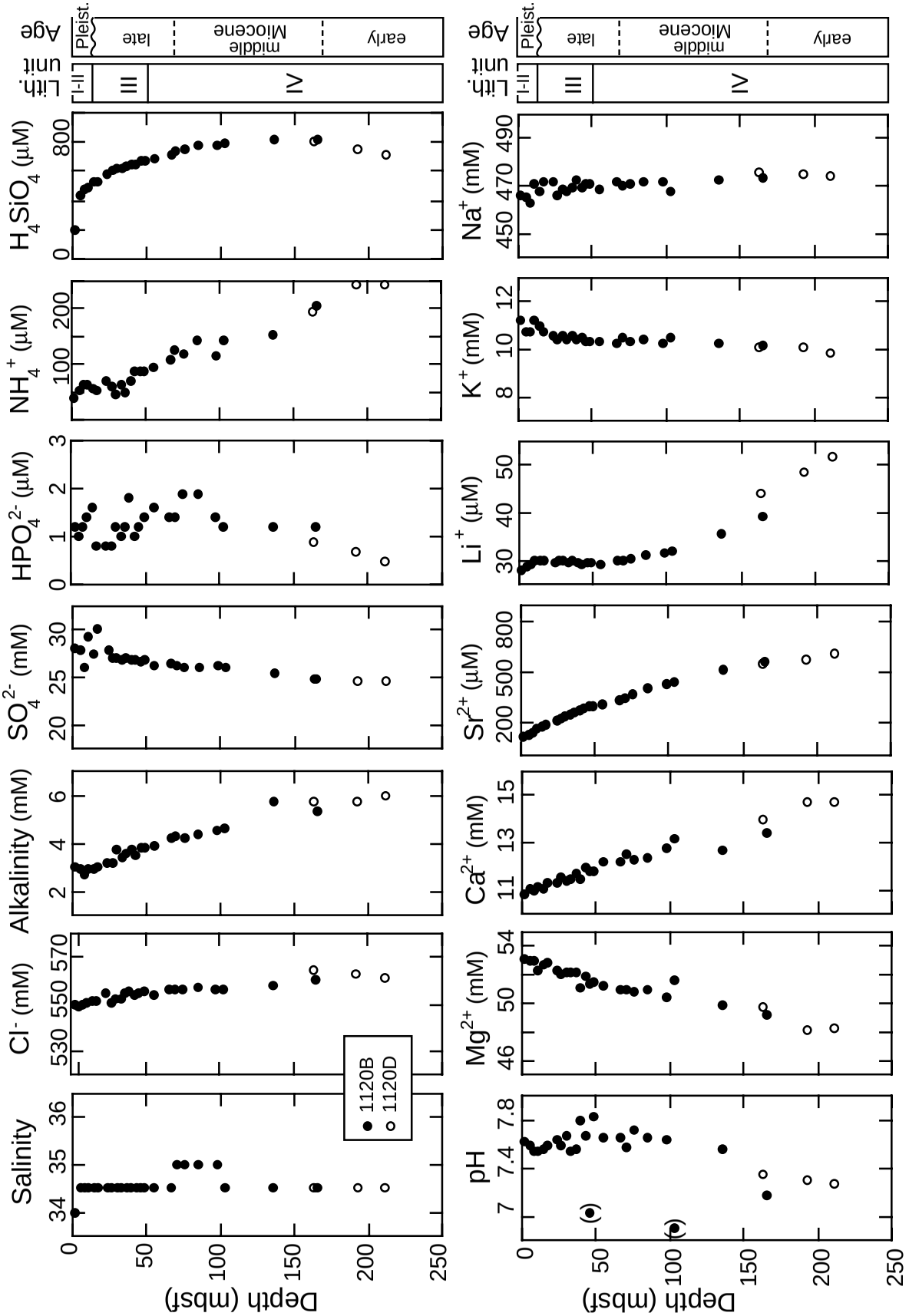

Figure F14. Depth profiles of interstitial-water constituents at Site 1120. Parentheses in pH column denote the erroneous analytical data.

Figure F15. Carbonate contents in sediments from Holes 1120B and 1120D.

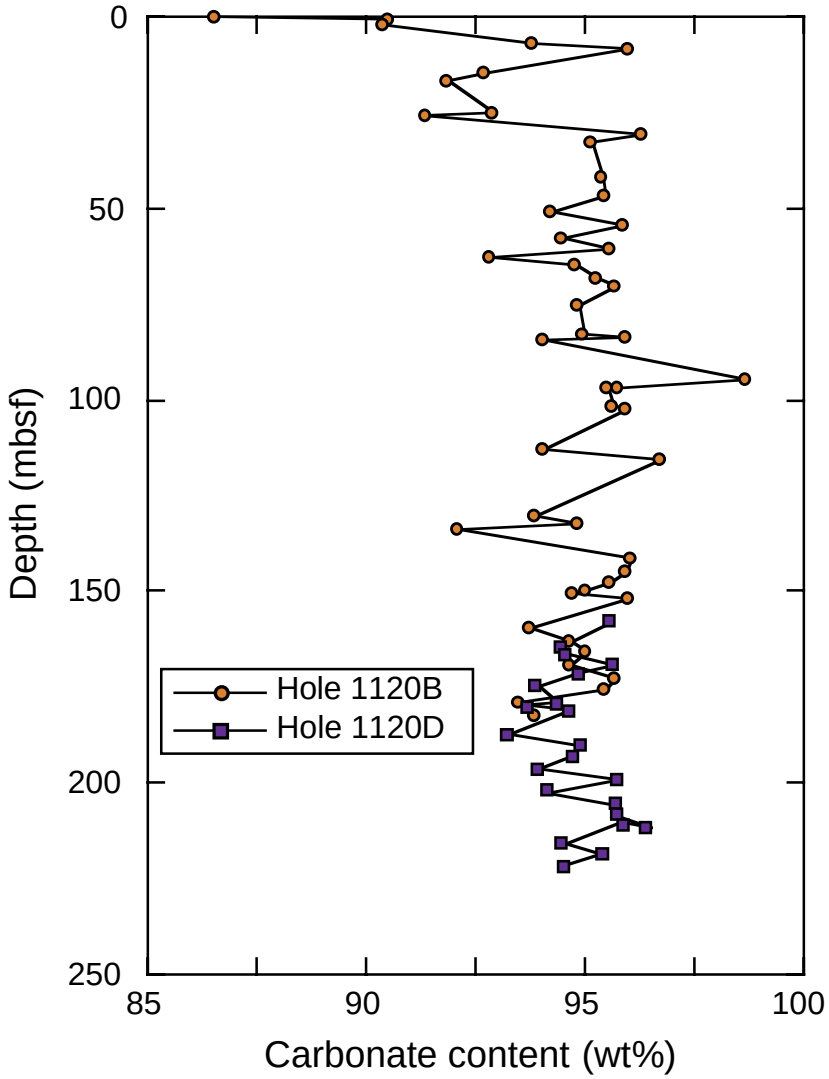

Figure F16. Index properties measured from Holes 1120B and 1120D.

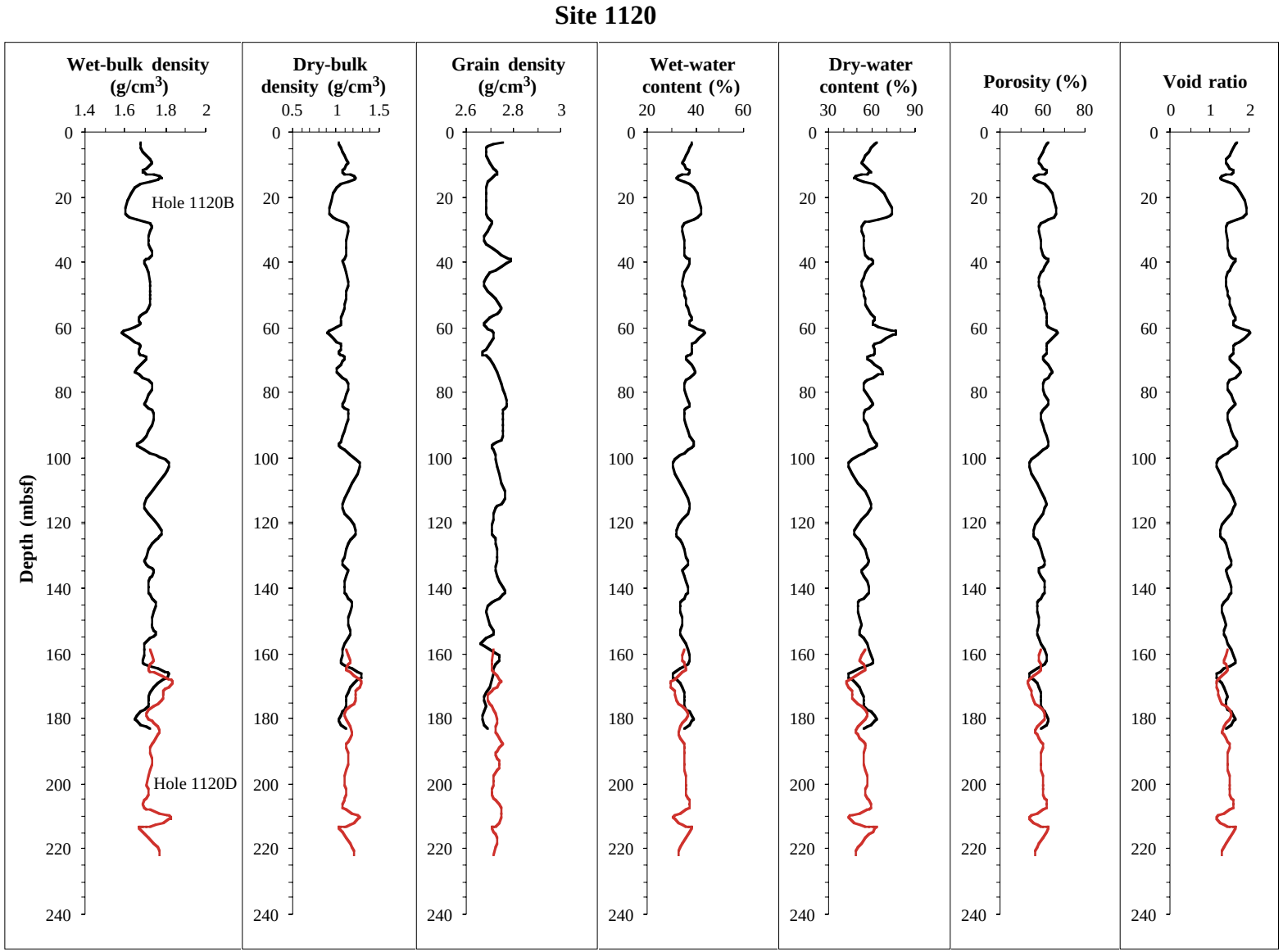

Figure F17. MST measurements from Holes 1120B and 1120D including GRAPE density, magnetic susceptibility, natural gamma-ray intensity, and *P*-wave velocity.

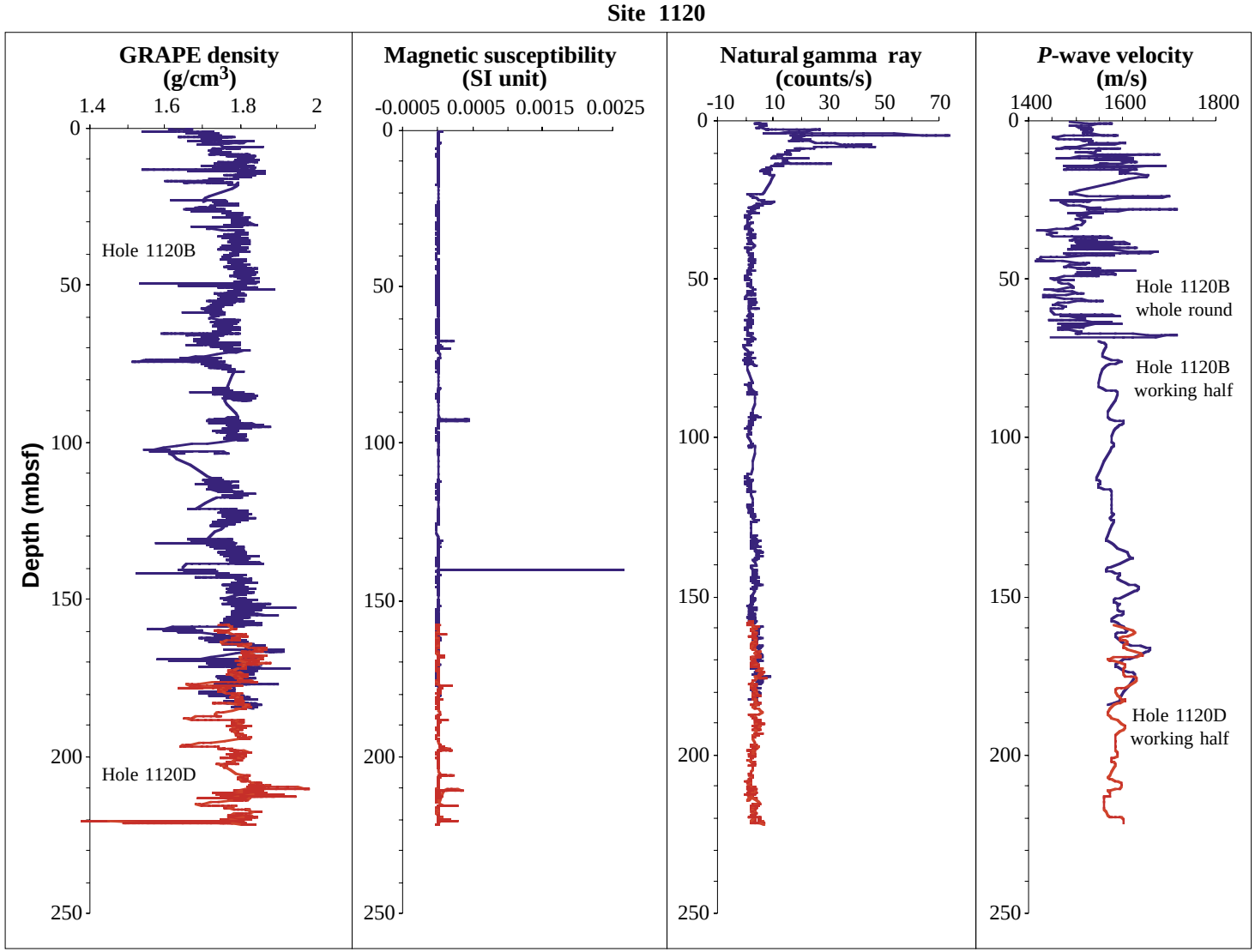

Figure F18. GRAPE density measurements from Holes 1120B and 1120D.

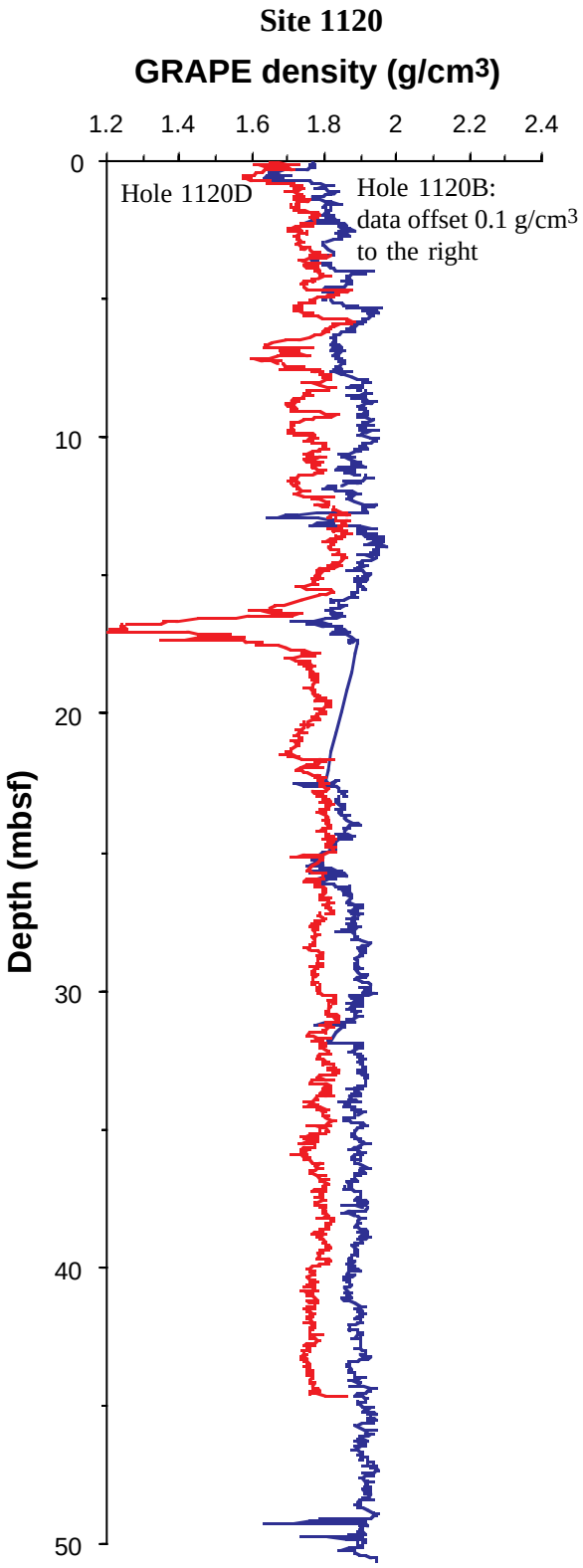

Figure F19. Vane shear strength measured in cores from Hole 1120B and Torvane shear strength measured from cores in Hole 1120C.

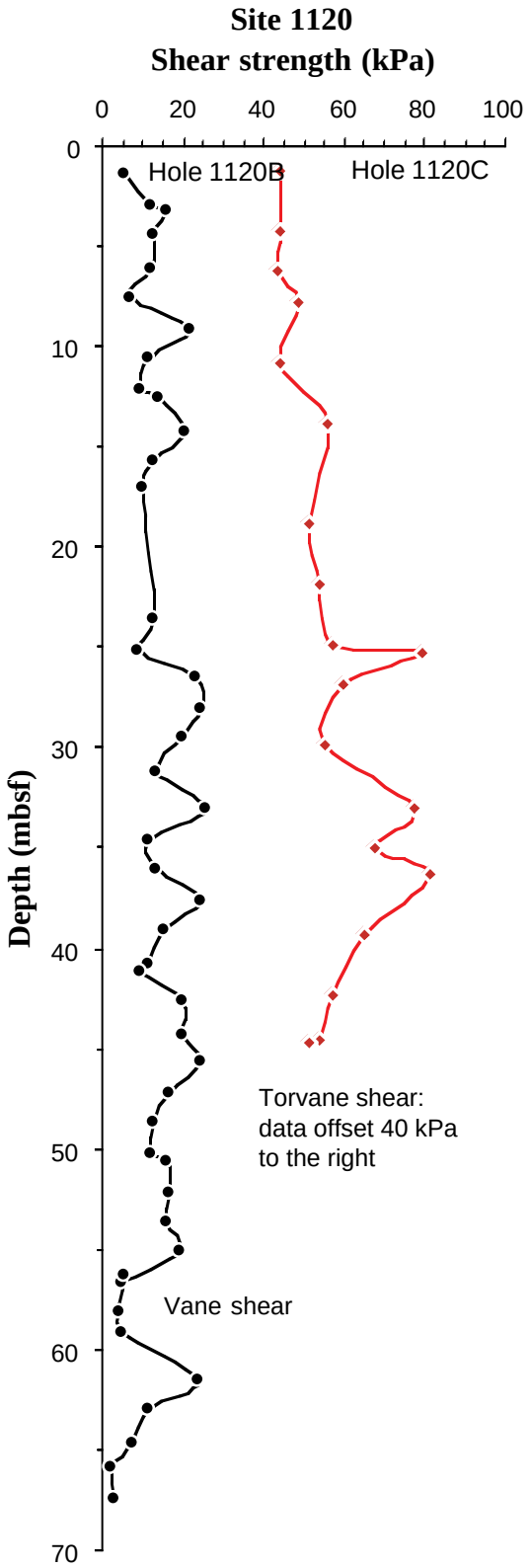

Figure F20. Temperature measurements made by the Adara temperature tool at (**A**) the mudline and (**B**) on Core 181-1120B-6H.

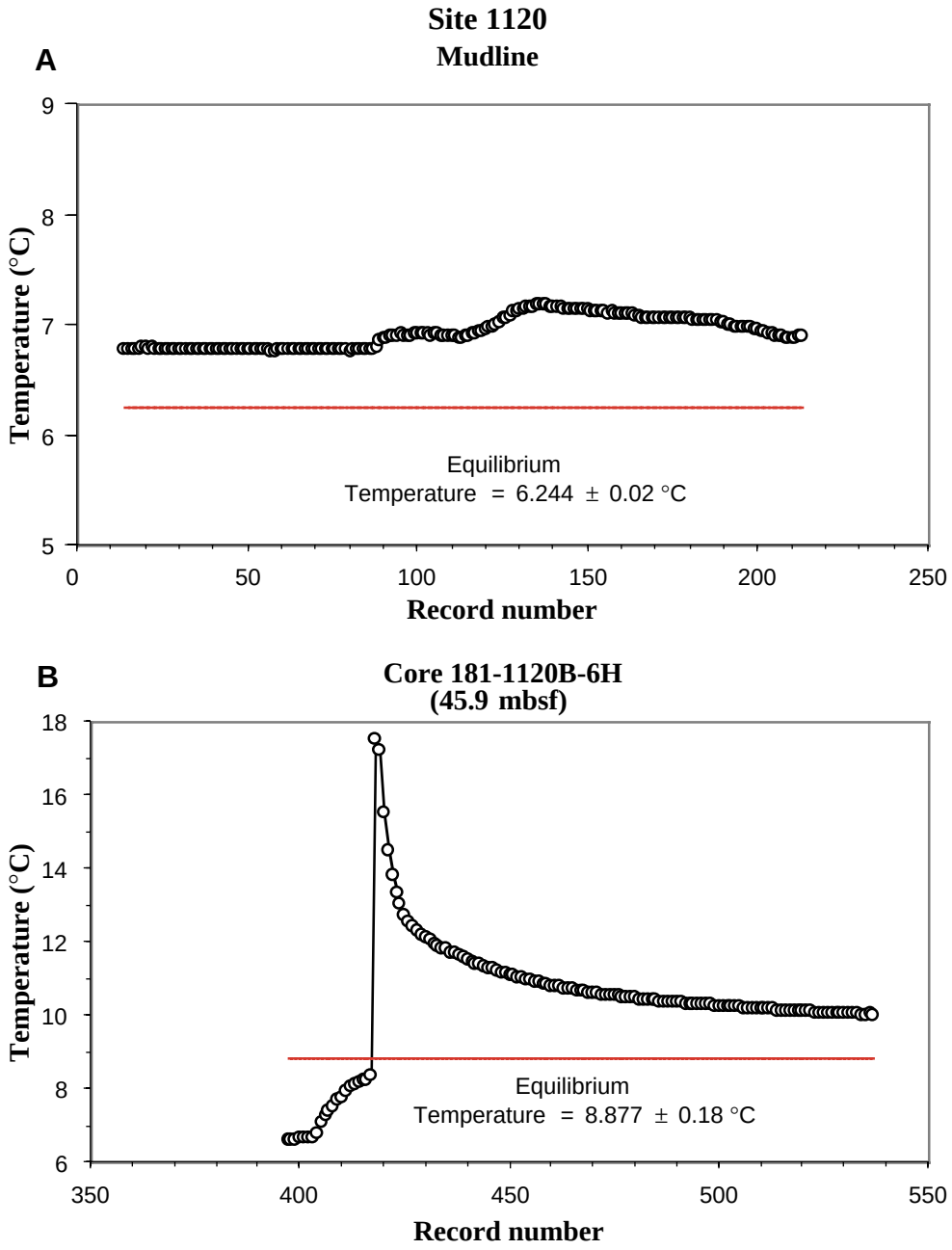

Table T1. Site 1120 expanded coring summary. (**See table note.** Continued on next six pages.)

Core	Date (August 1998)	Time (UTC)	Core depth (mbsf) Top	Core depth (mbsf) Bottom	Length (m) Cored	Length (m) Recovered	Recovery (%)	Section	Length (m) Liner	Length (m) Curated	Section depth (mbsf) Top	Section depth (mbsf) Bottom	Catwalk samples	Comment
181-1120A-														
1H	27	1755	0	4.6	4.6	4.6	100							
								1	1.5	1.5	0	1.5	PAL, PAL, PAL, PAL	
								2	1.5	1.5	1.5	3	PAL, PAL, PAL	
								3	1.42	1.42	3	4.42	PAL, PAL, PAL, PAL	
								CC	0.18	0.18	4.42	4.6	PAL	
									4.60	4.60				
				Totals:	4.6	4.6	100							
181-1120B-														
1H	27	1855	0	3.3	3.3	3.36	101.8							
								1	1.5	1.5	0	1.5	IW	
								2	1.5	1.5	1.5	3	HS	
								3	0.2	0.2	3	3.2		
								CC	0.16	0.16	3.2	3.36	PAL	
									3.36	3.36				
2H	27	1930	3.3	12.8	9.5	9.58	100.8							
								1	1.5	1.5	3.3	4.8	IW	
								2	1.5	1.5	4.8	6.3		
								3	1.5	1.5	6.3	7.8	IW	
								4	1.5	1.5	7.8	9.3		
								5	1.5	1.5	9.3	10.8	HS, IW	
								6	1.5	1.5	10.8	12.3		
								7	0.4	0.4	12.3	12.7		
								CC	0.18	0.18	12.7	12.88	PAL	
									9.58	9.58				
3H	27	2000	12.8	22.3	9.5	4.9	51.6							
								1	1.5	1.5	12.8	14.3	IW	
								2	1.5	1.5	14.3	15.8	HS	
								3	1.4	1.4	15.8	17.2	IW	
								4	0.25	0.25	17.2	17.45		
								CC	0.25	0.25	17.45	17.7	PAL	
									4.90	4.90				
4H	27	2035	22.3	31.8	9.5	9.26	97.5							
								1	1.5	1.5	22.3	23.8	IW	
								2	1.5	1.5	23.8	25.3		
								3	1.45	1.45	25.3	26.75	IW, PAL, PAL	
								4	1.5	1.5	26.75	28.25		
								5	1.5	1.5	28.25	29.75	HS, IW	
								6	1.5	1.5	29.75	31.25		
								CC	0.31	0.31	31.25	31.56	PAL	
									9.26	9.26				
5H	27	2110	31.8	41.3	9.5	9.64	101.5							
								1	1.5	1.5	31.8	33.3	IW	
								2	1.5	1.5	33.3	34.8		
								3	1.5	1.5	34.8	36.3	IW	
								4	1.5	1.5	36.3	37.8		
								5	1.5	1.5	37.8	39.3	HS, IW	
								6	1.5	1.5	39.3	40.8		

Table T1 (continued).

Core	Date (August 1998)	Time (UTC)	Core depth (mbsf) Top	Core depth (mbsf) Bottom	Length (m) Cored	Length (m) Recovered	Recovery (%)	Section	Length (m) Liner	Length (m) Curated	Section depth (mbsf) Top	Section depth (mbsf) Bottom	Catwalk samples	Comment
								7	0.37	0.37	40.8	41.17		
								CC	0.27	0.27	41.17	41.44	PAL	
									9.64	9.64				
6H	27	2205	41.3	50.8	9.5	9.78	102.9							
								1	1.5	1.5	41.3	42.8	IW	
								2	1.5	1.5	42.8	44.3		
								3	1.5	1.5	44.3	45.8	IW	
								4	1.5	1.5	45.8	47.3		
								5	1.5	1.5	47.3	48.8	HS, IW	
								6	1.5	1.5	48.8	50.3		
								7	0.36	0.36	50.3	50.66		
								CC	0.42	0.42	50.66	51.08	PAL	
									9.78	9.78				
7H	27	2235	50.8	60.3	9.5	8.66	91.2							
								1	1.5	1.5	50.8	52.3		
								2	1.5	1.5	52.3	53.8		
								3	1.5	1.5	53.8	55.3	IW	
								4	1.5	1.5	55.3	56.8	HS	
								5	1.5	1.5	56.8	58.3		
								6	0.93	0.93	58.3	59.23		
								CC	0.23	0.23	59.23	59.46	PAL	
									8.66	8.66				
8H	27	2335	60.3	68.3	8	8.03	100.4							
								1	1.5	1.5	60.3	61.8		
								2	1.5	1.5	61.8	63.3		
								3	1.5	1.5	63.3	64.8		
								4	1.5	1.5	64.8	66.3	IW	
								5	1.5	1.5	66.3	67.8	HS	
								6	0.38	0.38	67.8	68.18		
								CC	0.15	0.15	68.18	68.33	PAL	
									8.03	8.03				
9X	28	35	68.3	72.6	4.3	2.57	59.8							
								1	1.5	1.5	68.3	69.8	IW	
								2	0.89	0.89	69.8	70.69	HS	
								CC	0.18	0.18	70.69	70.87	PAL	
									2.57	2.57				
10X	28	110	72.6	82.2	9.6	4.86	50.6							
								1	1.5	1.5	72.6	74.1		
								2	1.5	1.5	74.1	75.6	IW, HS	
								3	1.5	1.5	75.6	77.1		
								4	0.14	0.14	77.1	77.24		
								CC	0.22	0.22	77.24	77.46	PAL	
									4.86	4.86				
11X	28	140	82.2	91.8	9.6	4.45	46.4							
								1	1.5	1.5	82.2	83.7		
								2	1.5	1.5	83.7	85.2	IW	
								3	1.17	1.17	85.2	86.37	HS	
								CC	0.28	0.28	86.37	86.65	PAL	
									4.45	4.45				

Table T1 (continued).

Core	Date (August 1998)	Time (UTC)	Core depth (mbsf) Top	Core depth (mbsf) Bottom	Length (m) Cored	Length (m) Recovered	Recovery (%)	Section	Length (m) Liner	Length (m) Curated	Section depth (mbsf) Top	Section depth (mbsf) Bottom	Catwalk samples	Comment
12X	28	210	91.8	101.4	9.6	7.4	77.1							
								1	1.5	1.5	91.8	93.3		
								2	1.5	1.5	93.3	94.8		
								3	1.5	1.5	94.8	96.3		
								4	1.5	1.5	96.3	97.8	IW	
								5	1.22	1.22	97.8	99.02	HS	
								CC	0.18	0.18	99.02	99.2	PAL	
									7.40	7.40				
13X	28	240	101.4	111	9.6	2.21	23							
								1	1.5	1.5	101.4	102.9	IW	
								2	0.37	0.37	102.9	103.27	HS	
								CC	0.34	0.34	103.27	103.61	PAL	
									2.21	2.21				
14X	28	310	111	120.6	9.6	6.56	68.3							
								1	1.5	1.5	111	112.5		
								2	1.5	1.5	112.5	114		
								3	1.5	1.5	114	115.5	PAL, PAL	
								4	1.5	1.5	115.5	117		
								5	0.4	0.4	117	117.4	HS	
								CC	0.16	0.16	117.4	117.56	PAL	
									6.56	6.56				
15X	28	345	120.6	130.1	9.5	6.28	66.1							
								1	1.5	1.5	120.6	122.1		
								2	1.5	1.5	122.1	123.6		
								3	1.5	1.5	123.6	125.1		
								4	1.5	1.5	125.1	126.6	HS	
								CC	0.28	0.28	126.6	126.88	PAL	
									6.28	6.28				
16X	28	410	130.1	139.8	9.7	8.73	90							
								1	1.5	1.5	130.1	131.6		
								2	1.5	1.5	131.6	133.1		
								3	1.5	1.5	133.1	134.6		
								4	1.5	1.5	134.6	136.1	IW	
								5	1.5	1.5	136.1	137.6	HS, HS	
								6	1	1	137.6	138.6		
								CC	0.23	0.23	138.6	138.83	PAL	
									8.73	8.73				
17X	28	440	139.8	149.4	9.6	8.49	88.4							
								1	1.5	1.5	139.8	141.3		
								2	1.5	1.5	141.3	142.8		
								3	1.5	1.5	142.8	144.3		
								4	1.5	1.5	144.3	145.8		
								5	1.5	1.5	145.8	147.3	HS	
								6	0.7	0.7	147.3	148		
								CC	0.29	0.29	148	148.29	PAL	
									8.49	8.49				
18X	28	510	149.4	159	9.6	9.23	96.1							
								1	1.5	1.5	149.4	150.9		

Table T1 (continued).

Core	Date (August 1998)	Time (UTC)	Core depth (mbsf) Top	Core depth (mbsf) Bottom	Length (m) Cored	Length (m) Recovered	Recovery (%)	Section	Length (m) Liner	Length (m) Curated	Section depth (mbsf) Top	Section depth (mbsf) Bottom	Catwalk samples	Comment
								2	1.5	1.5	150.9	152.4		
								3	1.5	1.5	152.4	153.9		
								4	1.5	1.5	153.9	155.4		
								5	1.5	1.5	155.4	156.9	HS	
								6	1.5	1.5	156.9	158.4		
								CC	0.23	0.23	158.4	158.63	PAL	
									9.23	9.23				
19X	28	535	159	168.7	9.7	7.93	81.8							
								1	1.5	1.5	159	160.5		
								2	1.5	1.5	160.5	162		
								3	1.5	1.5	162	163.5		
								4	1.5	1.5	163.5	165	IW	
								5	1.5	1.5	165	166.5	HS	
								CC	0.43	0.43	166.5	166.93	PAL	
									7.93	7.93				
20X	28	600	168.7	178.4	9.7	8.44	87							
								1	1.5	1.5	168.7	170.2		
								2	1.5	1.5	170.2	171.7		
								3	1.5	1.5	171.7	173.2		
								4	1.5	1.5	173.2	174.7		
								5	1.5	1.5	174.7	176.2	HS	
								6	0.77	0.77	176.2	176.97		
								CC	0.17	0.17	176.97	177.14	PAL	
									8.44	8.44				
21X	28	635	178.4	188	9.6	6.15	64.1							
								1	1.5	1.5	178.4	179.9		
								2	1.5	1.5	179.9	181.4		
								3	1.5	1.5	181.4	182.9		
								4	1.35	1.35	182.9	184.25	HS	
								CC	0.3	0.3	184.25	184.55	PAL	
									6.15	6.15				
				Totals:	188	146.51	77.90							
181-1120C-														
1H	28	1500	0	6.6	6.6	6.59	99.8							
								1	1.5	1.5	0	1.5		
								2	1.5	1.5	1.5	3		
								3	1.5	1.5	3	4.5		
								4	1.5	1.5	4.5	6		
								5	0.39	0.39	6	6.39		
								CC	0.2	0.2	6.39	6.59	PAL	
									6.59	6.59				
2H	28	1545	6.6	16.1	9.5	9.12	96							
								1	1.5	1.5	6.6	8.1		
								2	1.5	1.5	8.1	9.6		
								3	1.5	1.5	9.6	11.1		
								4	1.5	1.5	11.1	12.6		
								5	1.5	1.5	12.6	14.1		

Table T1 (continued).

Core	Date (August 1998)	Time (UTC)	Core depth (mbsf) Top	Core depth (mbsf) Bottom	Length (m) Cored	Length (m) Recovered	Recovery (%)	Section	Length (m) Liner	Length (m) Curated	Section depth (mbsf) Top	Section depth (mbsf) Bottom	Catwalk samples	Comment
								6	1.44	1.44	14.1	15.54		
								CC	0.18	0.18	15.54	15.72	PAL	
									9.12	9.12				
3H	29	1615	16.1	25.6	9.5	9.51	100.1							
								1	1.5	1.5	16.1	17.6		
								2	1.5	1.5	17.6	19.1		
								3	1.5	1.5	19.1	20.6		
								4	1.5	1.5	20.6	22.1		
								5	1.5	1.5	22.1	23.6		
								6	1.41	1.41	23.6	25.01		
								7	0.3	0.3	25.01	25.31		
								CC	0.3	0.3	25.31	25.61	PAL	
									9.51	9.51				
4H	29	1655	25.6	35.1	9.5	9.95	104.7							
								1	1.5	1.5	25.6	27.1		
								2	1.5	1.5	27.1	28.6		
								3	1.5	1.5	28.6	30.1		
								4	1.5	1.5	30.1	31.6		
								5	1.5	1.5	31.6	33.1		
								6	1.5	1.5	33.1	34.6		
								7	0.72	0.72	34.6	35.32		
								CC	0.23	0.23	35.32	35.55	PAL	
									9.95	9.95				
5H	29	2255	35.1	44.6	9.5	9.78	102.9							
								1	1.5	1.5	35.1	36.6		
								2	1.5	1.5	36.6	38.1		
								3	1.5	1.5	38.1	39.6		
								4	1.5	1.5	39.6	41.1		
								5	1.5	1.5	41.1	42.6		
								6	1.5	1.5	42.6	44.1		
								7	0.68	0.68	44.1	44.78		
								CC	0.1	0.1	44.78	44.88	PAL	All to PAL
									9.78	9.78				
				Totals:	44.6	44.95	100.8							
181-1120D-														
10	31	0845	0	157.4	0	0	N/A							
1X	31	0925	157.4	167	9.6	9.63	100.3							
								1	1.5	1.5	157.4	158.9		
								2	1.5	1.5	158.9	160.4		
								3	1.5	1.5	160.4	161.9		
								4	1.5	1.5	161.9	163.4	IW	
								5	1.5	1.5	163.4	164.9	HS	
								6	1.5	1.5	164.9	166.4		
								7	0.48	0.48	166.4	166.88		
								CC	0.15	0.15	166.88	167.03	PAL	
									9.63	9.63				
2X	31	0955	167	176.7	9.7	9.73	100.3							

Table T1 (continued).

Core	Date (August 1998)	Time (UTC)	Core depth (mbsf) Top	Core depth (mbsf) Bottom	Length (m) Cored	Length (m) Recovered	Recovery (%)	Section	Length (m) Liner	Length (m) Curated	Section depth (mbsf) Top	Section depth (mbsf) Bottom	Catwalk samples	Comment
								1	1.5	1.5	167	168.5	PAL	
								2	1.5	1.5	168.5	170		
								3	1.5	1.5	170	171.5	PAL	
								4	1.5	1.5	171.5	173	PAL	
								5	1.5	1.5	173	174.5	HS	
								6	1.5	1.5	174.5	176	PAL	
								7	0.44	0.44	176	176.44		
								CC	0.29	0.29	176.44	176.73	PAL	
									9.73	9.73				
3X	31	1025	176.7	186.3	9.6	8.28	86.3							
								1	1.5	1.5	176.7	178.2		
								2	1.5	1.5	178.2	179.7		
								3	1.5	1.5	179.7	181.2		
								4	1.5	1.5	181.2	182.7		
								5	1.5	1.5	182.7	184.2	HS	
								6	0.52	0.52	184.2	184.72		
								CC	0.26	0.26	184.72	184.98	PAL	
									8.28	8.28				
4X	31	1055	186.3	195.9	9.6	8.48	88.3							
								1	1.5	1.5	186.3	187.8		
								2	1.5	1.5	187.8	189.3		
								3	1.5	1.5	189.3	190.8		
								4	1.5	1.5	190.8	192.3	IW	
								5	1.5	1.5	192.3	193.8	HS	
								6	0.78	0.78	193.8	194.58		
								CC	0.2	0.2	194.58	194.78	PAL	
									8.48	8.48				
5X	31	1120	195.9	205.5	9.6	7.77	80.9							
								1	1.5	1.5	195.9	197.4		
								2	1.5	1.5	197.4	198.9		
								3	1.5	1.5	198.9	200.4		
								4	1.5	1.5	200.4	201.9		
								5	1.5	1.5	201.9	203.4		
								CC	0.27	0.27	203.4	203.67	PAL	
									7.77	7.77				
6X	31	1159	205.5	210.1	4.6	8.72	189.6							
								1	1.5	1.5	205.5	207		
								2	1.5	1.5	207	208.5		
								3	1.5	1.5	208.5	210		
								4	1.5	1.5	210	211.5		
								5	1.5	1.5	211.5	213	HS	
								6	1	1	213	214		
								CC	0.22	0.22	214	214.22	PAL	
									8.72	8.72				
7X	31	1235	210.1	215.1	5	3.55	71							
								1	1.5	1.5	210.1	211.6	IW	
								2	1.5	1.5	211.6	213.1	HS	
								3	0.2	0.2	213.1	213.3		

Table T1 (continued).

Core	Date (August 1998)	Time (UTC)	Core depth (mbsf) Top	Core depth (mbsf) Bottom	Length (m) Cored	Length (m) Recovered	Recovery (%)	Section	Length (m) Liner	Length (m) Curated	Section depth (mbsf) Top	Section depth (mbsf) Bottom	Catwalk samples	Comment
								CC	0.35	0.35	213.3	213.65	PAL	
									3.55	3.55				
8X	31	1310	215.1	218.7	3.6	6.75	187.5							
								1	1.5	1.5	215.1	216.6		
								2	1.5	1.5	216.6	218.1		
								3	1.5	1.5	218.1	219.6		
								4	1.5	1.5	219.6	221.1	HS	
								5	0.53	0.53	221.1	221.63		
								CC	0.22	0.22	221.63	221.85	PAL	
									6.75	6.75				
9X	31	1340	218.7	220.7	2	3.26	163							
								1	1.5	1.5	218.7	220.2		
								2	1.48	1.48	220.2	221.68	HS	
								CC	0.28	0.28	221.68	221.96	PAL	
									3.26	3.26				
				Totals:	63.3	66.17	104.50							

Note: PAL = paleontology, IW = interstitial water, HS = headspace, N/A = not available. This table is also available in **ASCII format.**

Table T2. Main criteria used for distinguishing lithostratigraphic units.

Unit	Depth (mbsf)	Characteristics
I	0–4.6	Nannofossils = A; foraminifers = A–C; quartz/feldspar = P; beds <0.5 m distinguished by colors; unit sits on unconformity.
II	4.6–11.2	Nannofossils = A; foraminifers = A–C; glauconite = P; beds >1.0 m; colors less distinct than in Unit I.
III	11.2–54.9	Nannofossils = A; foraminifers = C; sponge spicules = P; bedding differentiation weak.
IV	54.9–220.7	Nannofossils = A; foraminifers = P; bedding very poor.

Note: A = abundant, C = common, P = present.

Table T3. Biostratigraphic events identified at Site 1120.(See table note. Continued on next page.)

Event	Group	NZ stage	Zone (base)	Epoch	Age (Ma)	Sample	Depth (mbsf)
FO *Emiliania huxleyi*	N	Wq	NN21	late Pleistocene	0.24	1120A-1H-2, 28-29cm	1.78
FO *Globorotalia truncatulinoides*	F	Wc			0.8	1120A-1H-2, 85-87cm	2.35
FO dominant *Globorotalia inflata*	F	Wc			0.7	1120A-1H-2, 85-87cm	2.35
LO *Pseudoemiliania lacunosa*	N	Wc/Wq	NN20	mid-Pleistocene	0.42	1120A-1H-3, 30-32cm	3.3
LO *Globorotalia puncticuloides*	F	e Wc		mid-Pleistocene	0.7	1120A-1H-3, 130-32cm	4.3
Acme *Gephyrocapsa* (small)	N			mid-Pleistocene	0.9-1.2	1120B-1H-CC	3.3
FO *Globorotalia crassacarina*	F	Wm/Wn			~2.5	1120C-1H-CC	6.6
FO *Globorotalia puncticuloides*	F	Wp			3.6	1120B-2H-4, 90-95 cm	6.6
FO *Gephyrocapsa* (small)	N			Miocene/Pliocene	~5-6	1120B-2H-CC	12.8
LO Acme *Dictyococcites antarcticus*	N				~5-6	1120B-2H-CC	12.8
FO *Globorotalia sphericomiozea*	F	m Tk		late Miocene	5.6	1120B-2H-CC	12.8
LO *Globorotalia miotumida*	F	m Tk		late Miocene	5.6	1120B-2H-CC	12.8
LO *Simonseniella barboi*	D				2	1120B-3H-2, 86-87cm	14.5
LO *Hemidiscus triangula*	D				5.3	1120B-3H-2, 86-87cm	14.5
FO *Hemidiscus triangula*	D				5.6	1120B-3H-CC	22.3
LO *Rectuvigerina ongleyi*	F	l Tt		late Miocene	~8	1120B-3H-CC	22.3
FO *Globorotalia juanai*	F	Tt/Tk			6.6	1120B-3H-CC	
LO *Globorotalia* cf. *margaritae*	F				? 4.3	1120B-3H-CC	25.6
LO *Hemidiscus karstenii* f.1	D				5.7	1120B-4H-CC	31.8
FCO *Neogloboquadrina pachyderma*	F	Tt		late Miocene	9.2	1120B-4H-CC	31.8
FO *Prunopyle titan*	R				5.1	1120B-5H-CC	41.3
LO *Globoquadrina dehiscens*	F	e/l Tt			9.9	1120B-9X-CC	
LO *Bolboforma pentaspinosa*	B			late Miocene	~7	1120B-5H-CC	41.3
LO *Helotholus praevema*	R				4.6	1120B-5H-CC	41.3
LO *Cyrtocapsella japonica*	R			late Miocene	10.11	1120B-6H-CC	50.8
Acme *Cyrtocapsella japonica*	R			late Miocene	10.2	1120B-7H-CC	60.3
LO *Bolboforma subfragoris*	B				10.5	1120B-7H-CC	60.3
LO *Denticulopsis dimorpha*	D				10.6	1120B-8H-CC	68.3
LO *Orbulina suturalis*	F	e Tt			~10.5	1120B-9X-CC	72.6
Acme *Globorotalia miotumida* (dextral)	F	e Tt			10.7-10.9	1120B-9X-CC	72.6
FO *Bolboforma pentaspinosa*	B				11.5	1120B-10X-CC	82.2
LO *Coccolithus miopelagicus*	N				10.5	1120B-10X-CC	82.2
LO *Cycladophora humerus*	R				10.5	1120B-10X-CC	82.2
FO Bolboforma subfragoris	B				11.5	1120B-10X-CC	82.2
LO *C. miopelagicus*	N				10.94	1120B-10X-CC	82.2
LCO *Cyrtocapsella tetrapera*	R			middle Miocene	12.6	1120B-11X-CC	91.8
FO *Dendrospyris megalocephalis*	R				12.7	1120B-11X-CC	91.8
LO *Globorotalia praemenardii*	F	Sl/Sw		middle Miocene	13	1120B-12X-CC	101.4
LO *Globorotalia conica* and *G. amuria*	F	Sl/Sw		middle Miocene	13	1120B-12X-CC	101.4
FO *C. macintyrei*	N				12.34	1120B-12X-CC	101.4
FO *Orbulina universa*	F	m Sl			14.5	1120B-12X-CC	
FO *Denticulopsis dimorpha*	D				12.2	1120B-14X-3, 60-61	115
LO *C. premacintyrei*	N			middle Miocene	12.65	1120B-14X-CC	120.6
LO *C. floridanus*	N				12.65	1120B-15X-CC	130.1
FO *Eucyrtidium inflatum*	R			middle Miocene	12.3	1120B-16X-CC	139.8
FO *Orbulina suturalis*	F	Sc/Sl		middle Miocene	15.1	1120B-17X-CC	149.4
LO *Praeorbulina circularis*	F			middle Miocene	14.8	1120B-17X-CC	149.4
FO *Praeorbulina glomerosa*	F	m Sc			15.6	1120B-18X-4, 90-95	
LO *Sphenolithus heteromorphus*	N		NN6	middle Miocene	>13.6	1120B-19X-CC	168.7
FO *Globorotalia praemenardii*	F	m Sc		middle Miocene	15.8	1120B-17X-CC	168.7
FO *Sphenolithus heteromorphus*	N		NN4		18.2	1120B-20X-CC	178.4
LO Acme *Globorotalia zealandica*	F	m/l Pl		early Miocene	16.7	1120B-20X-CC	178.4
LO *Globorotalia praescitula*	F	m/l Pl		early Miocene	16.7	1120B-20X-CC	178.4
FO *Globorotalia miozea*	F	m/l Pl		early Miocene	16.7	1120D-2X-1, 50-55	167.5
LO *C. dissimilis*	N				17.8	1120D-3X-CC	186.3
FO *Eucyrtidium punctatum*	R			early Miocene	17	1120D-3X-CC	186.3
FO *C. leptoporus*	N				18.2	1120D-3X-CC	186.3
FO *C. premacintyrei*	N				17.4	1120D-3X-CC	186.3

Table T3 (continued).

Event	Group	NZ stage	Zone (base)	Epoch	Age (Ma)	Sample	Depth (mbsf)
FO *G. rotula*	N				19.8	1120D-4X-CC	195.9
FO *Globorotalia zealandica*	F	e/m Pl		early Miocene	18.5	1120D-4X-CC	195.9
LO *Globorotalia incognita*	F	e Pl		early Miocene	18.5	1120D-5X-CC	205.5
FO *Globorotalia bella*	F	e Pl		early Miocene	19	1120D-5X-CC	205.5
FO *Globorotalia praescitula*	F	Po/Pl		early Miocene	19	1120D-6X-4, 90-95 cm	205.5
FCO *Helicosphaera carteri*	N			early Miocene	>19.2	1120D-6X-CC	210.1
LO *R. bisecta*	N				24	1120D-7X-CC	215.1
FO *Globigerinoides trilobus*	F	Po/Pl		early Miocene	19	1120D-7X-CC	215.1
FO *Globorotalia incognita*	F	m Po		early Miocene	21.6	1120D-9X-CC	220.7

Notes: N = calcareous nannofossil, F = foraminifer, D = diatom, R = radiolarian, B = bolboformid. Wq = Haweran, Wc = Castlecliffian, Wm = Mangapanian, Wn = Nukumaruan, Wp = Waipipian, Tk = Kapitean, Tt = Tongaporutuan, Sl = Lillburnian, Sw = Waiauan, Sc = Clifdenian, Pl = Altonian, Po = Otaian, e = early, m = middle, l = late. See also Figure F7, p. 46, in the "Explanatory Notes" chapter.

Table T4. Calcareous nannofossil datum levels useful at this site and their assigned age estimates.

Depth* (mbsf)	Event	Age (Ma)	References
1.5	FO *Emiliania huxleyi*	0.24	Naish et al. (1998)
2.8	LO *Pseudoemiliania lacunosa*	0.42	Sato and Kameo (1996)
74.1	LO *Coccolithus miopelagicus*	10.94	Backman and Raffi (1997)
101.3	FO *Calcidiscus macintyrei*	12.34	Raffi and Flores (1995)
101.3	LO *Calcidiscus premacintyrei*	12.65	Raffi and Flores (1995)
125.4	LO *Cyclicargolithus floridanus*	13.19	Raffi and Flores (1995)
166.9	LO *Sphenolithus heteromorphus*	13.52	Backman and Raffi (1997)
166.9	LO Acme *Discoaster deflandrei*	16.21	Raffi and Flores (1995)
174.4	LO *Sphenolithus dissimilis*	17.8	Gartner (1992)
189.8	FO *Calcidiscus premacintyrei*	17.4	Gartner (1992)
199.2	FO *Calcidiscus leptoporus*	18.2	Gartner (1992)
177.0	FO *Sphenolithus heteromorphus*	18.6	Backman et al. (1990)
299.2	FO *Geminilithella rotula*	19.8	Young et al. (1994)
215.6	LO *Ilselithina fusa*	22.3	Gartner (1992)
221.9	FO *Discoaster druggi*	23.2	Berggren et al. (1995)

Note: * = the depth of each datum is assigned at the midpoint between observed samples.

Table T5. Identification and abundance of nannofossils observed at Site 1120.

Core, section, interval (cm)	Depth (mbsf)	*Calcidiscus leptoporus*	*Calcidiscus macintyrei*	*Calcidiscus premacintyrei*	*Coccolithus miopelagicus*	*Coccolithus pelagicus*	*Cyclicargolithus abisectus*	*Cyclicargolithus floridanus*	*Dictyococcites antarcticus*	*Dictyococcites bisectus*	*Dictyococcites productus*	*Discoaster deflandrei*	*Discoaster dilatus*	*Discoaster druggii*	*Discoaster variabilis*	*Emiliania huxleyi*	*Geminilithella rotula*	*Gephyrocapsa* (medium)	*Gephyrocapsa* (small)	*Helicosphaera ampliaperta*	*Helicosphaera carteri*	*Helicosphaera euphratis*	*Helicosphaera intermedia*	*Helicosphaera obliqua*	*Helicosphaera paleocarteri*	*Pontosphaera* spp.	*Pseudoemiliania lacunosa*	*Pyrocyclus* spp.	Reticulofenestra sp. Z	*Reticulofenestra gelida*	*Reticulofenestra* (medium)	*Reticulofenestra pseudoumbilicus*	*Reticulofenestra* (small)	*Scyphosphaera* spp.	*Sphenolithus compactus*	*Sphenolithus dissimilis*	*Sphenolithus heteromorphus*	*Sphenolithus moriformis*	*Syracosphaera* spp.
181-1120A-																																						
1H-1, 0-1	0	A				C					C					A		C	C		F											A						
1H-1, 4-6	0.04	A				F					F					A		C	C		F										R	C						
1H-1, 54-56	0.54	F				C		R								C		A	A		F											A						
1H-2, 28-29	1.78	C				C										F		C	D		C											D						C
1H-2, 85-87	2.35	C																R	A		F																	R
1H-3, 30-31	3.3	C				A													D		C						F						A					
181-1120B-																																						
1H-CC, 11-16	3.31	C				C													D		C						R						C					
181-1120A-																																						
1H-3, 130-132	4.3	A				C				R									D		F						R				A		C					
181-1120B-																																						
2H-CC, 13-18	12.83	F				A			C		F	R							F		F					C						C	C	C				F	
3H-CC, 20-25	17.65	F				C			A												F					R				A		A					C	
4H-CC, 26-31	31.46	F				A			D	R											F							F		C		C					C	
5H-CC, 22-27	41.39	C	C					R	A	R											F							R		C		A					C	
6H-CC, 37-42	51.03	C	F			A															C									C		C						
7H-CC, 18-23	59.41	F	F			C			D												R							F		C		F						
8H-CC, 10-15	68.28					F		R	A		R																	F		D							C	
9X-CC, 8-18	70.77	F	C			F			A												F							F		A		C					F	
10X-CC, 12-22	77.36	C	F		C	C		R	A																													
11X-CC, 18-28	86.55	C	F		C	C		R	C												A											C						
12X-CC, 8-18	99.1	C	R		F	A		C	A								R				C							C				C					F	R
13X-CC, 24-34	103.51	C		C		C		R	A			R	R				R				F							F			A	C					F	
14X-CC, 6-16	117.46	C		F		A	R		A								R				C										A	C					C	
15X-CC, 18-28	126.78	C		A		A		R	A						C		C				C		F								A							
16X-CC, 13-23	138.73	F		C		C		C	C				F		R		C				C										A						F	C
17X-CC, 19-29	148.09			C		A		A	D				R		R		F				C					R		F					A					R	
18X-CC, 13-23	158.53			C		A		A					F				F				C																C	
19X-CC, 38-43	166.88			A				A	C				F				C				C	R				C		F				F	C			R	C	
181-1120D-																																						
1X-CC, 5-15	166.93			C		D		A	F			R	F				F				C					C		R					C					C	
2X-1, 50-55	167.5	R		A		C		A	C				R								C					C					A				F		C	
2X-3, 130-135	171.3	F		C		A		A	A				C								C					C		F			A				F	F	C	
2X-4, 60-65	172.1	F		F		A		C	C			R	C				F				C	F				F		F			A	C				F	C	
2X-CC, 24-29	176.68	C		C		A	R	C	A			A	C				C				A	C	R	R				F								R		A	
181-1120B-																																						
20X-CC, 7-17	177.04	F		C		C		C	A			C	C				F				F	F	R					R								C	C	
21X-CC, 20-30	184.45	C		R		A	R	A	D	R		R	R				R								R			R			C	C	A				C	
181-1120D-																																						
3X-CC, 21-26	184.93	C		F		A		A	D											R	A	F			R	R		F			A						C	
4X-CC, 10-20	194.68	F				A	R	C	A				F				F				C	R			R			F				F				R		C	
5X-CC, 22-27	203.62					A		C				C	C												R			F			A						C	
7X-CC, 20-35	213.5					A	C	A	C			C	F	C														F	A		C						C	
6X-CC, 12-22	214.12					C		C	A			C														F		F	C		A						C	
8X-CC, 12-22	221.75					A		A	A			C	C	C														C			F						C	
9X-CC, 18-28	221.86					A		A	D				F	C														C			F						C	

Note: Abundance of species: D = dominant, A = abundant, C = common, F = few, and R = rare.

Table T6. Identification and abundance of planktonic foraminifers observed at Site 1120. (**See table note.** Continued on next page.)

Core, section, interval (cm)	Depth (mbsf)	NZ stage	Epoch	*Bolboforma pentaspinosa*	*Bolboforma subfragoris*	*Catapsydrax dissimilis*	*Catapsydrax unicavus*	*Dentoglobigerina altispira altispira*	*Fohsella peripheroronda*	*Globigerina bulloides*	*Globigerina euapertura*	*Globigerina praebulloides*	*Globigerina quinqueloba*	*Globigerina* spp.	*Globigerina umbilicata*	*Globigerinella aequilateralis*	*Globigerinita glutinata*	*Globigerinoides trilobus*	*Globoquadrina dehiscens*	*Globoquadrina venezuelana*	*Globorotalia amuria*	*Globorotalia conica*	*Globorotalia crassaformis crassacarina*	*Globorotalia crassaformis* (sinistral)	*Globorotalia crassula*	*Globorotalia explicationis*	*Globorotalia incognita*	*Globorotalia inflata*	*Globorotalia juanai*	*Globorotalia miotumida*	*Globorotalia miozea*	*Globorotalia* cf. *panda*	*Globorotalia panda*	*Globorotalia praemenardii*	*Globorotalia praescitula*	*Globorotalia puncticulata*	*Globorotalia puncticuloides*	*Globorotalia scitula*	*Globorotalia sphericomiozea*	*Globorotalia truncatulinoides*	*Globorotalia zealandica*	*Neogloboquadrina acostaensis*	*Neogloboquadrina dutertrei*	*Neogloboquadrina humerosa*	*Neogloboquadrina pachyderma*	*Orbulina suturalis*	*Orbulina universa*	*Paragloborotalia bella*	*Paragloborotalia continuosa*	*Paragloborotalia mayeri*	*Praeorbulina circularis*	*Sphaeroidinellopsis disjuncta*	*Zeaglobigerina woodi*
181-1120A-																																																		
1H-1, 4-6	0.04	Wn-Wq	late Quaternary							F																	R									R				F										
1H-2, 85-87	2.35	Wn-Wq	late Quaternary								R													R			R									P								P						
1H-3, 130-132	4.3	Wn-Wc	Pliocene–early Pleistocene							F			F										R	R									F							F									
1H-CC, 8-18	4.5	Wn-Wc	Pliocene–early Pleistocene										R	F									P	R									R																
181-1120B-																																																			
1H-CC, 11-16	3.31	Wn-Wc	Pliocene–early Pleistocene							F			R	A								P	P					P						R	F															
181-1120C-																																																			
1H-CC, 10-20	6.49	Wn-Wc	Pliocene–early Pleistocene							A			F	D									P	R									F									R								
181-1120B-																																																			
2H-CC, 13-18	12.83	Tk	late Miocene							A			R	F												P				R								R												
181-1120C-																																																			
2H-CC, 8-18	15.62	Tk	late Miocene											D															P	R							R			P	R								
181-1120B-																																																			
3H-CC, 20-25	17.65	Tt-e Tk	late Miocene											A															R			R																	
181-1120C-																																																			
3H-CC, 20-30	25.51	Tt-e Tk	late Miocene							D				D	F															R												R			P			R	
181-1120B-																																																		
4H-3, 35-37	25.65	Tt-e Tk	late Miocene							A				A																R		R										F		R			P		R
4H-3, 129-132	26.59	Tt-e Tk	late Miocene							F				A																		F										A					P		R
181-1120C-																																																		
4H-CC, 13-23	35.45	Tt-e Tk	late Miocene											D																																					
181-1120B-																																																		
5H-CC, 22-27	41.39	Tt-e Tk	late Miocene	A						R			R			P														R																P			R	
181-1120C-																																																		
5H-CC, 0-10	44.78	Tt-e Tk	late Miocene											D																																					
181-1120B-																																																		
7H-CC, 18-23	59.41	Tt-e Tk	late Miocene	F	F																									R			P																
8H-CC, 10-15	68.28	e Tt	late Miocene		A					R																				R																			R
9X-CC, 8-18	70.77	e Tt	late Miocene	A						F			R						P											P			P										R	P	P			P		R
10X-CC, 12-22	77.36	Sw-e Tt	late Miocene	F	F					R																				P			R					R					P	P	P			P		

Table T6 (continued).

Core, section, interval (cm)	Depth (mbsf)	NZ stage	Epoch	*Bolboforma pentaspinosa*	*Bolboforma subfragoris*	*Catapsydrax dissimilis*	*Catapsydrax unicavus*	*Dentoglobigerina altispira altispira*	*Fohsella peripheroronda*	*Globigerina bulloides*	*Globigerina euapertura*	*Globigerina praebulloides*	*Globigerina quinqueloba*	*Globigerina* spp.	*Globigerina umbilicata*	*Globigerinella aequilateralis*	*Globigerinita glutinata*	*Globigerinoides trilobus*	*Globoquadrina dehiscens*	*Globoquadrina venezuelana*	*Globorotalia amuria*	*Globorotalia conica*	*Globorotalia crassacarina*	*Globorotalia crassaformis* (sinistral)	*Globorotalia crassula*	*Globorotalia explicationis*	*Globorotalia incognita*	*Globorotalia inflata*	*Globorotalia juanai*	*Globorotalia miotumida*	*Globorotalia miozea*	*Globorotalia* cf. *panda*	*Globorotalia panda*	*Globorotalia praemenardii*	*Globorotalia praescitula*	*Globorotalia puncticulata*	*Globorotalia puncticuloides*	*Globorotalia scitula*	*Globorotalia sphericomiozea*	*Globorotalia truncatulinoides*	*Globorotalia zealandica*	*Neogloboquadrina acostaensis*	*Neogloboquadrina dutertrei*	*Neogloboquadrina humerosa*	*Neogloboquadrina pachyderma*	*Orbulina suturalis*	*Orbulina universa*	*Paragloborotalia bella*	*Paragloborotalia continuosa*	*Paragloborotalia mayeri*	*Praeorbulina circularis*	*Sphaeroidinellopsis disjuncta*	*Zeaglobigerina woodi*
12X-CC, 8-18	99.1	Sl-Sw	middle Miocene						P	R				F							P	R			P				F															P			R
16X-CC, 13-23	138.73	Sl	middle Miocene							R												P							R														R			P			F
17X-19-29	148.09	l Sc-e Sl	middle Miocene							F				F							R								R														P			P	P		F
18X-CC, 13-23	158.53	Sc-Sl	middle Miocene							F								P												R																				F
19X-CC, 38-43	166.88	Sc-Sl	middle Miocene						P	R									P											R																				R
20X-CC, 7-17	177.04	m/l Pl	early Miocene							R		P		A					P											R					R							P						R	F
21X-CC, 20-30	184.45	m Pl	early Miocene									P		A				R																P							P							F
181-1120D-																																																		
2X-1, 50-55	167.5	m Pl	early Miocene					P					R	A	P				R											P																		P			
2X-6, 126-131	175.76	m Pl	early Miocene				P							A				F		R										P				F							P						P			R
3X-CC, 21-26	184.93	m Pl	early Miocene															P																R							P								F
4X-CC, 10-20	194.68	m Pl	early Miocene									R																						R							R								F
5X-CC, 22-27	203.62	e Pl	early Miocene							F				A					F	P						P								P												P			R	F
6X-CC, 12-22	214.12	l Po	early Miocene				P							A																																			R		
7X-CC, 20-35	213.5	l Po	early Miocene											A				P								P																							P		
8X-CC, 12-22	221.75	l Po	early Miocene			P				F	P	R		A			P		F							P																									F
9X-CC, 18-28	221.86	l Po	early Miocene								P	R		A					R							P																										

Notes: New Zealand stages: Wn = Nukumaruan, Wq = Haweran, Wc = Castlecliffian, Tk = Kapitean, Sw = Waiauan, e = early, m = middle, l = late. Abundance of species: D = dominant, A = abundant, F = few/frequent, R = rare, and P = present.

Table T7. Identification and abundance of diatoms observed at Site 1120.

Core, section, interval (cm)	Depth (mbsf)	Abundance of diatom valves	*Actinocyclus ingens*	*Actinocyclus ingens* var. *planus*	*Actinocyclus karstenii*	*Azpeitia endoi*	*Azpeitia tabularis*	*Bladulphia tuomeyi*	*Cestodiscus reticulatus*	*Coscinodiscus marginatus*	*Coscinodiscus radiatus*	*Denticulopsis dimorpha*	*Denticulopsis hustedtii*	*Denticulopsis meridionalis*	*Diploneis* sp.	*Eucampia balaustium*	*Hemiaulus* sp.	*Hemidiscus karstenii* f.1	*Hemidiscus triangularis*	*Hyalodiscus* sp.	*Neobrunia mirabilis*	*Nitzschia barronii*	*Nitzschia kerguelensis*	*Nitzschia kolbackeckii*	*Nitzschia panduliformis*	*Nitzschia ritscherii*	*Paralia sulcata*	*Pseudopodosira* sp.	*Pyxilla proboscidea*	*Rhizosolenia hebetata* f. *hiemalis*	*Simonseniella barboi*	*Stephanopyxis turris intermedia*	*Stephanopyxis turris turris*	*Thalassionema nitzschioides*	*Thalassionema nitzschioides* var. *parva*	*Thalassiosira insigna*	*Thalassiosira inura*	*Thalassiosira lentiginosa*	*Thalassiosira oestrupii*	*Thalassiothrix longissima*	*Xanthiopyxis ovalis*	*Xanthiopyxis* sp.	Sponge spicules
181-1120A-																																										
1H-1, 0-1	0	B																																								R
1H-1, 4-6	0.04	B																																								C
1H-1, 29-31	0.29	T																																			T					C
1H-1, 54-56	0.54	B																																								R
1H-2, 85-87	2.35	B																																								T
1H-3, 130-132	4.3	R																																			R					A
1H-CC, 8-18	4.5	F	R													R				F		R	T			R				F						R	R	T	R		F
181-1120B-																																										
1H-CC, 11-16	3.31	T																																								R
2H-CC, 13-18	12.83	R								T																																R
3H-CC, 20-25	17.65	C			T					T									C							T				T	C				T					R
4H-CC, 26-31	31.46	F	T				T			F	T			T				T		T										T			R			R					A
5H-CC, 22-27	41.39	C	R				R						T	T				R												R	R				R			R	T		C
6H-CC, 37-42	51.03	F	F				R		T				R				T	T															T					F			A
7H-CC, 18-23	59.41	F	R															T												F								F			C
8H-CC, 10-15	68.28	C	F									C																R		R							F	F			C
9X-CC, 8-18	70.77	C		T						R		C	R	T									T				R			T								R			C
10X-CC, 12-22	77.36	C	F	T		F	R			R		C	R										R	T		R	R		T								F			C
11X-CC, 18-28	86.55	R	F	F								F	T														R										F			C
12X-CC, 8-18	99.1	R								T													T				F	R													A
13X-CC, 24-34	103.51	R		T																													R								C
14X-3, 60-60	114.6	F	R			T				F		T	F																								F	T			C
14X-3, 84-85	114.84	T																																				T			C
14X-CC, 6-16	117.46	T																																							C
15X-CC, 18-28	126.78	R									T												R							T							T			C
16X-CC, 13-23	138.73	R															R						R				T										T	R		C
17X-CC, 19-29	148.09	R							T								R						R														R			A
18X-CC, 13-23	158.53	T																																							F
19X-CC, 38-43	166.88	B																																							F
20X-CC, 7-17	177.04	B																																							R
21X-CC, 20-30	184.45	T																																							C
181-1120D-																																									
1X-CC, 5-15	166.93	B																																								T
2X-CC, 24-29	176.68	B																																								R
3X-CC, 21-26	184.93	T						T																									T								F
4X-CC, 10-20	194.68	B																																								B
5X-CC, 22-27	203.62	B																																								B
6X-CC, 12-22	214.12	B																																								B
7X-CC, 20-35	213.5	B																																								B
8X-CC, 12-22	221.75	B																																								B
9X-CC, 18-28	221.86	B																																								B

Note: Total and relative abundance of diatoms: A = abundant, C = common, F = few, R = rare, T = trace, and B = barren.

Table T8. Identification and abundance of radiolarians observed at Site 1120. (**See table note.** Continued on next three pages.)

Core, section, interval (cm)	Depth (mbsf)	Preservation	Group abundance	*Actinomma popofskii*	*Actinomma* sp.	*Actinomma* sp. A	*Actinomma* sp. B	*Actinomma* sp. C	*Antarctissa denticulata*	*Antarctissa longa*	*Antarctissa strelkovi*	*Anthocyrtidium* sp.	*Axoprunum angelinum*	*Botryostrobus aquilonaris*	*Botryostrobus* sp.	*Calocyclas* sp. A	*Carpocanistrum* sp.	*Carpocanopsis bramlettei*	*Carpocanopsis* sp.	*Cenosphaera* sp.	*Cenosphaera* sp. (large)	*Cenosphaera* sp. (small)	*Ceratocyrtis* sp.	*Cycladophora bicornis amphora*	*Cycladophora humerus*	*Cycladophora* sp.	*Cyrtocapsella cornuta*	*Cyrtocapsella elongata*	*Cyrtocapsella japonica*	*Cyrtocapsella* sp.	*Cyrtocapsella tetrapera*	*Dendrospyris megalocephalis*	*Diartus* sp. C	*Diartus* sp.	*Dictyophimus* sp.	*Disolenia* sp.	*Druppatractus irregularis*	*Druppatractus* sp.	*Euchitonia* sp.	*Eucyrtidium calvertense*	*Eucyrtidium cienkowskii* group	*Eucyrtidium inflatum*	*Eucyrtidium punctatum*	*Eucyrtidium* sp.	*Eucyrtidium teuscheri teuscheri*	*Gondwanaria* sp.	*Heliodiscus asteriscus*	*Helotholus praevema*	*Hexacontium* sp.	*Hexalonche philosophica*	*Lamprocyrtis maritaris*
181-1120A-																																																	
1H-1, 4-6	0.04	M	R		R																																												
1H-1, 29-31	0.29		B																																														
1H-1, 54-56	0.54	G	T																																														
1H-2, 85-87	2.35		B																																														
1H-CC, 8-18	4.5	G	C	F	R				C	F	A			T			R									T																				R			
181-1120B-																																																	
1H-CC, 11-16	3.31		B																																														
2H-CC, 13-18	12.83		T																																														
3H-CC, 20-25	17.65	G	C		A							T																																			T	R		
4H-3, 129-132	26.59																																																	
4H-CC, 26-31	31.46	VG	C		C	A											R									R																						
5H-CC, 22-27	41.39	G	C				A								R				A				R	C		R							R	F											C	R		R	
6H-CC, 37-42	51.03	G	C				A											F						T					C																	R			
7H-CC, 18-23	59.41	G	C		A		A	R									R							R					A						T			R		T				T		R			
8H-CC, 10-15	68.28	G	C				A										F							F					A								C	R		R					C			R
9X-CC, 8-18	70.77	G	C		R												R												A								R	T	F	R									
10X-CC, 12-22	77.36	M	C														T						R	F	R			R	C								C	C	C	F			R		R		F		
11X-CC, 18-28	86.55	G	C		R												R									C			R		A	T	C			R	R	A								R			
12X-CC, 8-18	99.1	G	F																						R					R								R											
13X-CC, 24-34	103.51	G	F																											T				R			F	F							T			
14X-3, 60-60	114.6	M	F																											C				F				R								T			
14X-3, 84-85	114.84	M	R		R								T																	T				R			T												
14X-CC, 6-16	117.46	M	F																											R								F											
15X-CC, 18-28	126.78	M	R																											F								R											
16X-CC, 13-23	138.73	G	C										R				R						R				R		R	A							F			R			R			R			
17X-CC, 19-29	148.09	G	C		F												R													C							C								R	T	F	
18X-CC, 13-23	158.53	G	C														T			A							A			C							C				A			T		R		R	
19X-CC, 38-43	166.88	G	T																	R																	R												
20X-CC, 7-17	177.04		B																																														
21X-CC, 20-30	184.45	P	R													T	T				A	A							T	R							R												

Table T8 (continued).

Core, section, interval (cm)	Depth (mbsf)	Preservation	Group abundance	*Larcopyle* sp.	*Lithelius minor*	*Lithelius nautiloides*	*Lithopera neotera*	*Lithopera?* form A	*Lophocyrtis* (*Cyclampterium*) sp.	*Lychnocanoma conica*	*Lychnocanoma elongata*	*Lychnocanoma* sp.	*Lychnocanoma* sp. B	*Nassellaria* form B	*Periphaena* sp.	*Peripyramis* sp.	*Phormospyris stabilis*	*Phorticium clevei*	*Prunopyle* sp.	*Prunopyle titan*	*Pterocanium* sp.	*Pterocanium trilobum*	*Pylospira* sp.	*Siphocampe grantmackiei*	*Siphocampe* sp.	*Siphonosphaera* sp.	*Spongodiscus osculosus*	*Spongodiscus* sp.	*Spongoplegma antarcticum*	*Spongotrochus glacialis*	*Spumellaria* form A	*Stichocorys* sp.	*Stichocorys delmontensis*	*Stichocorys peregrina*	*Stylacontarium acquilonium*	*Stylacontarium bispiculum*	*Stylatractus* sp.	*Stylatractus universus*	*Stylodictya* sp.	*Tetrapyle octacantha*	*Thecosphaera miocenica*	*Thecosphaera* sp.	*Thecosphaera* sp. (large)	*Thecosphaera* sp. (small)	*Theocorythium* sp.	*Theocorythium vetulum*	*Triceraspyris antarctica*	*Triceraspyris coronata*	*Triceraspyris* sp.
181-1120A-																																															
1H-1, 4-6	0.04	M	R																										R								T										
1H-1, 29-31	0.29		B																																												
1H-1, 54-56	0.54	G	T																										R																			
1H-2, 85-87	2.35		B																																												
1H-CC, 8-18	4.5	G	C	A		A												F			R						T	A	F	R							T							T	R	R	
181-1120B-																																															
1H-CC, 11-16	3.31		B	T																																											
2H-CC, 13-18	12.83		T																																												
3H-CC, 20-25	17.65	G	C	R											R													F			F		R			T							F				
4H-3, 129-132	26.59																																														
4H-CC, 26-31	31.46	VG	C												R	T						T									R				A	R	T	R							
5H-CC, 22-27	41.39	G	C	R								T			R					R								A							F			T	T		A			R			F
6H-CC, 37-42	51.03	G	C	R								T																R							F	R		T		C					R	T
7H-CC, 18-23	59.41	G	C	R				R				R				T	T		R				R											R	T		R		A				R	R	
8H-CC, 10-15	68.28	G	C	F				R				F					F											R							C	C		R		R	R			C		
9X-CC, 8-18	70.77	G	C		R			A								R	F						T					F							C	R		F		A						
10X-CC, 12-22	77.36	M	C	C			F					R					F		R									A			R				R	F		C				A	A			
11X-CC, 18-28	86.55	G	C	F				R																				F							F	F				A		A				
12X-CC, 8-18	99.1	G	F											F														F							R					A	C						
13X-CC, 24-34	103.51	G	F	F										F														F							F	R	T			C			R				
14X-3, 60-60	114.6	M	F	R										R									R					F										R			R						
14X-3, 84-85	114.84	M	R																																T						R						
14X-CC, 6-16	117.46	M	F											R																					R	R											
15X-CC, 18-28	126.78	M	R	R																			R												R	R											
16X-CC, 13-23	138.73	G	C	R									R				R						R		R								R	R	A	T		R		A						
17X-CC, 19-29	148.09	G	C						R	F	T		R				R						F	R		T									A			R		A						
18X-CC, 13-23	158.53	G	C	R					T	R	R	R					R								T	C			R						A	R										
19X-CC, 38-43	166.88	G	T																																												
20X-CC, 7-17	177.04		B																																												
21X-CC, 20-30	184.45	P	R	R																								R							R					R							

Table T8 (continued).

Core, section, interval (cm)	Depth (mbsf)	Preservation	Group abundance	*Actinomma popofskii*	*Actinomma* sp.	*Actinomma* sp. A	*Actinomma* sp. B	*Actinomma* sp. C	*Antarctissa denticulata*	*Antarctissa longa*	*Antarctissa strelkovi*	*Anthocyrtidium* sp.	*Axoprunum angelinum*	*Botryostrobus aquilonaris*	*Botryostrobus* sp.	*Calocyclas* sp. A	*Carpocanistrum* sp.	*Carpocanopsis bramlettei*	*Carpocanopsis* sp.	*Cenosphaera* sp.	*Cenosphaera* sp. (large)	*Cenosphaera* sp. (small)	*Ceratocyrtis* sp.	*Cycladophora bicornis amphora*	*Cycladophora humerus*	*Cycladophora* sp.	*Cyrtocapsella cornuta*	*Cyrtocapsella elongata*	*Cyrtocapsella japonica*	*Cyrtocapsella* sp.	*Cyrtocapsella tetrapera*	*Dendrospyris megalocephalis*	*Diartus* sp. C	*Diartus* sp.	*Dictyophimus* sp.	*Disolenia* sp.	*Druppatractus irregularis*	*Druppatractus* sp.	*Euchitonia* sp.	*Eucyrtidium calvertense*	*Eucyrtidium cienkowskii* group	*Eucyrtidium inflatum*	*Eucyrtidium punctatum*	*Eucyrtidium* sp.	*Eucyrtidium teuscheri teuscheri*	*Gondwanaria* sp.	*Heliodiscus asteriscus*	*Helotholus praevema*	*Hexacontium* sp.	*Hexaloncha philosophica*	*Lamprocyrtis maritaris*
181-1120D-																																																		
1X-CC, 5-15	166.93	M	T																																																
2X-CC, 24-29	176.68		B																																																
3X-CC, 21-26	184.93	P	C		R												T													R					R		F				C					T			
4X-CC, 10-20	194.68		B																																															
5X-CC, 22-27	203.62		B																																															
6X-CC, 12-22	214.12		B																																															
7X-CC, 20-35	213.5		B																																															
8X-CC, 12-22	221.75		T														T																																	
9X-CC, 18-28	221.86		B																																															

Note: Preservation: VG = very good, G = good, M = moderate, and P = poor; total (group) and relative abundance of radiolarians: C = common, F = few, R = rare, T = trace, and B = barren.

Table T8 (continued).

Core, section, interval (cm)	Depth (mbsf)	Preservation	Group abundance	*Larcopyle* sp.	*Lithelius minor*	*Lithelius nautiloides*	*Lithopera neotera*	*Lithopera?* form A	*Lophocyrtis* (*Cyclampterium*) sp.	*Lychnocanoma conica*	*Lychnocanoma elongata*	*Lychnocanoma* sp.	*Lychnocanoma* sp. B	*Nassellaria* form B	*Periphaena* sp.	*Peripyramis* sp.	*Phormospyris stabilis*	*Phorticium clevei*	*Prunopyle* sp.	*Prunopyle titan*	*Pterocanium* sp.	*Pterocanium trilobum*	*Pylospira* sp.	*Siphocampe grantmackiei*	*Siphocampe* sp.	*Siphonosphaera* sp.	*Spongodiscus osculosus*	*Spongodiscus* sp.	*Spongoplegma antarcticum*	*Spongotrochus glacialis*	*Spumellaria* form A	*Stichocorys* sp.	*Stichocorys delmontensis*	*Stichocorys peregrina*	*Stylacontarium acquilonium*	*Stylacontarium bispiculum*	*Stylatractus* sp.	*Stylatractus universus*	*Stylodictya* sp.	*Tetrapyle octacantha*	*Thecosphaera miocenica*	*Thecosphaera* sp.	*Thecosphaera* sp. (large)	*Thecosphaera* sp. (small)	*Theocorythium* sp.	*Theocorythium vetulum*	*Triceraspyris antarctica*	*Triceraspyris coronata*	*Triceraspyris* sp.
181-1120D-																																																
1X-CC, 5-15	166.93	M	T																																					R								
2X-CC, 24-29	176.68		B																																														
3X-CC, 21-26	184.93	P	C	R								F				R												R							A				R			R	A	A				
4X-CC, 10-20	194.68		B																																													
5X-CC, 22-27	203.62		B																																													
6X-CC, 12-22	214.12		B																																													
7X-CC, 20-35	213.5		B																																													
8X-CC, 12-22	221.75		T																																													
9X-CC, 18-28	221.86		B																																													

Table T9. Composite depth section, Site 1120. (See table note. Continued on next three pages.)

Leg	Site	Hole	Core	Type	Section	Section length (m)	Depth (mbsf)	Offset (m)	Composite depth (mcd)
181	1120	A	1	H	1	1.50	0.00	0.00	0.00
181	1120	A	1	H	2	1.50	1.50	0.00	1.50
181	1120	A	1	H	3	1.42	3.00	0.00	3.00
181	1120	A	1	H	CC	0.18	4.42	0.00	4.42
181	1120	B	1	H	1	1.50	0.00	0.00	0.00
181	1120	B	1	H	2	1.50	1.50	0.00	1.50
181	1120	B	1	H	3	0.20	3.00	0.00	3.00
181	1120	B	1	H	CC	0.16	3.20	0.00	3.20
181	1120	B	2	H	1	1.50	3.30	0.44	3.74
181	1120	B	2	H	2	1.50	4.80	0.44	5.24
181	1120	B	2	H	3	1.50	6.30	0.44	6.74
181	1120	B	2	H	4	1.50	7.80	0.44	8.24
181	1120	B	2	H	5	1.50	9.30	0.44	9.74
181	1120	B	2	H	6	1.50	10.80	0.44	11.24
181	1120	B	2	H	7	0.40	12.30	0.44	12.74
181	1120	B	2	H	CC	0.18	12.70	0.44	13.14
181	1120	B	3	H	1	1.50	12.80	1.80	14.60
181	1120	B	3	H	2	1.50	14.30	1.80	16.10
181	1120	B	3	H	3	1.40	15.80	1.80	17.60
181	1120	B	3	H	4	0.25	17.20	1.80	19.00
181	1120	B	3	H	CC	0.25	17.45	1.80	19.25
181	1120	B	4	H	1	1.50	22.30	–0.94	21.36
181	1120	B	4	H	2	1.50	23.80	–0.94	22.86
181	1120	B	4	H	3	1.45	25.30	–0.94	24.36
181	1120	B	4	H	4	1.45	26.75	–0.94	25.81
181	1120	B	4	H	5	1.50	28.20	–0.94	27.26
181	1120	B	4	H	6	1.50	29.70	–0.94	28.76
181	1120	B	4	H	CC	0.31	31.20	–0.94	30.26
181	1120	B	5	H	1	1.50	31.80	0.45	32.25
181	1120	B	5	H	2	1.50	33.30	0.45	33.75
181	1120	B	5	H	3	1.50	34.80	0.45	35.25
181	1120	B	5	H	4	1.50	36.30	0.45	36.75
181	1120	B	5	H	5	1.50	37.80	0.45	38.25
181	1120	B	5	H	6	1.50	39.30	0.45	39.75
181	1120	B	5	H	7	0.37	40.80	0.45	41.25
181	1120	B	5	H	CC	0.27	41.17	0.45	41.62
181	1120	B	6	H	1	1.50	41.30	1.41	42.71
181	1120	B	6	H	2	1.50	42.80	1.41	44.21
181	1120	B	6	H	3	1.50	44.30	1.41	45.71
181	1120	B	6	H	4	1.50	45.80	1.41	47.21
181	1120	B	6	H	5	1.50	47.30	1.41	48.71
181	1120	B	6	H	6	1.50	48.80	1.41	50.21
181	1120	B	6	H	7	0.36	50.30	1.41	51.71
181	1120	B	6	H	CC	0.42	50.66	1.41	52.07
181	1120	B	7	H	1	1.50	50.80	1.41	52.21
181	1120	B	7	H	2	1.50	52.30	1.41	53.71
181	1120	B	7	H	3	1.50	53.80	1.41	55.21
181	1120	B	7	H	4	1.50	55.30	1.41	56.71
181	1120	B	7	H	5	1.50	56.80	1.41	58.21
181	1120	B	7	H	6	0.93	58.30	1.41	59.71
181	1120	B	7	H	CC	0.23	59.23	1.41	60.64
181	1120	B	8	H	1	1.50	60.30	1.41	61.71
181	1120	B	8	H	2	1.50	61.80	1.41	63.21
181	1120	B	8	H	3	1.50	63.30	1.41	64.71
181	1120	B	8	H	4	1.50	64.80	1.41	66.21
181	1120	B	8	H	5	1.50	66.30	1.41	67.71
181	1120	B	8	H	6	0.38	67.80	1.41	69.21
181	1120	B	8	H	CC	0.15	68.18	1.41	69.59
181	1120	B	9	X	1	1.50	68.30	1.41	69.71
181	1120	B	9	X	2	0.89	69.80	1.41	71.21
181	1120	B	9	X	CC	0.18	70.69	1.41	72.10
181	1120	B	10	X	1	1.50	72.60	1.41	74.01
181	1120	B	10	X	2	1.50	74.10	1.41	75.51
181	1120	B	10	X	3	1.50	75.60	1.41	77.01
181	1120	B	10	X	4	0.14	77.10	1.41	78.51
181	1120	B	10	X	CC	0.22	77.24	1.41	78.65
181	1120	B	11	X	1	1.50	82.20	1.41	83.61

Table T9 (continued).

Leg	Site	Hole	Core	Type	Section	Section length (m)	Depth (mbsf)	Offset (m)	Composite depth (mcd)
181	1120	B	11	X	2	1.50	83.70	1.41	85.11
181	1120	B	11	X	3	1.17	85.20	1.41	86.61
181	1120	B	11	X	CC	0.28	86.37	1.41	87.78
181	1120	B	12	X	1	1.50	91.80	1.41	93.21
181	1120	B	12	X	2	1.50	93.30	1.41	94.71
181	1120	B	12	X	3	1.50	94.80	1.41	96.21
181	1120	B	12	X	4	1.50	96.30	1.41	97.71
181	1120	B	12	X	5	1.22	97.80	1.41	99.21
181	1120	B	12	X	CC	0.18	99.02	1.41	100.43
181	1120	B	13	X	1	1.50	101.40	1.41	102.81
181	1120	B	13	X	2	0.37	102.90	1.41	104.31
181	1120	B	13	X	CC	0.34	103.27	1.41	104.68
181	1120	B	14	X	1	1.50	111.00	1.41	112.41
181	1120	B	14	X	2	1.50	112.50	1.41	113.91
181	1120	B	14	X	3	1.50	114.00	1.41	115.41
181	1120	B	14	X	4	1.50	115.50	1.41	116.91
181	1120	B	14	X	5	0.40	117.00	1.41	118.41
181	1120	B	14	X	CC	0.16	117.40	1.41	118.81
181	1120	B	15	X	1	1.50	120.60	1.41	122.01
181	1120	B	15	X	2	1.50	122.10	1.41	123.51
181	1120	B	15	X	3	1.50	123.60	1.41	125.01
181	1120	B	15	X	4	1.50	125.10	1.41	126.51
181	1120	B	15	X	CC	0.28	126.60	1.41	128.01
181	1120	B	16	X	1	1.50	130.10	1.41	131.51
181	1120	B	16	X	2	1.50	131.60	1.41	133.01
181	1120	B	16	X	3	1.50	133.10	1.41	134.51
181	1120	B	16	X	4	1.50	134.60	1.41	136.01
181	1120	B	16	X	5	1.50	136.10	1.41	137.51
181	1120	B	16	X	6	1.00	137.60	1.41	139.01
181	1120	B	16	X	CC	0.23	138.60	1.41	140.01
181	1120	B	17	X	1	1.40	139.80	1.41	141.21
181	1120	B	17	X	2	1.50	141.20	1.41	142.61
181	1120	B	17	X	3	1.50	142.70	1.41	144.11
181	1120	B	17	X	4	1.50	144.20	1.41	145.61
181	1120	B	17	X	5	1.50	145.70	1.41	147.11
181	1120	B	17	X	6	0.70	147.20	1.41	148.61
181	1120	B	17	X	CC	0.29	147.90	1.41	149.31
181	1120	B	18	X	1	1.50	149.40	1.41	150.81
181	1120	B	18	X	2	1.50	150.90	1.41	152.31
181	1120	B	18	X	3	1.50	152.40	1.41	153.81
181	1120	B	18	X	4	1.50	153.90	1.41	155.31
181	1120	B	18	X	5	1.50	155.40	1.41	156.81
181	1120	B	18	X	6	1.50	156.90	1.41	158.31
181	1120	B	18	X	CC	0.23	158.40	1.41	159.81
181	1120	B	19	X	1	1.50	159.00	1.41	160.41
181	1120	B	19	X	2	1.50	160.50	1.41	161.91
181	1120	B	19	X	3	1.50	162.00	1.41	163.41
181	1120	B	19	X	4	1.50	163.50	1.41	164.91
181	1120	B	19	X	5	1.50	165.00	1.41	166.41
181	1120	B	19	X	CC	0.43	166.50	1.41	167.91
181	1120	B	20	X	1	1.50	168.70	–0.69	168.01
181	1120	B	20	X	2	1.50	170.20	–0.69	169.51
181	1120	B	20	X	3	1.50	171.70	–0.69	171.01
181	1120	B	20	X	4	1.50	173.20	–0.69	172.51
181	1120	B	20	X	5	1.50	174.70	–0.69	174.01
181	1120	B	20	X	6	0.77	176.20	–0.69	175.51
181	1120	B	20	X	CC	0.17	176.97	–0.69	176.28
181	1120	B	21	X	1	1.50	178.40	–0.69	177.71
181	1120	B	21	X	2	1.50	179.90	–0.69	179.21
181	1120	B	21	X	3	1.50	181.40	–0.69	180.71
181	1120	B	21	X	4	1.35	182.90	–0.69	182.21
181	1120	B	21	X	CC	0.30	184.25	–0.69	183.56
181	1120	C	1	H	1	1.50	0.00	–0.24	–0.24
181	1120	C	1	H	2	1.50	1.50	–0.24	1.26
181	1120	C	1	H	3	1.50	3.00	–0.24	2.76
181	1120	C	1	H	4	1.50	4.50	–0.24	4.26
181	1120	C	1	H	5	0.39	6.00	–0.24	5.76
181	1120	C	1	H	CC	0.20	6.39	–0.24	6.15
181	1120	C	2	H	1	1.50	6.60	2.66	9.26
181	1120	C	2	H	2	1.50	8.10	2.66	10.76

Table T9 (continued).

Leg	Site	Hole	Core	Type	Section	Section length (m)	Depth (mbsf)	Offset (m)	Composite depth (mcd)
181	1120	C	2	H	3	1.50	9.60	2.66	12.26
181	1120	C	2	H	4	1.50	11.10	2.66	13.76
181	1120	C	2	H	5	1.50	12.60	2.66	15.26
181	1120	C	2	H	6	1.44	14.10	2.66	16.76
181	1120	C	2	H	CC	0.18	15.54	2.66	18.20
181	1120	C	3	H	1	1.50	16.10	2.90	19.00
181	1120	C	3	H	2	1.50	17.60	2.90	20.50
181	1120	C	3	H	3	1.50	19.10	2.90	22.00
181	1120	C	3	H	4	1.50	20.60	2.90	23.50
181	1120	C	3	H	5	1.50	22.10	2.90	25.00
181	1120	C	3	H	6	1.41	23.60	2.90	26.50
181	1120	C	3	H	7	0.30	25.01	2.90	27.91
181	1120	C	3	H	CC	0.30	25.31	2.90	28.21
181	1120	C	4	H	1	1.50	25.60	3.49	29.09
181	1120	C	4	H	2	1.50	27.10	3.49	30.59
181	1120	C	4	H	3	1.50	28.60	3.49	32.09
181	1120	C	4	H	4	1.50	30.10	3.49	33.59
181	1120	C	4	H	5	1.50	31.60	3.49	35.09
181	1120	C	4	H	6	1.50	33.10	3.49	36.59
181	1120	C	4	H	7	0.72	34.60	3.49	38.09
181	1120	C	4	H	CC	0.23	35.32	3.49	38.81
181	1120	C	5	H	1	1.50	35.10	2.99	38.09
181	1120	C	5	H	2	1.50	36.60	2.99	39.59
181	1120	C	5	H	3	1.50	38.10	2.99	41.09
181	1120	C	5	H	4	1.50	39.60	2.99	42.59
181	1120	C	5	H	5	1.50	41.10	2.99	44.09
181	1120	C	5	H	6	1.50	42.60	2.99	45.59
181	1120	C	5	H	7	0.68	44.10	2.99	47.09
181	1120	C	5	H	CC	0.10	44.78	2.99	47.77
181	1120	D	1	X	1	1.50	157.40	0.49	157.89
181	1120	D	1	X	2	1.50	158.90	0.49	159.39
181	1120	D	1	X	3	1.50	160.40	0.49	160.89
181	1120	D	1	X	4	1.50	161.90	0.49	162.39
181	1120	D	1	X	5	1.50	163.40	0.49	163.89
181	1120	D	1	X	6	1.50	164.90	0.49	165.39
181	1120	D	1	X	7	0.48	166.40	0.49	166.89
181	1120	D	1	X	CC	0.15	166.88	0.49	167.37
181	1120	D	2	X	1	1.50	167.00	0.81	167.81
181	1120	D	2	X	2	1.50	168.50	0.81	169.31
181	1120	D	2	X	3	1.50	170.00	0.81	170.81
181	1120	D	2	X	4	1.50	171.50	0.81	172.31
181	1120	D	2	X	5	1.50	173.00	0.81	173.81
181	1120	D	2	X	6	1.50	174.50	0.81	175.31
181	1120	D	2	X	7	0.44	176.00	0.81	176.81
181	1120	D	2	X	CC	0.29	176.44	0.81	177.25
181	1120	D	3	X	1	1.50	176.70	0.81	177.51
181	1120	D	3	X	2	1.50	178.20	0.81	179.01
181	1120	D	3	X	3	1.50	179.70	0.81	180.51
181	1120	D	3	X	4	1.50	181.20	0.81	182.01
181	1120	D	3	X	5	1.50	182.70	0.81	183.51
181	1120	D	3	X	6	0.52	184.20	0.81	185.01
181	1120	D	3	X	CC	0.26	184.72	0.81	185.53
181	1120	D	4	X	1	1.50	186.30	0.81	187.11
181	1120	D	4	X	2	1.50	187.80	0.81	188.61
181	1120	D	4	X	3	1.50	189.30	0.81	190.11
181	1120	D	4	X	4	1.50	190.80	0.81	191.61
181	1120	D	4	X	5	1.50	192.30	0.81	193.11
181	1120	D	4	X	6	0.78	193.80	0.81	194.61
181	1120	D	4	X	CC	0.20	194.58	0.81	195.39
181	1120	D	5	X	1	1.50	195.90	0.81	196.71
181	1120	D	5	X	2	1.50	197.40	0.81	198.21
181	1120	D	5	X	3	1.50	198.90	0.81	199.71
181	1120	D	5	X	4	1.50	200.40	0.81	201.21
181	1120	D	5	X	5	1.50	201.90	0.81	202.71
181	1120	D	5	X	CC	0.27	203.40	0.81	204.21
181	1120	D	6	X	1	1.50	205.50	0.81	206.31
181	1120	D	6	X	2	1.50	207.00	0.81	207.81
181	1120	D	6	X	3	1.50	208.50	0.81	209.31
181	1120	D	6	X	4	1.50	210.00	0.81	210.81
181	1120	D	6	X	5	1.50	211.50	0.81	212.31

Table T9 (continued).

Leg	Site	Hole	Core	Type	Section	Section length (m)	Depth (mbsf)	Offset (m)	Composite depth (mcd)
181	1120	D	6	X	6	1.00	213.00	0.81	213.81
181	1120	D	6	X	CC	0.22	214.00	0.81	214.81
181	1120	D	7	X	1	1.50	210.10	0.81	210.91
181	1120	D	7	X	2	1.50	211.60	0.81	212.41
181	1120	D	7	X	3	0.20	213.10	0.81	213.91
181	1120	D	7	X	CC	0.35	213.30	0.81	214.11
181	1120	D	8	X	1	1.50	215.10	0.81	215.91
181	1120	D	8	X	2	1.50	216.60	0.81	217.41
181	1120	D	8	X	3	1.50	218.10	0.81	218.91
181	1120	D	8	X	4	1.50	219.60	0.81	220.41
181	1120	D	8	X	5	0.53	221.10	0.81	221.91
181	1120	D	8	X	CC	0.22	221.63	0.81	222.44
181	1120	D	9	X	1	1.50	218.70	0.81	219.51
181	1120	D	9	X	2	1.48	220.20	0.81	221.01
181	1120	D	9	X	CC	0.28	221.68	0.81	222.49

Note: This table is also available in **ASCII format.**

Table T10. Splice tie points, Site 1120.

Site	Hole	Core	Type	Section	Depth in section (cm)	Depth (mbsf)	Depth (mcd)		Site	Hole	Core	Type	Section	Depth in section (cm)	Depth (mbsf)	Depth (mcd)
1120	C	1	H	4	92	5.42	5.18	Tie to	1120	B	2	H	1	144	4.74	5.18
1120	B	2	H	5	104	10.34	10.78	Tie to	1120	C	2	H	2	1	8.12	10.78
1120	C	2	H	5	36	12.96	15.62	Tie to	1120	B	3	H	1	101	13.82	15.62
1120	B	3	H	4	16	17.36	19.16	Tie to	1120	C	3	H	1	16	16.26	19.16
1120	C	3	H	6	88	24.48	27.38	Tie to	1120	B	4	H	5	6.5	28.32	27.38
1120	B	4	H	6	120	30.95	30.01	Tie to	1120	C	4	H	1	92	26.52	30.01
1120	C	4	H	6	84	33.94	37.43	Tie to	1120	B	5	H	4	68	36.98	37.43
1120	B	5	H	6	24	39.54	39.99	Tie to	1120	C	5	H	2	40	37.00	39.99
1120	C	5	H	4	120	40.80	43.79	Tie to	1120	B	6	H	1	108	42.38	43.79
1120	B	6	H	7	34	50.64	52.05									

Note: This table is also available in **ASCII format.**

Table T11. Reliable biostratigraphic events identified at Site 1120.

Event	Group	Age (Ma)	Sample	Depth (mbsf)
1 FO *Emiliania huxleyi*	N	0.24	1120A-1H-2, 28-29cm	1.78
2 FO *Globorotalia truncatulinoides*	F	~0.8	1120A-1H-2, 85-87cm	2.35
3 FCO dominant *Globorotalia inflata*	F	~0.7	1120A-1H-2, 85-87cm	2.35
4 LO *Pseudoemiliania lacunosa*	N	0.42	1120A-1H-3, 30-32 cm	3.3
5 FO *Globorotalia crassacarina*	F	~2.5	1120B-1H-CC	3.36
6 LCO *Globorotalia puncticuloides*	F	~0.7	1120A-1H-3, 30-32 cm	4.3
7 LO *Simonseniella barboi*	D	2	1120A-1H-CC	4.6
8 FO *Globorotalia puncticuloides*	F	3.6	1120C-1H-CC	6.6
9 LO *Globorotalia miotumida*	F	5.6	1120B-2H-CC	12.9
10 FO *Globorotalia sphericomiozea*	F	5.6	1120C-2H-CC	15.7
11 LO *Hemidiscus triangularis*	D	5.3	1120B-3H-CC	17.7
12 FCO *Neogloboquadrina pachyderma*	F	9.2	1120B-4H-3, 129-132 cm	26.6
13 LO *Hemidiscus karstenii* f. 1	D	5.7	1120B-4H-CC	31.56
14 FO *Prunopyle titan*	R	5.1	1120B-5H-CC	41.4
15 LO *Bolboforma pentaspinosa*	B	~7	1120B-5H-CC	41.4
16 LO *Helotholus praevema*	R	4.6	1120B-5H-CC	41.4
17 LO *Cyrtocapsella japonica*	R	10.11	1120B-6H-CC	51.1
18 Acme *Cyrtocapsella japonica*	R	10.2	1120B-7H-CC	59.5
19 LO *Bolboforma subfragoris*	B	10.5	1120B-7H-CC	59.5
20 LO *Denticulopsis dimorpha*	D	10.6	1120B-8H-CC	68.3
21 LO *Orbulina suturalis*	F	~10.5	1120B-9X-CC	70.8
22 Kaiti acme *Globorotalia miotumida* (dextral)	F	10.8-10.9	1120B-9X-CC	72.6
23 FO *Bolboforma pentaspinosa*	B	11.5	1120B-10X-CC	77.5
24 LO *Cycladophora humerus*	R	10.5	1120B-10X-CC	77.5
25 FO *Bolboforma subfragoris*	B	11.5	1120B-10X-CC	77.5
26 LO *Coccolithus miopelagicus*	N	10.94	1120B-10X-CC	77.5
27 LCO *Cyrtocapsella tetrapera*	R	12.6	1120B-11X-CC	86.6
28 FO *Dendrospyris megalocephalis*	R	12.7	1120B-11X-CC	86.6
29 LO *Globorotalia praemenardii*	F	~13.2	1120B-12X-CC	99.2
30 LO *Globorotalia conica*	F	13	1120B-12X-CC	99.2
31 LO *Globorotalia amuria*	F	13.2	1120B-12X-CC	99.2
32 FO *Calcidiscus macintyrei*	N	12.34	1120B-12X-CC	99.2
33 LO *Calcidiscus premacintyrei*	N	12.65	1120B-13X-CC	103.5
34 FO *Denticulopsis dimorpha*	D	12.2	1120B-14X-3, 60-61	114.6
35 FO *Eucyrtidium inflatum*	R	12.3	1120B-16X-CC	138.8
36 FO *Orbulina suturalis*	F	15.1	1120B-17X-CC	148.3
37 Range *Praeorbulina circularis*	F	14.8-15.6	1120B-17X-CC	148.3
38 LO *Sphenolithus heteromorphus*	N	13.52	1120B-19X-CC	166.9
39 FO *Globorotalia miozea*	F	16.7	1120D-2X-6, 126-131	175.8
40 FO *Globorotalia praemenardii*	F	15.8	1120B-20X-CC	177.1
41 FO *Sphenolithus heteromorphus*	N	18.6	1120B-20X-CC	177.1
42 LO *Globorotalia praescitula*	F	16.7	1120B-20X-CC	177.1
43 FO *Eucyrtidium punctatum*	R	17	1120D-3X-CC	185.0
44 FO *Calcidiscus premacintyrei*	N	17.4	1120D-3X-CC	185.0
45 FO *Globorotalia zealandica*	F	18.6	1120D-4X-CC	194.8
46 FO *Calcidiscus leptoporus*	N	18.2	1120D-4X-CC	194.8
47 FO *Geminilithella rotula*	N	19.8	1120D-4X-CC	194.8
48 FCO *Helicosphaera carteri*	N	19.2	1120D-4X-CC	194.8
49 LO *Globorotalia incognita*	F	18.5	1120D-5X-CC	203.7
50 FO *Globorotalia praescitula*	F	19	1120D-5X-CC	203.7
51 FO *Globigerinoides trilobus*	F	~19	1120D-7X-CC	213.65
52 LO *Globigerina euapertura*	F	22.5	1120D-8X-CC	221.8
53 ?FO *Globorotalia incognita*	F	21.6	1120D-9X-CC	222.0

Notes: Numbers in "Event" column correspond to events plotted in Figure **F6,** p. 31. N = nannofossils, F = foraminifers, D = diatoms, R = radiolarians, and B = bolboformids.

Table T12. Slightly simplified age/sedimentation rate data for Site 1120.

Age interval (Ma)	Sedimentation rate (m/m.y.)
0.24	7.42
0.42	8.44
1.05	0.16
3.40	1.36
5.50	2.60
5.70	95.00
7.00	7.31
10.10	3.28
10.50	78.50
11.50	0.10
12.34	22.86
12.60	147.69
15.10	3.76
15.80	28.00
16.70	1.10
17.00	54.30
18.50	0.00
19.00	78.40
21.60	5.96

Note: Data derived from Table T11, p. 71, and used to plot compacted sedimentation rates in Figure F6, p. 31.

Table T13. Composition of interstitial waters, Site 1120.

Core, section, interval (cm)	Depth (mbsf)	Depth (mcd)	Salinity	Cl^- (mM)	pH	Alkalinity (mM)	Na^+ (mM)	Mg^{2+} (mM)	Ca^{2+} (mM)	SO_4^{2-} (mM)	HPO_4^{2-} (µM)	NH_4^+ (µM)	H_4SiO_4 (µM)	K^+ (mM)	Li^+ (µM)	Sr^{2+} (µM)
181-1120B-																
1H-1, 145-150	1.45	1.45	34.0	550	7.62	2.99	466	53.1	10.8	28.0	1.2	39	203	11.2	28	106
2H-1, 145-150	4.75	5.19	34.5	549	7.58	2.86	465	53.0	11.1	27.9	1.0	53	436	10.8	28	124
2H-3, 145-150	7.75	8.19	34.5	550	7.53	2.74	463	53.0	11.0	26.0	1.2	63	469	10.7	29	139
2H-5, 145-150	10.75	11.19	34.5	551	7.53	2.95	471	52.3	11.1	29.2	1.4	63	485	11.2	30	154
3H-1, 145-150	14.25	16.05	34.5	551	7.55	2.92	467	52.7	11.0	27.5	1.6	56	526	11.0	30	165
3H-3, 135-140	17.15	18.95	34.5	551	7.59	2.97	472	52.9	11.3	30.1	0.8	53	533	10.7	30	177
4H-1, 140-150	23.70	22.76	34.5	555	7.63	3.22	472	52.3	11.3	27.9	0.8	69	586	10.6	29	207
4H-3, 135-145	26.65	25.71	34.5	550	7.58	3.22	466	52.0	11.6	27.0	0.8	60	612	10.4	30	217
4H-5, 140-150	29.60	28.66	34.5	552	7.66	3.69	468	52.2	11.3	27.0	1.2	47	619	10.5	30	230
5H-1, 140-150	33.20	33.65	34.5	552	7.53	3.43	468	52.2	11.5	26.8	1.0	64	623	10.4	29	245
5H-3, 140-150	36.20	36.65	34.5	555	7.55	3.57	470	52.2	11.7	27.0	1.2	50	634	10.6	30	259
5H-5, 140-150	39.20	39.65	34.5	555	7.79	3.70	473	51.1	11.4	26.9	1.7	68	641	10.4	30	265
6H-1, 140-150	42.70	44.11	34.5	554	7.67	3.46	469	51.8	11.9	26.9	1.0	88	650	10.5	29	276
6H-3, 140-150	45.70	47.11	34.5	555	7.02	3.78	471	51.3	11.7	26.5	1.2	86	665	10.3	30	288
6H-5, 140-150	48.70	50.11	34.5	555	7.83	3.79	471	51.5	11.8	26.8	1.4	88	665	10.4	29	294
7H-3, 140-150	55.20	56.61	34.5	554	7.65	3.86	468	51.2	12.2	26.3	1.6	94	683	10.3	29	308
8H-4, 140-150	66.20	67.61	34.5	557	7.65	4.19	472	51.0	12.2	26.4	1.4	108	713	10.3	30	331
9X-1, 140-150	69.70	71.11	35.0	556	7.57	4.26	470	51.0	12.5	26.2	1.4	126	740	10.5	30	345
10X-2, 140-150	75.50	76.91	35.0	556	7.72	4.17	471	50.8	12.3	26.1	1.9	117	751	10.3	30	370
11X-2, 140-150	85.10	86.51	35.0	557	7.65	4.45	471	50.9	12.3	26.1	1.9	142	771	10.4	31	400
12X-4, 140-150	97.70	99.11	35.0	557	7.64	4.52	471	50.4	12.7	26.2	1.4	116	773	10.2	32	426
13X-1, 140-150	102.80	104.21	34.5	557	6.90	4.60	467	51.6	13.2	25.9	1.2	143	790	10.5	32	438
16X-4, 140-150	136.00	137.41	34.5	558	7.56	5.71	472	49.9	12.7	25.4	1.2	151	817	10.2	36	507
19X-4, 140-150	164.90	166.31	34.5	560	7.17	5.31	473	49.2	13.4	24.9	1.2	203	819	10.2	39	563
181-1120D-																
1X-4, 140-150	163.30	163.79	34.5	564	7.35	5.67	475	49.7	13.9	24.9	0.9	193	801	10.1	44	553
4X-4, 140-150	192.20	193.01	34.5	563	7.30	5.66	475	48.1	14.7	24.6	0.7	242	749	10.1	49	578
7X-1, 140-150	211.50	212.31	34.5	561	7.26	5.96	474	48.3	14.7	24.7	0.5	242	711	9.8	52	607

Note: This table is also available in **ASCII format.**

Table T14. Inorganic carbon, carbonate, total carbon, total organic carbon, total nitrogen, and total sulfur for sediments from Holes 1120B and 1120D. (**See table note.** Continued on next page.)

Core, section, interval (cm)	Depth (mbsf)	IC (%)	$CaCO_3$ (%)	TC (%)	TOC (%)	TN (%)	TS (%)
181-1120B-							
1H-1, 28-29	0.28	10.4	86.6	10.69	0.29	0.06	0.04
1H-1, 54-55	0.54	10.87	90.56	10.89	0.02	0.04	0
1H-2, 84-85	2.34	10.85	90.42				
2H-3, 50-51	6.80	11.26	93.82				
2H-4, 50-51	8.30	11.53	96.06				
3H-2, 8-9	14.38	11.13	92.73				
3H-3, 109-110	16.89	11.03	91.91	11.03	ND	0.02	ND
4H-2, 96-97	24.76	11.15	92.92				
4H-3, 26-27	25.56	10.97	91.38				
4H-6, 110-111	30.80	11.56	96.32				
5H-1, 80-81	32.60	11.42	95.17				
6H-1, 50-51	41.80	11.45	95.42				
6H-4, 56-57	46.36	11.46	95.5				
6H-7, 30-31	50.60	11.32	94.3				
7H-3, 74-75	54.54	11.51	95.91				
7H-5, 80-81	57.60	11.35	94.54				
8H-1, 40-41	60.70	11.48	95.64				
8H-2, 88-89	62.68	11.15	92.88	11.56	0.41	0.02	ND
8H-4, 5-6	64.85	11.38	94.8				
9X-1, 31-32	68.61	11.44	95.3				
9X-2, 82-83	70.62	11.5	95.76				
10X-2, 105-106	75.15	11.39	94.89				
11X-1, 81-82	83.01	11.4	94.99				
11X-2, 24-25	83.94	11.52	95.95				
11X-2, 85-86	84.55	11.3	94.1				
12X-3, 15-16	94.95	11.85	98.73				
12X-4, 61-62	96.91	11.5	95.82				
12X-4, 69-70	96.99	11.47	95.57				
13X-1, 12-13	101.52	11.49	95.69				
13X-1, 80-81	102.20	11.52	95.98				
14X-2, 45-46	112.95	11.3	94.1				
14X-4, 45-46	115.95	11.62	96.78				
16X-1, 40-41	130.50	11.27	93.9				
16X-2, 70-71	132.30	11.39	94.86				
16X-3, 76-77	133.86	11.06	92.14				
17X-2, 45-46	141.65	11.54	96.11				
17X-4, 45-46	144.65	11.52	95.95				
17X-6, 45-46	147.65	11.48	95.62				
18X-1, 16-17	149.56	11.41	95.08				
18X-1, 90-91	150.30	11.38	94.78				
18X-2, 108-109	151.98	11.53	96.06	11.53	ND	0.02	ND
19X-1, 77-78	159.77	11.26	93.78				
19X-3, 77-78	162.77	11.37	94.68				
19X-5, 77-78	165.77	11.41	95.04				
20X-1, 77-78	169.47	11.36	94.67				
20X-3, 77-78	172.47	11.49	95.73				
20X-5, 77-78	175.47	11.46	95.49				
21X-1, 79-81	179.19	11.23	93.54				
21X-3, 79-81	182.19	11.28	93.93				
181-1120D-							
1X-1, 70-71	158.10	11.48	95.61				
1X-5, 120-121	164.60	11.34	94.5				
1X-7, 30-31	166.70	11.36	94.64				
2X-2, 45-46	168.95	11.49	95.7				
2X-4, 16-17	171.66	11.39	94.86				
2X-6, 42-43	174.92	11.28	93.95				
3X-2, 80-81	179.00	11.33	94.37				
3X-3, 24-25	179.94	11.24	93.65				
3X-4, 9-10	181.29	11.37	94.67				
4X-1, 124-125	187.54	11.2	93.29				
4X-3, 83-84	190.13	11.39	94.85				
4X-5, 97-98	193.27	11.38	94.77				
5X-1, 50-51	196.40	11.28	93.94				
5X-3, 50-51	199.40	11.5	95.82				
5X-5, 50-51	202.40	11.3	94.12				

Table T14 (continued).

Core, section, interval (cm)	Depth (mbsf)	IC (%)	$CaCO_3$ (%)	TC (%)	TOC (%)	TN (%)	TS (%)
6X-1, 50-51	206.00	11.5	95.8				
6X-3, 50-51	209.00	11.5	95.8				
6X-5, 50-51	212.00	11.59	96.54				
7X-1, 50-51	210.60	11.51	95.87				
8X-1, 50-51	215.60	11.36	94.59				
8X-3, 50-51	218.60	11.45	95.38				
8X-5, 50-51	221.60	11.36	94.59				
9X-1, 50-51	219.20	11.39	94.84				

Notes: Carbonate is calculated assuming that all inorganic carbon is calcite. ND = not detected. This table is also available in **ASCII format.**

Table T15. List of index properties measured from Holes 1120B and 1120D. (See table note. Continued on next page.)

Leg	Hole	Core	Section	Interval (cm)	Depth (mbsf)	Wet-water content (%)	Dry-water content (%)	Wet-bulk density (g/cm^3)	Dry density (g/cm^3)	Grain density (g/cm^3)	Porosity (%)	Void ratio
181	1120B	1H	3	10-12	3.10	38.3	62.1	1.671	1.031	2.750	62.5	1.67
181	1120B	2H	1	108-110	4.38	37.2	59.2	1.674	1.051	2.682	60.8	1.55
181	1120B	2H	4	124-126	9.04	34.5	52.6	1.724	1.130	2.693	58.1	1.38
181	1120B	2H	6	128-130	12.08	37.1	59.1	1.685	1.060	2.725	61.1	1.57
181	1120B	3H	1	132-134	14.12	31.7	46.4	1.778	1.214	2.700	55.0	1.22
181	1120B	3H	3	113-115	16.93	38.9	63.6	1.646	1.006	2.681	62.5	1.67
181	1120B	4H	2	127-129	25.07	42.1	72.7	1.594	0.923	2.679	65.6	1.90
181	1120B	4H	4	126-128	28.01	35.1	54.0	1.717	1.115	2.707	58.8	1.43
181	1120B	5H	1	121-123	33.01	35.0	53.9	1.708	1.109	2.668	58.4	1.41
181	1120B	5H	4	125-127	37.55	35.2	54.4	1.725	1.117	2.747	59.3	1.46
181	1120B	5H	5	125-127	39.05	37.4	59.6	1.695	1.062	2.783	61.9	1.62
181	1120B	6H	1	122-124	42.52	35.2	54.3	1.712	1.109	2.694	58.8	1.43
181	1120B	6H	3	127-129	45.57	34.5	52.6	1.718	1.126	2.672	57.9	1.37
181	1120B	6H	5	125-127	48.55	34.9	53.6	1.716	1.117	2.691	58.5	1.41
181	1120B	7H	2	127-129	53.57	36.2	56.7	1.706	1.089	2.742	60.3	1.52
181	1120B	7H	4	132-134	56.62	37.8	60.8	1.666	1.036	2.694	61.5	1.60
181	1120B	7H	6	75-77	59.05	37.5	59.9	1.667	1.043	2.673	61.0	1.56
181	1120B	8H	1	111-113	61.41	43.3	76.3	1.582	0.897	2.708	66.9	2.02
181	1120B	8H	3	125-127	64.55	38.0	61.2	1.665	1.033	2.697	61.7	1.61
181	1120B	8H	5	112-114	67.42	37.9	60.9	1.658	1.030	2.664	61.3	1.59
181	1120B	9X	1	96-98	69.26	35.7	55.6	1.703	1.094	2.697	59.4	1.47
181	1120B	10X	1	105-107	73.65	39.8	66.0	1.643	0.990	2.731	63.8	1.76
181	1120B	10X	3	110-112	76.70	35.1	54.1	1.726	1.120	2.746	59.2	1.45
181	1120B	11X	1	130-132	83.50	37.4	59.7	1.692	1.059	2.771	61.8	1.62
181	1120B	11X	3	80-82	86.00	34.6	52.9	1.738	1.136	2.752	58.7	1.42
181	1120B	12X	1	130-132	93.10	36.9	58.5	1.696	1.070	2.751	61.1	1.57
181	1120B	12X	3	130-132	96.10	38.6	63.0	1.655	1.015	2.702	62.4	1.66
181	1120B	12X	5	110-112	98.90	33.6	50.7	1.746	1.159	2.717	57.3	1.34
181	1120B	13X	1	111-113	102.51	30.3	43.4	1.814	1.265	2.727	53.6	1.16
181	1120B	14X	1	134-136	112.34	36.6	57.6	1.704	1.081	2.759	60.8	1.55
181	1120B	14X	3	127-129	115.27	36.9	58.6	1.687	1.064	2.717	60.8	1.55
181	1120B	15X	1	139-141	121.99	31.9	46.7	1.775	1.210	2.701	55.2	1.23
181	1120B	15X	3	136-138	124.96	33.6	50.5	1.749	1.162	2.723	57.3	1.34
181	1120B	16X	1	132-134	131.42	36.6	57.9	1.695	1.074	2.728	60.7	1.54
181	1120B	16X	3	131-133	134.41	34.3	52.3	1.733	1.138	2.716	58.1	1.39
181	1120B	16X	5	136-138	137.46	35.9	56.0	1.710	1.096	2.737	60.0	1.50
181	1120B	17X	1	133-135	141.13	36.3	57.0	1.708	1.087	2.759	60.6	1.54
181	1120B	17X	3	132-134	144.02	33.4	50.0	1.749	1.165	2.707	57.0	1.32
181	1120B	17X	5	131-133	147.01	33.2	49.8	1.742	1.163	2.676	56.6	1.30
181	1120B	18X	1	133-135	150.73	34.2	52.0	1.729	1.137	2.693	57.8	1.37
181	1120B	18X	3	124-126	153.64	33.7	50.8	1.743	1.156	2.709	57.3	1.34
181	1120B	18X	5	130-132	156.70	35.7	55.5	1.693	1.089	2.656	59.0	1.44
181	1120B	19X	1	121-123	160.21	37.0	58.8	1.689	1.063	2.732	61.1	1.57
181	1120B	19X	3	126-128	163.26	36.8	58.3	1.690	1.067	2.720	60.8	1.55
181	1120B	19X	5	121-123	166.21	29.9	42.6	1.817	1.274	2.713	53.0	1.13
181	1120B	20X	1	130-132	170.00	33.9	51.4	1.733	1.145	2.692	57.5	1.35
181	1120B	20X	3	141-143	173.11	35.0	53.8	1.710	1.112	2.675	58.4	1.41
181	1120B	20X	5	138-140	176.08	34.9	53.6	1.714	1.116	2.682	58.4	1.40
181	1120B	21X	1	135-137	179.75	38.5	62.6	1.647	1.013	2.662	61.9	1.63
181	1120B	21X	3	135-137	182.75	34.9	53.5	1.716	1.118	2.687	58.4	1.40
181	1120D	1X	1	134-136	158.74	35.2	54.3	1.717	1.113	2.713	59.0	1.44
181	1120D	1X	3	130-132	161.70	33.8	51.1	1.740	1.151	2.706	57.5	1.35
181	1120D	1X	5	130-132	164.70	35.3	54.6	1.711	1.107	2.700	59.0	1.44
181	1120D	2X	1	107-109	168.07	29.5	41.8	1.834	1.293	2.740	52.8	1.12
181	1120D	2X	3	110-112	171.10	31.3	45.5	1.786	1.227	2.700	54.6	1.20
181	1120D	2X	5	115-117	174.15	31.7	46.4	1.773	1.211	2.685	54.9	1.22
181	1120D	3X	1	135-137	178.05	36.1	56.6	1.702	1.087	2.722	60.1	1.51
181	1120D	3X	3	137-139	181.07	34.5	52.7	1.733	1.135	2.730	58.4	1.40
181	1120D	3X	5	130-132	184.00	32.8	48.8	1.761	1.184	2.717	56.4	1.30
181	1120D	4X	1	87-89	187.17	35.2	54.4	1.725	1.117	2.750	59.4	1.46
181	1120D	4X	3	110-112	190.40	34.9	53.7	1.723	1.121	2.718	58.8	1.43
181	1120D	4X	5	125-127	193.55	34.9	53.5	1.728	1.125	2.732	58.8	1.43
181	1120D	5X	1	136-138	197.26	35.7	55.6	1.707	1.097	2.714	59.6	1.47
181	1120D	5X	3	127-129	200.17	36.0	56.3	1.701	1.088	2.709	59.8	1.49
181	1120D	5X	5	120-122	203.10	35.6	55.4	1.706	1.098	2.704	59.4	1.46
181	1120D	6X	1	137-139	206.87	36.9	58.4	1.694	1.070	2.744	61.0	1.57

Table T15 (continued).

Leg	Hole	Core	Section	Interval (cm)	Depth (mbsf)	Wet-water content (%)	Dry-water content (%)	Wet-bulk density (g/cm^3)	Dry density (g/cm^3)	Grain density (g/cm^3)	Porosity (%)	Void ratio
181	1120D	6X	3	129-131	209.79	30.2	43.2	1.821	1.271	2.743	53.7	1.16
181	1120D	6X	5	125-127	212.75	35.3	54.5	1.716	1.111	2.717	59.1	1.45
181	1120D	7X	2	116-118	212.76	38.3	62.2	1.659	1.023	2.700	62.1	1.64
181	1120D	8X	1	130-132	216.40	35.5	55.1	1.713	1.105	2.724	59.4	1.47
181	1120D	8X	3	130-132	219.40	33.3	49.9	1.754	1.170	2.721	57.0	1.33
181	1120D	9X	2	122-124	221.42	32.7	48.6	1.762	1.185	2.712	56.3	1.29

Note: This table is also available in **ASCII format.**